

**Induction of DNA double-strand breaks at various stages  
of the cell cycle using the comet assay**

***A Thesis***

**Submitted in Partial Fulfilment of Requirement for Ph. D. Degree  
of Science (Biology).**

***By***

**Atef Mahmoud Mahmoud Attia**

***At***

**(The Centre of Radiology, Georg- August University,  
Goettingen, Germany)**

***To***

**(The Faculty of Biology, Georg-August University,  
Goettingen, Germany)**

**2002**

D7

Referent : Prof. Dr. Fritz

Korreferent : Prof. Dr. Hardeland

**Tag der mündlichen Prüfung : 30 Oktober 2002**

## CONTENTS

### CHAPTER 1

<b>INTRODUCTION</b>	<b>-1-</b>
<b>1.1 ) DNA and ionizing radiation</b>	<b>-1-</b>
<b>1.2 ) Methods used for measuring the degree of DNA condensation and supercoiling in individual cells at various stages of the cell cycle</b>	<b>-4-</b>
<b>1.2.1) Methods based on automatic image analysis of nuclear morphology</b>	<b>-4-</b>
<b>1.2.2 ) Flow cytofluorometric (FCM) methods</b>	<b>-5-</b>
<b>1.2.2.1 ) FCM- methods based on differential stainibility of cells after denaturation procedures</b>	<b>-5-</b>
<b>1.2.2.2 ) FCM- methods based on different light scatter properties</b>	<b>-6-</b>
<b>1.3 ) Methods used for measuring DNA damage in individual cells</b>	<b>-7-</b>
<b>1.4) Analysis of the cell cycle distribution and estimation of the fraction of cells in different phases of the cell cycle</b>	<b>-9-</b>
<b>1.4.1) Analysis of DNA histograms measured by comet assay- based cytofluorometry</b>	<b>-9-</b>
<b>1.4.2) Mathematical model for analysis of DNA- histograms measured by comet assay- based cytofluorometry</b>	<b>-9-</b>
<b>1.4.3) Software computer program for analysis of DNA- histograms and estimating the fraction of cells in different phases of the cell cycle</b>	<b>-10-</b>
<b>1.5) Biophysical model for analysis of the degree of condensation and relative molecular size of DNA in individual cells, at various stages of the cell cycle</b>	<b>-10-</b>
<b>1.5.1) Relative DNA condensation</b>	<b>-11-</b>
<b>CHAPTER 2</b>	
<b>MATERIALS AND METHODS</b>	<b>-13-</b>
<b>2.1 ) Cell culture</b>	<b>-13-</b>
<b>2.2 ) Cell preparation</b>	<b>-13-</b>

2.3 )	<b>Microgel preparation</b>	<b>-13-</b>
2.4 )	<b>Fraction of cells in different phases of the cell cycle, measured by comet assay-based cytofluorometry</b>	<b>-14-</b>
24.1 )	<b>Cell lysis and chemical treatment</b>	<b>-14-</b>
2.4.2 )	<b>Microscopic image analysis</b>	<b>-14-</b>
2.4.3 )	<b>Analysis of DNA hisograms</b>	<b>-14-</b>
2.5 )	<b>The degree of condensation and relative molecular size of DNA in individual cells, measured by the comet assay-based cytofluorometry</b>	<b>-15-</b>
2.6)	<b>Effects of X-rays on DNA structure in individual cells, at different stages of the cell cycle</b>	<b>-15-</b>
2.6.1 )	<b>X-ray irradiation of human skin fibroblasts</b>	<b>-15-</b>
2.6.2 )	<b>DNA damage in individual cells, measured by single cell gel electrophoresis (neutral comet assay)</b>	<b>-15-</b>
2.6.2.1)	<b>Neutral lysis and microgel electrophoresis</b>	<b>-15-</b>
2.6.2.2)	<b>Comet analysis and visualization</b>	<b>-16-</b>
2.6.3 )	<b>Fraction of damaged DNA in human skin fibroblasts, at different stages of the cell cycle</b>	<b>-16-</b>
2.6.4 )	<b>DSB- induction in human skin fibroblasts, at different stages of the cell cycle</b>	<b>-17-</b>
2.7 )	<b>Data analysis</b>	<b>-17-</b>
<b>CHAPTER 3</b>		
	<b>RESULTS</b>	<b>-18-</b>
3.1 )	<b>Mathematical analysis of comet flourescence histograms for estimating the fraction of cells in different phases of the cell cycle based cytofluorometry</b>	<b>-18-</b>
3.2 )	<b>Densitometrical and geometrical parameters of unirradiated nucleoids, at various stages of the cell cycle</b>	<b>-18</b>
3.3 )	<b>The degree of condensation and relative size of DNA in single cells , at various stages of the cell cycle</b>	<b>-18-</b>
3.4 )	<b>The tail length of unirradiated nucleoids at various stages of the cell cycle</b>	<b>-19-</b>
3.5 )	<b>The tail intensity of unirradiated nucleoids at various stages of the cell cycle</b>	<b>-19</b>

3.6)	Effects of the electrophoretic field on the nuclear morphology of unirradiated nucleoids, at various stages of the cell cycle	-19-
3.7)	Effects of ionizing radiation on the DNA- structure and nuclear morphology of HSF2- fibroblasts	-19
3.7.1 )	Effects of ionizing radiation on the amount of DNA migrated from individual cells, measured by the neutral comet assay	-20-
3.7.2 )	Effects of ionizing radiation on the fluorescence density of individual cells, at various stages of the cell cycle	-20-
3.7.3 )	Effects of ionizing radiation on the comet area of individual cells at various stages of the cell cycle	-21-
3.7.4 )	Effects of ionizing radiation on the comet fluorescence of individual cells at various stages of the cell cycle	-21-
3.7.5 )	Effects of ionizing radiation on the degree of condensation of DNA in individual cells at various stages of the cell cycle	-21-
3.7.6 )	Effects of ionizing radiation on the relative molecular size of DNA in individual cells at various stages of the cell cycle	-21-
3.7.7 )	Effects of ionizing radiation on the fluorescence- decrement induced by electrophoresis of HSF2- fibroblasts at various stages of the cell cycle	-21-
3.7.8 )	Effects of ionizing radiation on the DNA damage in HSD2- fibroblasts at stages of the cell cycle	-22-
3.7.9 )	Effects of ionizing radiation on DSB-induction in individual cells at various stages of the cell cycle	-22-
<b>CHAPTER 4</b>		
	<b>DISCUSSION</b>	<b>-23</b>
<b>CHAPTER 5</b>		
	<b>CONCLUSION</b>	<b>-38-</b>
<b>CHAPTER 6</b>		
	<b>SUMMARY/ZUSAMMENFASSUNG</b>	<b>-39-</b>
	<b>REFERENCES</b>	<b>-41-</b>

# ***INTRODUCTION***

## **Introduction**

### **1.1) DNA and Ionizing radiation**

Ionizing radiation is a deleterious environmental agent. Its physico-chemical interaction with cellular DNA produces variety of primary lesions, such as single strand breaks (SSB), double strand breaks (DSB), DNA protein crosslinks and damage to purine and pyrimidine bases (Coquerelle and Hagen, 1978 ;Olive, 1999). DSBs are generally considered to be of greater biological consequence than SSBs, since they can lead directly to chromosome aberrations and loss of genetic material (Bryant., 1984; Natarajan and Obe 1978). Evaluation of these primary lesions is an essential step in the examination of the sequence of events leading to mutagenic, carcinogenic and lethal effects of radiation. A number of biophysical and biochemical methods have been used to quantitate radiation induced primary lesions in cellular DNA (Ager *et al.*, 1990; Flick *et al.*, 1989; Lehman and Stevans, 1977; Löbrich *et al.*, 1993; Ruiz de Amodovar *et al.*, 1994; Friedl, *et al.*, 1995). However, the neutral comet assay (single cell gel electrophoresis) is preferred because of its simplicity, rapidity and its potential to measure DNA damage and heterogeneity in response at the level of a single cell.

In 1984 Östling and Johanson described the first protocol of the comet assay, which is based on migration of DNA in an electric field. Cells embedded in agarose on frosted slides were lysed, subjected briefly to 5 V/cm for 5 min and, stained with a fluorescent DNA binding dye. Individual cells resembling 'comets', with a head and tail, were viewed using an epifluorescence microscope. The method is quantified by measuring  $F_{tail}/F_{head}+F_{tail}$ , where  $F_{tail}$  and  $F_{head}$  are the tail fluorescence and head fluorescence, respectively. The relative fluorescence of tails, with respect to the head fluorescence. More recently, the same authors have used this method successfully to study the effects of ionizing radiation on DNA damage in Chinese hamster ovary cells grown in vitro (Östling, and Johanson, 1987). However, there is doubt that Östling's protocol measures DNA double strand breaks in individual cells. The neutral method of Östling appeared to be sensitive to the effect of single strand breaks on DNA supercoiling. The lysis conditions used by these authors were likely to be ineffective in removing all proteins so that the major influence of radiation appeared to be the release of a halo of DNA by loss of DNA supercoiling, creating a sensitive assay for the presence of single strand breaks.

In 1990, Olive *et al.*, have developed further this method by optimizing the lysing solution, lysing time, electrophoresis time, and providing an image analysis system to define appropriate features of the comet as a measure of DNA damage in single cells. However, this method has several disadvantages, which are general for all Olive's protocols (Olive *et al.*, 1992; Olive *et al.*, 1993; Olive and Banath, 1995; Banath *et al.*, 1998). Among these disadvantages are: 1) No enzymatic or chemical treatment is involved to remove RNA conjugated with nuclear chromatin in individual cells, which leads to a considerable error and uncertainty in the estimation of the nuclear DNA content. This disadvantage makes this method inapplicable for measuring the nuclear DNA content and for the analysis of DNA-histograms and independent of the cell cycle distribution. Therefore accurate estimations of DNA damage at different stages of the cell cycle are not possible. 2) The more vigorous lysing conditions at elevated temperatures (50° C) used in this method is too aggressive for some human cell lines and leads to an unacceptable background damage (Ross *et al.*, 1995). Recently, (Singh and Stephens, 1997) have improved the comet assay to increase its sensitivity and reproducibility to detect DNA damage induced by doses as low as 0,125 Gy of X-ray. However, this method has several disadvantages like the more vigorous alkaline conditions used to remove RNA after electrophoresis, which leads to severe alterations in the

DNA conformation and total fluorescence, making it inapplicable for measuring the nuclear DNA-content, for the analysis of the cell cycle distribution using DNA- histograms and in turn for measuring the DNA damage, at different stages of the cell cycle. Therefore, we aimed from the present study to develop this technique experimentally to overcome the previously mentioned back draws.

A unique feature of the comet assay is its ability to measure DNA damage, simultaneously with the DNA content in individual cells. Recently, *Olive et al.*, (1992) have utilized this advantage and introduced a new technique for measuring DNA damage at different positions of the cell cycle, basing on the tail moment versus the comet fluorescence bivariate analysis. This technique has been successfully utilized to measure the effects of ionizing radiation on the DNA damage in individual cells, at different stages of the cell cycle (*Olive P. L. and Banath, 1993a, b, 1995 and Olive, 1999*). However, this analytical method has several disadvantages: 1) Sorting windows for G1 and G2- phase cells were defined, basing on approximate positions in the DNA histogram (*Olive et al., 1993 a*); 2) An approximate sorting window for S- phase cells was defined in the middle channel between the G1 and G2- peaks, which is not always true for all cell lines (*Olive and Banath , 1992, 1993a*); 3) Most important the same mean (mode) values of DNA histograms of unirradiated cells were used for irradiated cells, although these values vary with dose of ionizing radiation (*Olive P. L. and Banath, 1993 a, b 1995*). This method of analysis leads to an unacceptable error and uncertainty in the measured DNA damage of cells in different phases of the cell cycle; 4) Only 200 cells have been scored per slide, which is statistically not enough to get reproducible results and reliable conclusion about the effect of cell cycle position on DNA damage. Therefore, we aimed from this study to develop this method to get more accurate, reliable and reproducible results of DNA damage in individual cells at different stages of the cell cycle. With this regard, in this thesis a newly developed analytical method is introduced, based on the mathematical analysis of the DNA histograms and the total fluorescence versus tail intensity bivariate analysis, which allows a simultaneous estimation of cell fraction and DNA damage in single cells at different stages of the cell cycle.

A unique feature of the comet assay is its ability to measure DNA damage in individual cells (rather than the mean DNA damage) and the heterogeneity in response of cells within a population. Previous studies on (semi) synchronous populations of cells, using a variety of strand break assays, have failed to reveal a difference in either the number of initial radiation induced breaks or their rates of rejoining as a function of cell cycle position (*Humphrey et al., 1968; Lett and Sun, 1970; Watanabe and Dikomey, 1984*). However, a considerable heterogeneity was observed when asynchronous cells were used which could be attributed primarily to the presence of a high proportion of S-phase cells (*Olive et al., 1990, 1991, 1992, 1993; Olive and Banath, 1993 b, 1995 and Olive, 1999*). The results of these studies revealed a lower tendency of DNA migration from S-phase cells, as compared to G1 and G2-cells. These results have been confirmed in previous studies (*Iliakis et al., 1991 a, b, 1993; Mateos et al., 1996*) by using pulsed field gel electrophoresis or (*Radford and Broudhurst, 1988; Sweigert et al., 1988; Okayasu et al., 1988*) by using neutral filter elution.

Retardation of DNA migration appears to be at its maximum value in late-G1/early-S (*Olive et al., 1992*). It seems likely that the DNA replication structures are primarily responsible for inhibitory migration of replicating DNA during gel electrophoresis. Also changes in DNA packaging, which occur during S-phase and tightly bound proteins associated with DNA replication may also inhibit migration. DNA in cells at the G1-S border seemed particularly susceptible to this effect. There is evidence to suggest that those regions of the genome the chromatin of which is least condensed during interphase and therefore most accessible to the



replication enzymes is synthesized in early-S phase. Highly condensed heterochromatin, on the other hand, is generally replicated very late in the S-phase (*Alberts et al., 1983*). While removing S-phase cells considerably reduced heterogeneity in tail moment, this was not true for all cases (*Olive et al., 1991*). About 20 % of the cells sorted for G1 and G2 migrated at the rate of S-phase cells, in some cell lines (*Olive et al., 1991*). Therefore, the factor, which inhibited migration primarily in early S of some cell lines, might also be present in other phases of the cell cycle of other lines. If so, one could argue that inherent differences in DNA packaging play a role in the sensitivity of some cell types to DNA damaging agents. A possible role for DNA higher order structure in radiation - induced DNA damage and repair has been suggested (*Olive et al., 1986; Wheele et al., 1988; Wlodek et al., 1990; Gordon, et al., 1990*) and the concept of the DNA organization and packaging might be one of the determinants of radiation sensitivity among cells in different phases and different cell types which requires further study. Therefore, the aim of this work was to study the effect of DNA condensation and packaging on the response of cells in different phases to ionizing radiation, by using a new approach of the neutral comet assay. This allows simultaneous estimation of DNA damage and the degree of DNA organization in individual cells at different stages of the cell cycle. Moreover, the potential of the developed technique to measure the degree of DNA condensation in individual cells allowed us to study the effects of ionizing radiation on the DNA structure in single cells at different stages of the cell cycle.

The results of dose response curves obtained by the neutral comet assay have shown a 2-4 times lower rate of DNA migration from S-phase cells as compared to cells in other phases of the cell cycle (*Olive et al., 1991, 1992*). This effect is clearly evidenced during the early-S stage. However, it was also observed in some cell populations in G1 and G2- phases (*Olive et al., 1991*) indicating that the factors responsible for retardation of DNA migration during S-phase may also be present during other phases of the cell cycle. Although these factors are known for S-phase cells (*Olive and Banath, 1992, 1993 b*), they are still obscure for cells in other phases of cell cycle.

More recently, (*Olive, 1999*) have observed a lower tendency of DNA migration from unirradiated S-phase cells, as compared to G1 and G2- phase cells and has concluded that the retardation of DNA- migration is inherent to S- phase cells and not a result of radiation. If so, the comet assay based on the current tail parameters may be not relevant to measure DNA damage in cells at different stages of the cell cycle. Therefore, the aim of this study was to develop this method to be able to measure DNA damage in cells at different stages of the cell cycle. This could be accomplished by using a new approach of the neutral comet assay, which allows estimation of DNA damage and DSB-induction in mammalian cells at different stages of the cell cycle by using non- conventional comet parameters like (the total fluorescence) rather than the current tail parameters.

It is not known whether the differences observed in comet tail parameters of unirradiated cells in relation to the cell cycle have biological relevance or they simply reflect the influence of DNA- structure on its migration during gel electrophoresis (*Olive and Banath, 1993 a*). To resolve this problem, a new approach of the neutral comet assay was used to study the effects of ionizing radiation on DNA damage and DSB- induction in cells at different stages of the cell cycle. A comparison of the results obtained by this approach with those obtained by the conventional tail parameters allowed us to resolve this problem.

Another back draw in using the current tail parameters arise from the fact that not all damaged DNA is able to migrate into the tail, since only a fraction of the DNA pieces, which untangled near the surface of the comet, may be in a suitable position to migrate (*Olive et al., 1992*). The

suggested approach introduced in this study allowed measurement of the whole DNA damage in mammalian cells, since it is based on the fluorescence decrement induced by ionizing radiation, which represents the whole DNA in the cell nucleus, rather than the DNA in the tail region. More details on those new approaches will be described in the following few pages.

## 1. 2.) **Methods used for measuring the degree of DNA condensation and supercoiling in individual cells, at various stages of the cell cycle.**

Several methods have been used for measuring the degree of condensation and supercoiling in individual cells, at various stages of the cell cycle. These methods could be classified into three groups namely:

### 1.2.1) *Methods based on automatic image analysis of nuclear morphology.*

These methods utilize the correlation between the chromatin structure and nuclear morphology to evaluate the condensation state of nuclear chromatin at various stages of the cell cycle. By means of the image analyzing computer quantimet 720 D (*Sawicki et al., 1974*) have analyzed the nuclear chromatin of exponentially growing mouse fibroblasts, stained with the Feulgen's method. Cells with 2C and 3C and 4C content of DNA were considered as being in the G1, mid-S and G2 stages of cell cycle. It was found that the projected area of nuclei increases with the cell cycle and that the mean optical density of chromatin increases from G1 through S to G2 phase, indicating an increased chromatin condensation with progression of cells through the cell cycle. The curves showing the areas of chromatin at different optical density thresholds are different for cells in the G1, S and G2 phases. The results demonstrated cyclic changes in the chromatin morphology in the interphase nuclei during the cell cycle. However this method cannot be applied for measuring the chromatin morphology in other subphases of cell cycle. To overcome this problem (*Kendall and Swenson, 1976*) have measured various geometric and densitometric parameters, by means of the automated image analyzer Quantimet 720-D in Feulgen-stained HeLa cells synchronized by selective mitotic detachment and released from synchronization and examined at different times of the cell cycle. Similar studies was performed by *Nicolini et al., (1977a)*, who examined various geometrical and densitometrical parameters of Feulgen-stained HeLa S3 cells, by means of automated image analysis.

To study the effect of serum stimulation on the chromatin morphology, *Kendall et al., (1977)* examined the alteration in the nuclear morphology of Feulgen stained smears of WI-38 cells that were either confluent, or that received a nutritional stimulus to proliferate 3 h before collection. These experiments showed that it is possible to observe changes in morphometric and densitometric parameters of nuclei that correlate with structural and functional differences in isolated chromatin from quiescent G<sub>0</sub> and proliferating G<sub>1</sub>-cells that have been demonstrated by other means.

In another study published by *Nicolini et al., (1977b)* have studied, by means of automated image analysis (Quantimet 720 D), various geometric and densitometric parameters (area, projection, perimeter, integrated optical density, form factor, mean bound path and fractional areas) of Feulgen-stained WI48 human diploid fibroblasts, confluent (G<sub>0</sub>) and 3 h after nutritional stimulus (G<sub>0</sub>+G<sub>1</sub>). The frequency distribution of area and perimeter from the stimulated population show two distinct peaks (G<sub>0</sub> and G<sub>1</sub>), while no significant differences existed between mean values for IOD (DNA content). The parameters versus optical density level threshold are consistent with the above findings, showing distributions indicative of chromatin dispersion during the G<sub>0</sub>-G<sub>1</sub> transition.

Although the ability of these methods to detect differences in the chromatin structure between cells in different phases of the cell cycle, however they have the disadvantages of being tedious, non practical and require a large number of cells and high degree of synchronization to be applicable for measuring the nuclear morphology at various phases and subphases of the cell cycle. The main disadvantage of those methods is the low sensitivity for measuring the chromatin morphology of cells at different subphases with the same cell population examined, because of the small differences in the chromatin structure among G1-subphases and between G2 and M-phases of the cell cycle.

### 1.2.2) *Flow cytofluorometric (FCM) methods.*

Several more sensitive and more practical methods have been developed, based on the flow cytofluorometry (FCM), which have the potential for detecting the differences in the chromatin structure between G2 and M-cells and among cells at different G1 subphases of cell cycle at the same time, within the same cell population. Several fixation procedures, cell treatment and staining techniques have been used in these methods to enhance the difference in chromatin structure of cells in the various phases and subphases of the cell cycle, thus enabling flow cytometric detection of early-G1 from late-G1 cells and M-cells clearly separated from G2-phase cells, by using fluorescence as well as light scatter measurements. However, this effect was found only after certain pretreatments of the cells or cell nuclei, either before or during staining. These methods can be classified into two classes:

#### 1.2.2.1) *FCM methods based on differential stainability of cells after denaturation procedures.*

The principle of these methods based on the differential staining of double versus single stranded (denatured) DNA with acridine orange (AO) in cells depleted of RNA. The differential staining of double versus single stranded DNA occurs because AO intercalates into double stranded and fluoresces green ( $F_{530}$ ) whereas the dye stacking on denatured (single stranded) sections of DNA results in metachromatic red fluorescence ( $F > 600$ ). The extent of DNA denaturation is expressed as  $\alpha_t$ , which represents the ratio of  $F_{>600}$  to ( $F > 600 + F_{530}$ );  $\alpha_t = F_{>600} / (F > 600 + F_{530})$ . The extent of DNA denaturation is proportional to the degree of chromatin condensation (*Dazyńkiewicz et al., 1980*). Therefore, in most of these methods,  $\alpha_t$  was used as a measure of the chromatin condensation in individual cells at different phases of the cell cycle.

Some of these methods are based on the differential stainability induced by the heat denaturation (*Dazyńkiewicz et al., 1977a*). Other FCM-methods are based on the difference in DNA condensation among cells in different phases of the cell cycle, based on the differences in DNA stainability induced by acid denaturation (*Dazyńkiewicz et al., 1977c*) and (*Dazyńkiewicz et al., 1977d*).

Even though those methods are of special value for analysis of the cell cycle-specific effects of antitumor drugs they are characterized by the following:

- 1) It is difficult to assess the importance of the observed differences in DNA stability to denaturation (*Dazyńkiewicz et al., 1987*).
- 2) The phenomenon is of practical value only when it is used in conjunction with flow cytometry to identify the various cell types of subpopulations of cells of different metabolic or kinetic properties. However, the problems of cell loss, induced by chromatin and DNA degradation during preparation and clumping of cell nuclei during fluorometric

measurements, which are usually accompanied by a high error and uncertainty, reduce this ability.

3) The previous sources of error, besides the high background damage induced by chromatin and DNA degradation during preparation and acid / heat treatment of nuclei in suspension, reduce the ability and potential of this method for measuring the effects of DNA damaging agents on cells, at different stages of the cell cycle.

4) Local topological stresses on the DNA helix in chromatin (that could occur at the interphase between eu- and heterchromatic regions) conferring increased DNA sensitivity to S1-nuclease may be involved in the regulation of gene activity. However, because the phenomenon was observed, in these studies, at nonphysiological pH (2.6-3.0) of staining or at high temperatures ( $> 60^{\circ}$  C), during histone extraction, it is difficult to relate it to chromatin modulation in vivo, which represents one of the main disadvantages and back draws of these methods, which we aimed to overcome in this study.

#### 1. 2.2.2) *FCM-methods based on different light scatter properties.*

Depending on the orientation of cell nuclei and the direction of the exciting laser beam during the fluorescence and scattering measurements, these methods can be classified into four classes: 1) Methods based on the forward light scatter; 2) methods based on the light scatter in the  $90^{\circ}$  direction; 3) methods based on the perpendicular light scatter; 4) methods based on side scatter measurements.

By means of forward light scatter-cytofluorometry, *Larsen et al.*, (1986), could discriminate mitotic cells from G1, S and G2 cells by analysis of a nuclear suspension prepared with nonionic detergents, fixed with formaldehyde and stained with mithramycin. Mitotic nuclei showed 20-40 % increased mithramycin fluorescence, 30-60 % decreased forward light scatter, in comparison to G2-nuclei, indicating a higher degree of chromatin condensation in mitotic cells, as compared to G2-cells.

In 1988, *Zucker et al.*, could discriminate M-phase from G2-phase cells, by means of  $90^{\circ}$  light scatter versus PI-fluorescence cytometric analysis of nuclei obtained in Pollack's buffer. M-phase nuclei showed a lower PI-fluorescence and  $90^{\circ}$  light scatter than G2-phase nuclei, reflecting a higher chromatin condensation in the M-phase than G2-phase of cell cycle.

By means of perpendicular light scatter and EB-fluorescence measurements, *Cocco et al.*, (1988), could monitor and follow the alterations in chromatin condensation in isolated nuclei induced by phosphatidylserine (PS) or by (low pH) buffer-treatment. An increase in perpendicular light scatter and less efficient EB-binding was observed, indicating chromatin decondensation induced by these treatments. These alterations in chromatin structure were attributed to histone-H1 depletion from the treated nuclei, while chromatin decondensation without displacement of histone H1 is characterized only by an increase in perpendicular light scatter.

In 1989, *Giaretti et al.*, have developed a new technique, which allowed identification of additional compartments in the cell cycle and estimation of the degree of chromatin condensation at different stages of the cell cycle, by simultaneous measurements of light scattering and the cellular DNA content in propidium iodide (PI)-stained nucle1. Since, light scattering is correlated with chromatin condensation, as judged by microscopic evaluation of

cells sorted on the basis of light scatter. These results indicated a higher condensation of chromatin in mitotic and G1A cells than G2 and G1B cells, respectively.

By means of simultaneous cytometric measurements of ethidium bromide fluorescence and side scatter intensity of cell nuclei. *Nüsse et al., (1990)*, have identified several sub-compartments for cells having different chromatin structure. Metaphase cells and very early G1-phase cells (G1A1) with low side scatter intensities were discriminated from interphase cells with high side scatter intensities. The reason for this difference in light scatter intensities was attributed to the higher degree of chromatin condensation in early-G1 and M-cells than in interphase cells. The G1A-phase could be further subdivided into two sub-compartments; one with very low side scatter intensity (G1A1), attributed to a high degree of chromatin condensation in G1A-cells and other with an intermediate light scatter (G1A2), indicating a lower DNA condensation in cells during this stage of cell cycle. Additionally, the M-cells having a highly condensed chromatin could be identified with a relatively high resolution from G2-phase cells, although cells with side scatter intensities between those of G2- and M-phase cells were always found in the distributions. The disadvantage of this technique however is that cell clumping during a fluorometric measurement and loss of the suspended nuclei induced by chromatin shearing and DNA degradation can occur during preparation, which leads to errors and uncertainties in the estimation of these additional sub-compartments of the cell cycle (*Nüsse et al., 1990*).

In general, the flow cytometry assay (FMC) is the most rapid method (in terms of the data acquisition). Recently, this assay has been developed for measuring the alterations in DNA supercoiling in individual cells induced by ionizing radiation (*Milner et al., 1987*). Also, this technique has been used to demonstrate alterations in chromatin structure that correlate with radiosensitivity in several human tumor cell lines (*Vaughan et al., 1991, 1992*).

The main advantage of the FCM method is the ability to obtain sufficiently large data sets to investigate the heterogeneity of radiation damage and its repair. However, this method has several back draws and disadvantages :

- 1) The method is not well suited to investigating the supercoiling changes induced by progressively higher doses and PI-concentration.
- 2) The relationship of particle size to light scatter is not completely understood (e.g., the magnitude of scatter seems to be influenced by internal structure as well).
- 3) Occurrence of cell clumping, DNA degradation and the nucleoid disintegration during preparation and treatment of nuclei in suspensions, with the consequent presence of debris and a broadening of the DNA histogram.

### 1.3) Methods used for measuring DNA-damage in individual cells

Over the last 25 years, several methods have been developed to measure DNA strand breaks produced in individual cells. In 1978, *Rydberg and Johanson* described a method of single cell analysis based on differential lysis of irradiated cells in alkali. Later this technique was adopted for flow cytometry by first encapsulating cells in agarose beads before irradiation and alkaline lysis (*Rydberg, 1984*). The observation that treatment of cells with 2 M NaCl and anionic detergents produced 'nucleoids' composed of 50-100 kb loops of DNA attached to a

proteinaceous network (Cook and Brazell, 1978) led to the development of the halo assay (Roti Roti and Wright, 1987). In the halo assay, DNA strand breaks caused relaxation of supercoiled DNA and allowed expansion of the halo of DNA loops attached to the nuclear matrix proteins of individual cells.

In 1984, Östling and Johanson developed a method based on electrophoresis of cells embedded and lysed in agarose on a microscope slide. Lysis and electrophoresis were performed at pH 9.5, which means that no separation of DNA strands occurred. After electrophoresis of irradiated cells, the DNA, which is stained with a fluorescent dye, resembles a comet with a head and tail. With increasing dose more damaged DNA migrated out from the head. The method is quantified by measuring the relative fluorescence from tail and head of the comet.

Since its discovery in 1984, comet assay has been used in vitro and in vivo studies to assess DNA damage and repair induced by various agents in a variety of mammalian cells (Singh *et al.*, 1988, 1989, 1990, 1991, 1997; Olive *et al.*, 1990, 1992; Tice *et al.*, 1990). Its potential to measure DNA damage and its heterogeneity at the level of individual cells highlight its widespread applications in radiation biology, to evaluate single and double strand breaks, DNA base damage and crosslinks, detection of radioresistant hypoxic cells in solid tumors, of apoptotic cells and rejoining of DNA strand breaks. This assay has been used extensively in other applications like chromatin structure research, effects of UV, ultrasound and electromagnetic frequency radiation, biomonitoring of some cell types from human populations for susceptibility to DNA damage, genetic toxicology and analysis of irradiated food. These applications of comet assay have been reviewed extensively (Mckelvey-Martin *et al.*, 1993; Fairbairn *et al.*, 1995; Olive, 1999).

The clear advantage of the comet method over other techniques that measure DNA-damage is its ability to measure heterogeneities within complex populations. Electrophoresis pulls damaged DNA away from the nucleoid towards the anode. This allowed greater sensitivity for detecting DNA-damage and resolution of sub-populations of cells that showed different amounts of damage (Östling and Johanson, 1987). One disadvantage of this method is the sophisticated method used for estimating or evaluating DNA-damage, based on measuring the fluorescence at different distances (50, 75 and 100  $\mu\text{m}$ ) from the comet head but not the total fluorescence in the tail region. This method makes it unreliable for measuring the whole DNA-damage in individual cells

More recently, in 1990, Olive *et al.*, have improved this method by supplying it with an image analysis system to define appropriate features of the comet as a measure of DNA damage in single cells. The assay was also optimized for lysing solution, lysing time, electrophoresis time. However, this method has several disadvantages : 1) It used alkaline conditions for lysing the nuclei, while they are electrophoresed under the neutral conditions to measure DNA damage in individual cells. Therefore, the kind of DNA damage cannot be defined ; 2) Lysing of cells under alkaline conditions, with a consequent conversion of a considerable fraction of DNA to single stranded molecules, make it inapplicable for measuring the actual amounts of DSBs in individual cells. Furthermore, electrophoresis of alkaline lysed cells under neutral conditions leads to renaturing and tangling of DNA and to conversion of a considerable fraction of single-stranded DNA to double-stranded DNA. Therefore, this type of comet assay is insensitive to detect all SSBs in individual cells.

#### 1.4) Analysis of the cell cycle distribution and estimation of the fraction of cells in different phases of the cell cycle.

Flow cytometry has been used for estimating the fraction of cells in different phases of the cell cycle and analysis of cell kinetics (*Crissman and Tobey, 1974; Dean and Jett, 1974; Baish et al., 1975; Tobey et al., 1988; Wagner et al., 1993*). The comet assay has the advantage over this method in that it is being applicable for measuring the SSB and DSB-DNA damage with a high sensitivity, simultaneously with the DNA content of single cells, which provides us with a possibility of using this method for measuring the fractions of cells in different phases of the cell cycle.

##### 1.4.1) Analysis of DNA histograms measured by comet assay-based cytofluorometry.

800-1100 cells (nucleoids) stained with ethidium bromide (EB), visualized by an epifluorescence microscope supplied with a solid-state video camera, and image analysis system, were analyzed both for DNA damage and DNA content (the total nuclear fluorescence), simultaneously. The cells were sorted according to the DNA-content into 20 channels, using the total comet fluorescence as a measuring parameter, to yield a distribution of DNA-content (DNA histograms).

The DNA histograms contain information about the fraction of cells in the different phases of cell cycle. The distribution of DNA content of individual cells measured for exponentially growing HSF2-fibroblasts is shown in (Fig.1.1b) The peak at X1 represents the G1-cells, having a diploid (2C) DNA content; the peak at X3 represents the G2/M-cells, having a tetraploid (4C) DNA content. The S-cells, on the other hand, appear between the two peaks according to their intermediate DNA-content.

A quantitative determination of the fraction of cells in different phases is complicated by the overlapping of S-phase cells with G1 and G2-cells. To get quantitative results, under these distribution-conditions, a mathematical analysis of comet DNA fluorescence data is required. For this purpose, we have developed the mathematical model reported by (*Dean et al., 1974*) which normally used for analysis DNA histograms obtained by the flow cytometry, to be applicable for analysis of DNA histograms measured by the neutral comet assay.

In the following computer-based mathematical technique for calculating the fraction of cells in the G1, S and G2/M phases of cell cycle, from comet fluorescence spectra of DNA histograms will be presented.

##### 1.4.2) Mathematical model for analysis of DNA-histograms measured by comet assay-based cytofluorometry.

As mentioned previously, the DNA distribution showed three peaks, the first one for G1-cells, having a diploid (2C) DNA content, the second for G2/M-cells, which have a tetraploid (4C) DNA content, and the third for S-cells, which have DNA-contents between 2C and 4C. If the staining procedure was perfectly uniform and the cells were measured in a system that introduced no instrumental dispersion (broadening due to electronic noise, light scattering, etc.), the distribution of the cells in (Fig 1.1b) would appear, as shown in (Fig 1.1a).

In real experiments, there are a couple of error sources ( staining efficiency, instrumental, optical and electronic errors ), which lead to deviations in the experimental values. Thus, even

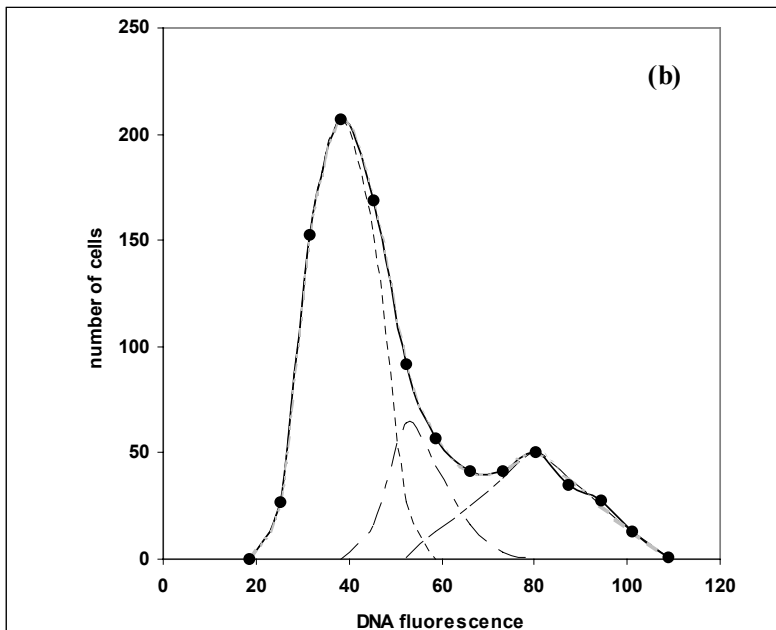
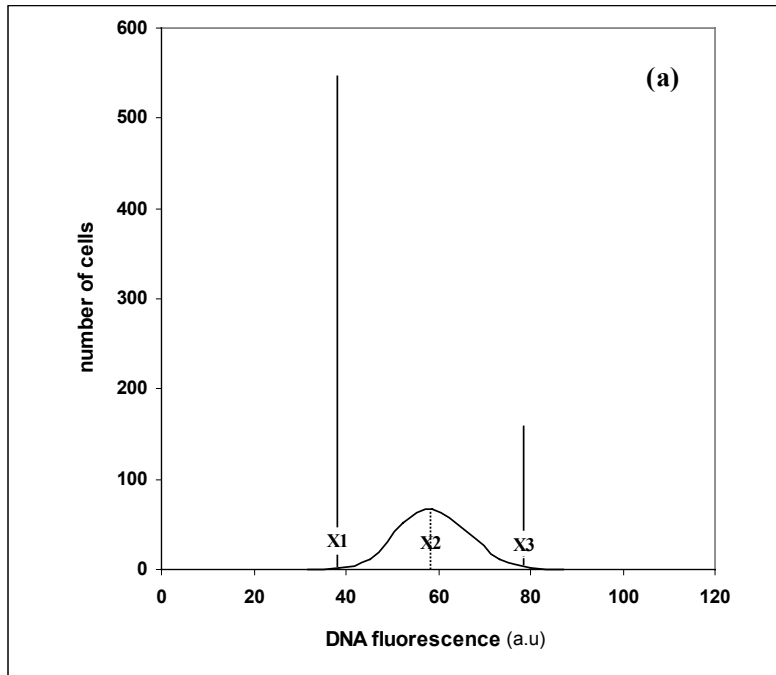


**Fig (1.1) DNA- histogram of exponentially growing HSD2 fibroblasts, under the ideal conditions and that measured experimentally measured by comet assay-based cytofluorometry**

X1 , X2 and X3 represent the mean (mode) values of the nuclear fluorescence of cells in G1 , S and G2/M phases, respectively.

The solid line shown in (Fig 1.1 b) represents the total fit function yielding the minimum deviation from the experimental points (solid circles) , obtained by the method of non-linear least squares.



for homogeneous cell populations G1 and G2/M-cells yield more or less broad distributions for the measured DNA-content (Fig 1.1b). In most of the DNA histograms, G1-phase distribution overlaps the beginning of S-phase and G2-phase distribution overlaps S-phase, at the late stages of replication. As a result of this overlapping, the peaks of G1 and G2 are no longer at X1 and X3. The difference between (Fig 1.1a) and (Fig 1.1b) is due to the broadening effects mentioned above. If the broadening is random from cell to cell, then the G1, S and G2/M cell populations could be described by normal distributions.

Considering the types of error, which lead to deviations of the experimental values from the real DNA-content, we can assume that the DNA fluorescence  $F_i$  of G1, S and G2/M cells is normally distributed ( $F_1=G1$ ,  $F_2=S$ ,  $F_3=G2/M$ ):

$$F_i(x) = \frac{A_i}{\sigma_i \cdot \sqrt{2\pi}} \cdot \exp \left[ -\frac{1}{2} \cdot \frac{\left( x - \bar{x}_i \right)^2}{(\sigma_i)^2} \right] \quad \text{----- (a)}$$

Where ( $A_i$ ) is the number of cells in a certain phase (G1), (S) or (G2/M),  $\bar{x}_i$  is the mean value of the corresponding fluorescence and ( $\sigma_i$ ) is the standard deviation.

The distribution of the fluorescence of all cells,  $Y_f(x)$  is the sum DNA fluorescence  $F_i(x)$

$$\therefore Y_f(x) = \sum_1^3 F_i(x) \quad \text{----- (b)}$$

The broken line shown in (1.1b) is the result of fitting the data (open circles) with the normal fit function,  $Y_f$ ; equation (b).

#### 1.4.3) Software computer program for analysis of DNA- histograms and estimating the fraction of cells in different phases of the cell cycle.

A software program, written by the language of advanced DBASE (IV), was used for analysis of DNA-histograms, based on the mathematical model described in Section (1.2.2). The results of this computer-based mathematical analysis will be shown in Section (2.1.1)

#### 1.5) Biophysical model for analysis of the degree of condensation and relative size of DNA in individual cells, at various stages of the cell cycle.

The ability of the developed technique to define compartments and sub-compartments for cells in different phases and sub-phases of cell cycle provided the possibility for developing a biophysical model for analysis of the relative condensation and relative molecular size of DNA in individual nucleoids, at different phases, by using various denistometrical and geometrical comet parameters. This in turn allowed the study of the effects of ionizing radiation on these parameters at the level of single cell, which will be discussed later in Section (2.1.2).

In this study the available geometrical and denistometrical parameters provided by the image software program of comet assay were used to develop the following model for analysis of

relative condensation and relative size of DNA in single cells, at various stages of the cell cycle.

### 1.5.1) *Relative DNA condensation.*

Relative condensation ( $RC$ ) in cell cycle stage ( $x$ ) i.e.  $x = G1$ , early-S, G2/M is given in the following equation:

$$RC(x) = DI \cdot \frac{F(G_0)}{F(x)} \cdot \frac{FD(x)}{FD(G_0)} = DI \cdot \frac{A(G_0)}{A(x)} \quad \text{----- (1)}$$

$$DI = 1.0 \text{ for } x = G1; DI = 1.23 \text{ for mid S and } DI = 2.0 \text{ for } x = G2$$

where  $F$  is the comet fluorescence of a certain cell stage,  $FD$  is the fluorescence density defined as  $F/A$  with  $A$  as comet area.

The relative size ( $RS$ ), a measure for the actual degree of DNA decondensation, could be estimated using the following equation:

$$RS = \frac{1}{RC(x)} \quad \text{----- (2)}$$

$\therefore RC(x)$  could be derived as follows:

$$C(x) = \frac{m(x)}{A(x)} \quad \text{----- (3)}$$

where  $C$  is the degree of nuclear DNA condensation,  $m$  is the DNA mass and  $A$  is the nuclear area.

$$m(x) = \frac{F(x)}{B(x)} \quad \text{----- (4)}$$

where  $B$  is the proportionality constant which depends on the EB-binding capacity i.e. number of EB-binding sites available in the nuclear DNA which depends on the DNA conformation.

From (3) and(4)

$$C(X) = \frac{1}{B(x)} \cdot \frac{F(x)}{A(x)} \quad \text{----- (5)}$$

$$FD(x) = \frac{F(x)}{A(x)} \quad \text{----- (6)}$$

$$C(x) = \frac{1}{B(x)} \cdot FD(x) \quad \text{----- (7)}$$

$$B(x) = \frac{F(x)}{DI \cdot m(Go)} \quad \text{----- (8)}$$

From equations 7 & 8  $RC(x)$  would then be equal to:

$$RC(x) = \frac{C(x)}{C(Go)} = \frac{DI \cdot m(Go) \cdot FD(x) \cdot F(Go)}{F(x) \cdot m(Go) \cdot FD(Go)}$$

$$\therefore RC(x) = DI \frac{F(Go)}{F(x)} \cdot \frac{FD(X)}{FD(Go)}$$

The molecular size  $MS$  is the inverse of the condensation.

$\therefore$  the relative DNA size is the inverse of  $RC(x)$

consequently ,

$$RS(x) = \frac{1}{RC(x)}$$

\*\*\*\*\*

## ***MATERIALS AND METHODS***

## **Materials and Methods**

### **2.1) Cell culture.**

Confluent human skin dermal fibroblasts (strains HSD1 and HSD2), passage-6, were prepared by cultivating cells at a cell density of 10 cells in minimal essential medium, containing 10% fetal calf serum (Gibco BRL). The cells were maintained in exponential growth by exchanging the medium 3 times weekly. After 7 days the cells reached the confluence. The cells were used for the experiments at the end of the eighth day.

For exponentially growing cultures, human skin dermal fibroblasts, strain HSD2, passage 7, were grown as monolayers in minimal essential medium (MEM) containing 10% fetal calf serum (Gibco BRL) and antibiotics in 80 ml culture flasks, at a cell density 10 cells. The cells were maintained in exponential growth by exchanging the medium 3 times weekly. The cells were used for the experiments after 5 days from cultivation. All incubations were at 37°C in a humidified incubator, in an atmosphere of 5% CO<sub>2</sub> and 95% air. Cells were counted by using a coulter counter (Coulter electronics LTD, Luton, BEDS, England).

### **2.2) Cell preparation.**

Cells were prepared by trypsinizing cultures using Ca/Mg-free 0.05% trypsin/0.02% EDTA solution (Seromed/ Biochem KG), for 3 minutes, at 37°C. After trypsinization, 5 ml of Ca/Mg free phosphate buffered saline (pH 7.3), pre-incubated at 37°C, was added. The number of cells in the suspension was counted by using a coulter counter. The cell suspension was centrifuged at 1500 rpm in Eppendorf tubes for 10 minutes. After centrifugation, the supernatant was removed and the cell pellet was used for the experiments.

### **2.3) Microgel preparation.**

Deckin's frosted slides were pretreated by pipetting 100 µl of 0.5% PBS-solution of normal melting point agarose (Sigma), pre-incubated at 40°C for 30 min. The agarose solution pipetted on the frosted slide was then covered with a 24x60 mm cover slip and allowed to solidify in a metal tray on ice. After 2 minutes, the cover slip was removed and the agarose layer was removed by the edge of a cover slip. The pretreated slides were covered by a second layer of 0.5% normal point agarose, which was allowed to gel on ice for 3 min and then to dry by incubation at 37°C in an airflow system. This dried agarose layer provides firm attachment for the subsequent layers.

Exponentially growing human skin dermal fibroblasts (strain HSD2) and confluent fibroblasts of the same strain were analyzed for the cell fraction in different phases of cell cycle. Cells were suspended in 0.5 ml of Ca/Mg-free PBS solution of 0.75% low melting agarose (Sigma), pre-incubated at 37°C for 30 min. 60 µl of this cell suspension, containing about 10,000 cells were embedded on the surface of the frosted slide and then covered with 24x50 mm cover slip and then allowed to solidify on ice for 4 min. The cover slip was removed carefully and the microgel was covered by 75 µl of 0.75% low melting point agarose and then covered with a 24\*50 mm cover slip. The slides were cooled in a steel tray on ice for 4 min. Cover glasses were then removed carefully and the slides containing the microgel were used for the experiments.

#### **2.4) Fraction of cells in different phases of the cell cycle, measured by comet assay-based cytofluorometry.**

The fraction of cells in G1, S and G2/M phases were measured for exponentially growing human skin fibroblasts (strain HSD2) and confluent fibroblasts (strains HSD1 And HSD2), by using the following method:

##### **2.4.1) Cell lysis and chemical treatment**

The frosted slides containing the microgel of the cell-agarose mixture were maintained for an hour in a freshly prepared lysing solution (3.5 M, 1% sodium N-lauroyl sarcosinate, 100 mM disodium EDTA, 10 mM Tris base, pH 8.3 and 1% Triton-X100) at 4 C. All chemicals were purchased from Merck company except disodium EDTA from Serva. After an hour of lysis, microgels were first treated with ribonuclease (RNase), (Boehringer 109134 ,10 µg per ml of the lysing solution but without Triton-X-100), at 37°C for 2 h and then treated with DNase-free proteinase , Biotechnology grade, amresco , 0.75 mg per ml of the lysing solution but without Triton-X-100, at 37°C for 1.5 h. Following RNase and proteinase K digestion, slides with microgels were treated with 0.15 M NaOH (Merck) for 1 min and then neutralized overnight in 0.4 M Tris (Paesel + Lorei). After neutralization, microgels were then rinsed in distilled water for 1 min and then dehydrated in ethanol for 15 min and dried at the room temperature. One slide at a time was stained with 100 µl of ethidium bromide (10 mg/1 ml) in distilled water.

##### **2.4.2) Microscopic image analysis**

800 to 1000 stained nucleoids on slide were viewed microscopically captured and analyzed. Examination of the slides was performed with an epifluorescence microscope attached to an intensified video camera and equipped with an excitation filter of 515-560 nm from 100-W mercury lamp and a barrier filter of 590 nm. The individual nucleoids were viewed, at a magnification power of 40. The cells were selected randomly avoiding areas near the edges of slides. The captured nucleoid images were analyzed by a software computer program, which digitizes and analyzes approximately 450 nucleoids per 1 h. Several features related to DNA structure and nuclear morphology, for example the total fluorescence and comet area were measured for each nucleoid. The total intensity of EB fluorescence was used as an indication of the DNA content per nucleoid.

##### **2.4.3) Analysis of DNA histograms.**

800 to 1000 nucleoids were sorted according to the DNA content into 20 sorting channels, covering the range of DNA content (0-180 au). The DNA histograms obtained were analyzed by means of a computer-based mathematical model, based on the assumption of the Gaussian normal distribution. A computer program, written in the advanced Dbase IV language, was used for fitting the DNA histograms with two different Gaussian normal functions, representing the cells in G1 and G2/M phases of cell cycle, by using the method of non-linear least squares (*Mason et al., 1989*). By taking the fluorescence values of the half width values of the Gaussian distributions, the sorting windows for G0 and G2/M cells can be defined. By the subtraction of the G1 and G2/M fluorescence from the total fluorescence distribution the S- distribution can be obtained. The fitting parameters A1, A2 and A3, which represent the fraction of cells in G1, S and G2/M phases, were determined for each histogram.

### **2.5) The degree of condensation and relative molecular size of DNA in individual cells, measured by the comet assay-based cytofluorometry.**

The simultaneous measurement of various denistometrical and geometrical comet parameters related to the nuclear morphology, besides the comet features related to DNA damage, allow estimation of the degree of DNA condensation in individual nucleoids. Based on the derived parameter of the total fluorescence and the comet area (i.e. the fluorescence density FD, the potential of the last two parameters), the degree of DNA condensation in individual cells in different phases of the cell cycle was estimated by using the biophysical model described in Section (1.5.1)

The relative size (RS) of DNA, which represents the degree of DNA dispersion, can be calculated using the equation in chapter 1.2.

### **2.6) Effects of X-ray on DNA structure in individual cells at different stages of the cell cycle.**

To study the effects of X-ray on the DNA structure, we have measured the tendency of DNA migration under the influence of electric field, the degree of condensation (RC) and relative size (RS) and the total fluorescence of DNA in individual cells, at different stages of cell cycle, before and after irradiation with 5, 10, 15 and 20 Gy of X-ray. Moreover, the fraction of damaged DNA and number of DSBs in mammalian cells at different phases were measured basing on the fluorescence decrement (FD) induced by ionizing radiation.

#### **2.6.1) X-ray irradiation of human skin fibroblasts.**

Cells embedded in microgels on frosted slides, prepared by the method described in (IV.3), were irradiated in metal tray on ice, using a 200-kvp X-ray unit, at a dose rate of 7.4 Gy/min, at different doses 5,10, 15 and 20 Gy, respectively. To measure the sensitivity of the method, cells embedded in microgels on frosted slides were irradiated on ice with low doses (1, 2, 3 and 4 Gy) of X-rays. Unirradiated cells were used as a control for the treated samples. The control and irradiated cells were then subjected to single cells gel electrophoresis.

#### **2.6.2) DNA damage in individual cells, measured by single cell gel electrophoresis (neutral comet assay).**

DNA damage in individual cells, basing on the relaxation of broken DNA loops under the influence of the electric field, can be measured by using the following method.

##### **2.6.2.1) Neutral lysis and microgel electrophoresis.**

The frosted slides containing the microgel of the cell-agarose mixture, prepared by the method described in (IV.3) were maintained for an hour in a freshly prepared lysing solution (3.5 M, 1% sodium N-lauroyl sarcosinate, 100 mM disodium EDTA, 10 mM Tris base, pH 8.3 and 1% Triton-X100) at 4 C. All chemicals were purchased from Merck except disodium EDTA from Serva. After an hour of lysis, microgels were first treated with ribonuclease (RNase) , (Boehringer 109134, 10 µg per ml of the lysing solution but without Triton-X-100), at 37°C for 2 h and then treated with DNase-free proteinase K, (Biotechnology grade, amresco, 0.75 mg per ml of the lysing solution but without Triton), at 37°C for 1.5 h.

Following RNase and proteinase K digestion, slides with microgels were immersed in a neutral electrophoretic buffer (50 mM Tris, 150 mM sodium acetate, pH adjusted to 8.3 by glacial acetic acid). Tris-(hydroxy methyl) aminmethane was purchased from (Paesel+ Lorei), while sodium acetate (analytical grade) was purchased from Serva.

The slides with microgels were then positioned on a modified Wide Mini Sub Cell-Electrophoretic Unit, modified so that both ends of each electrode were connected to the power supply. The electrophoretic unit was then filled with 500 ml of the electrophoretic buffer. After 3 min for equalibration, slides were subjected to an electric field of 0.6 V/cm at 40 mA for 15 min by using LKB 2197-electrofocusing constant power supply (LKB Bromma).

After electrophoresis, slides were removed from the unit, rinsed in distilled water for 2 min and then treated with 0.15 M NaOH (Merck) for 1 min and then neutralized overnight in 0.4 M Tris (pH 7.4). Microgels were then rinsed in distilled water for 1 min and then dehydrated in ethanol for 15 min and dried at room temperature. One slide at a time was stained with 100  $\mu$ l of EB (10 mg/1 ml) in distilled water.

#### 2.6.2.2) Comet analysis and visualization.

Examination of the slides was performed with an epifluorescence microscope, attached to an intensified video camera and equipped with an excitation filter of 515-560 nm from a 100-W mercury lamp and a barrier filter of 590 nm. The individual comets were viewed, at a magnification power of 40. 800 to 1100 comets were examined per slide. The cells were selected randomly avoiding areas near the edges of slides. The captured comet images were analyzed by a software computer program, which digitizes and analyzes approximately 350 comets per 1 h. Several features of the comet related to the DNA damage were calculated for each comet image: The tail length, which represents the size of broken DNA loops relaxed into the tail and measured as the distance from the mean of the head to the mean of the tail intensity distributions; the tail intensity, representing the number of broken loops relaxed into the tail and measured as the percentage value of the integrated fluorescence in the region from the mean head to the mean of the tail intensity distributions (relative to the total comet fluorescence). The total fluorescence was used as an indication of the DNA content per nucleoid. The tail moment was calculated as the product of the fraction of the total comet fluorescence in the tail and the tail length

#### 2.6.3) Fraction of damaged DNA in human skin fibroblasts at different stages of the cell cycle.

Partial alkaline unwinding of nuclear DNA, after neutral electrophoresis leads to conversion of double stranded DNA relaxed via DSB-induction to single stranded (damaged) DNA of a lower fluorescence. The fluorescence decrement induced by ionizing radiation is attributed mainly to extensive breakage of DNA induced by ionizing radiation and conversion of broken DNA to single stranded denatured DNA during lysis and alkaline treatment (*Olive et al., 1994*).

The principle of the developed method based on the differential staining of double versus single stranded (denatured) DNA with EB in cells depleted of RNA. The differential staining of double versus single stranded DNA occurs because EB intercalates into double stranded DNA and fluoresces red ( $F_{590}$ ), whereas the dye stacking on denatured (single stranded) sections of DNA results in metachromatic red fluorescence ( $F > 600$ ). Conversion of double



stranded DNA to single stranded damaged DNA leads to a decrease in the total fluorescence ( $F_{590}$ ) with an extent proportional to the degree of DNA damage. Since the major quantity of single stranded denatured DNA is induced at the SSB-sites of the broken loops made accessible to the alkaline action via DSB-induction and the consequent relaxation during neutral electrophoresis, the fluorescence decrement induced by X-rays observed under the suggested conditions of neutral lysis and electrophoresis is caused mainly by DSB-induction. Therefore, the percentage of DSB-damaged DNA can be calculated as the percentage decrement of the total fluorescence induced by ionizing radiation, by using the following equation:

$$\% \text{ damaged DNA} = \frac{F - F_o}{F_o} \cdot 100 = \frac{AF}{F_o} \quad \text{-----(1)}$$

$F$  is the total fluorescence of irradiated nucleoids,  $F_o$  is the total fluorescence of unirradiated nucleoids after electrophoresis (the intercept value of the fluorescence-dose response curves, Fig 3.18)

#### 2.6.4) DSB- induction in human skin fibroblasts at different stages of the cell cycle.

The induction rates of DNA double strand breaks in human skin fibroblasts was estimated by calibrating the rate values of DNA damage, using the rate of DSB-induction in G1-phase cells (21 DSBs/Gy.cell) (*Iliakis et al., 1991b*), as a reference value. The number of DNA double strand breaks induced by X-ray in human skin fibroblasts, at different stages of the cell cycle, can be calculated by using the rate values of DSB-induction, obtained by this method.

#### 2.7) Data analysis.

The results of DNA-histograms and fraction of cells in different phases for confluent human skin fibroblasts, represent the (mean  $\pm$ SD) of 4 independent experiments, while those for exponentially growing cells the (mean  $\pm$ SD) values was calculated for three independent experiments.

For comet assay experiments, the results were obtained from two independent experiments, one experiment was performed using confluent cells, 24 h after serum stimulation and the second was performed by using exponentially growing cells. The results of each measurement represents the (mean  $\pm$ SD) of different subpopulations of 750-800 confluent cells or 1000-1100 exponentially growing cells. The significance of the difference in response between the control and irradiated cells, at different doses, was assessed by the Student's test (*Baily Norman, 1959*) by using the following equation :

$$t = \frac{X - \bar{X}_1}{\sqrt{(SE)^2 + (SE_1)^2}} \quad \text{----- (2)}$$

Where  $X$  and  $\bar{X}_1$  are the mean values of the control and irradiated groups, respectively. The difference is considered significant when  $P < 0.05$  and highly significant when  $P < 0.02$ , where  $P$  is the probability of observing a value of  $t$ , with a given degrees of freedom, that is greater than the values shown by the Student's distribution.

# ***RESULTS***

## **Results**

### **3.1) Mathematical analysis of comet fluorescence histograms for estimating the fraction of cells in different phases of the cell cycle.**

The distribution of DNA content of individual cells measured for confluent population of (HSD2)-fibroblasts is shown in Fig. (3.1) , while those for exponentially growing (HSD2) fibroblasts is shown in Fig. (3.2). The first peak from the left represents the G0/G1-cells (with a diploid DNA content), the second represents the S-cells with an intermediate DNA values, while the third peak represents the G2/M-cells, having a tetraploid DNA content.

The DNA histogram of the confluent cells is characterized by a high peak of G0/G1-cells, small peaks of S and G2/M-cells, while the DNA histograms of the exponentially growing cells showed a high peak of G1-cells (relatively lower than that of confluent cells). The solid line in these distributions represents the computer fit to the experimental data (the solid circles), while the broken lines are fit functions for the distributions representing G1, S and G2/M-phases, respectively. The fraction values of cells in different phases of the cell cycle, calculated by this analysis for confluent and exponentially growing populations are shown in (Tables 3.1 and 3.2), respectively.

The results obtained for exponentially growing populations show fraction values of 59.9 ( $\pm 3.2$ ), 22.4 ( $\pm 6.0$ ) and 17.5 ( $\pm 4.4$ ) % for G1, S and G2/M-cells, respectively; while for confluent cultures, the fraction of G0/G1, S and G2/M-cells are 88.5 ( $\pm 2.34$ ), 6.4 ( $\pm 2.3$ ) and 5.3 ( $\pm 1.2$ ) %, respectively. The small values of standard deviation (shown between parentheses) indicate the high reproducibility of the method. In Fig.3.3 the cell cycle distributions of stimulated confluent (Fig. 3.1) and of exponentially growing (Fig. 3.2) cells were compared. This figure shows a remarkable shift of the distribution of exponentially growing cells compared to stimulated confluent cells.

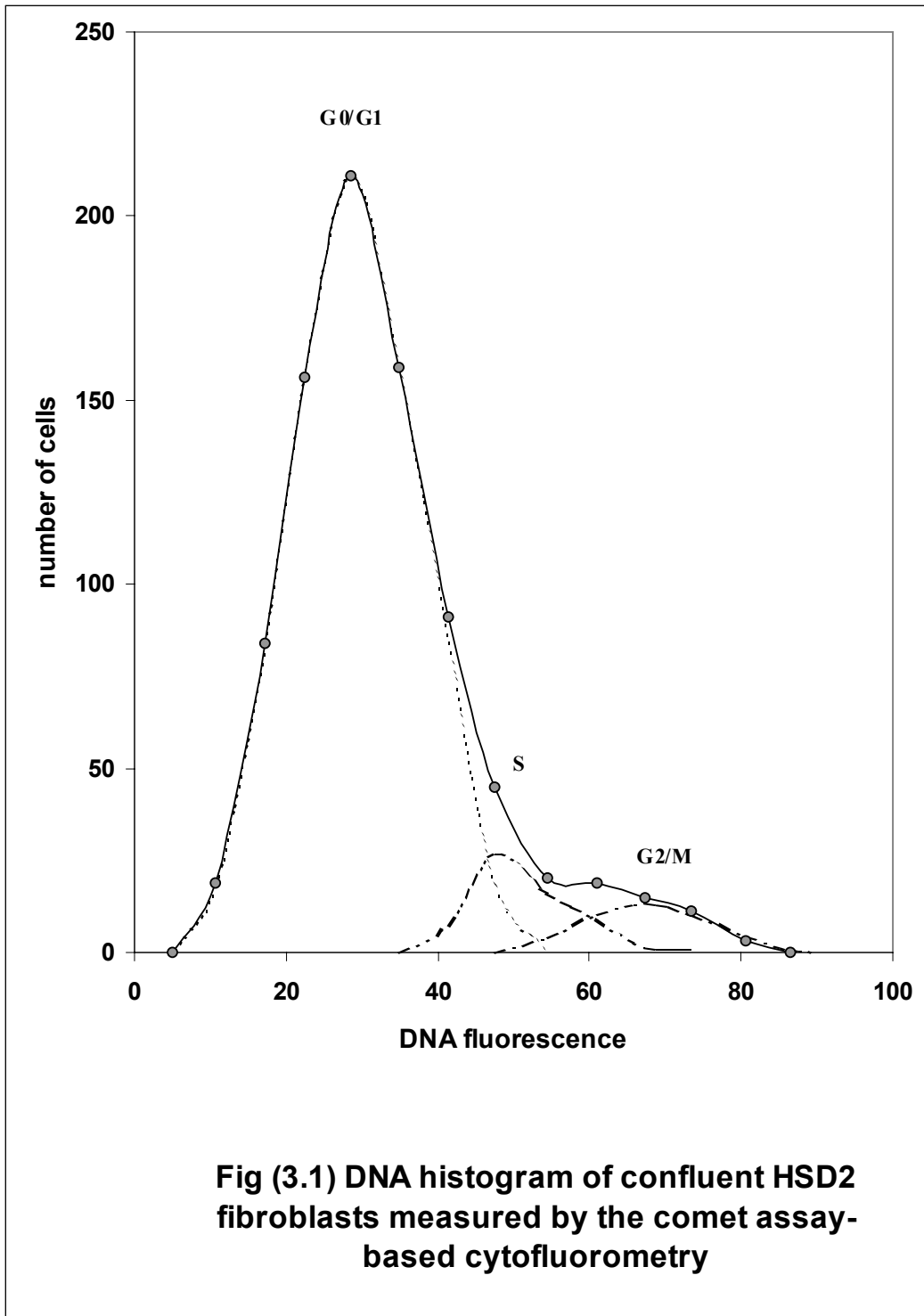
### **3.2) Densitometrical and geometrical parameters of unirradiated nucleoids, at various stages of the cell cycle.**

Table (3.3) shows the various geometrical and denistometrical comet parameters of unirradiated HSD2 nucleoids at diffrent stages of the cell cycle. A significant increase in all comet parameters is observed with transition of G0 cells to G1 and with progression through the cell cycle. Fig. (3.4) shows as an example the variation in comet area with cell cycle position. With transition of cells from G0 to G1 small increase in comet area is observed. With further progression through the cell cycle a remarkable increase in comet area is observed.

We have used the available comet parameters provided by the image software program to develop a biophysical model for analysis of the relative condensation and relative size of DNA in single cells, at different stages of the cell cycle. This model was described previously in Section (1.5).

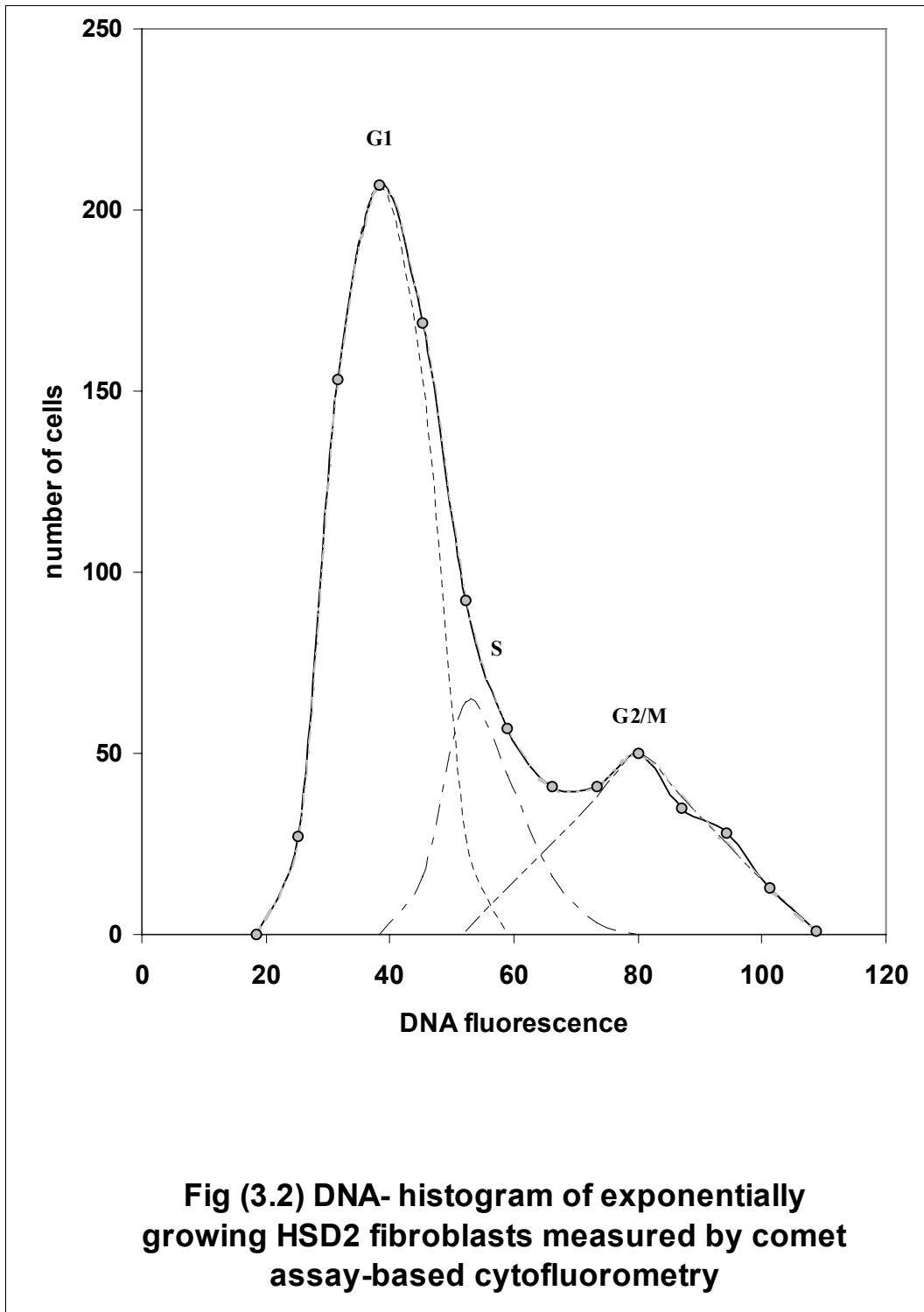
### **3.3) The degree of condensation and relative size of DNA in single cells at various stages of the cell cycle.**

The results of DNA-condensation (Table 3.4), calculated by equations 1 and 2 derived from the mathematical model given in section (1.5), showed a significant decondensation of DNA



The broken lines represent the normal fit functions of G1, S and G2/M cells, calculated by the fitting computer program, described in Section (1.1.2)

The solid line represents the total fit function yielding the minimum deviation from the experimental points (solid circles), obtained by the method of non-linear least squares.



The broken lines represent the normal fit functions of G1, S and G2/M cells, calculated by the fitting computer program, described in Section (1.1.2)

The solid line represents the total fit function yielding the minimum deviation from the experimental points (solid circles), obtained by the method of non-linear least squares.

**Table (3.1) Fractions of cells in different phases of the cell cycle for confluent human skin fibroblasts 24 h after serum stimulation measured by comet assay-based cytofluorometry.**

<i>Sample number</i>	<i>G0%</i>	<i>S%</i>	<i>G2/M%</i>
1	87.48	7.27	5.25
2	85.7	9.3	5.00
3	88.5	4.5	7.00
4	91.3	4.5	4.2
<i>Mean</i>	88.48	6.393	5.363
±	±	±	±
<i>SD</i>	2.342	2.337	1.18
±	±	±	±
SE	1.171	1.168	0.59

**Table (3.2) Fractions of cells in different phases of the cell cycle for exponentially growing human skin fibroblasts, measured by comet assay-based cytofluorometry.**

<i>Sample number</i>	<i>G1%</i>	<i>S%</i>	<i>G2/M%</i>
<b>1</b>	<b>62.00</b>	<b>15.65</b>	<b>22.32</b>
<b>2</b>	<b>56.28</b>	<b>27.16</b>	<b>16.56</b>
<b>3</b>	<b>61.58</b>	<b>24.55</b>	<b>13.63</b>
<b><i>Mean</i></b>	<b>59.953</b>	<b>22.453</b>	<b>17.503</b>
<b>±</b>	<b>±</b>	<b>±</b>	<b>±</b>
<b><i>SD</i></b>	<b>3.188</b>	<b>6.034</b>	<b>4.42</b>
<b>±</b>	<b>±</b>	<b>±</b>	<b>±</b>
<b><i>(SE)</i></b>	<b>(1.84)</b>	<b>(3.468)</b>	<b>(2.55)</b>

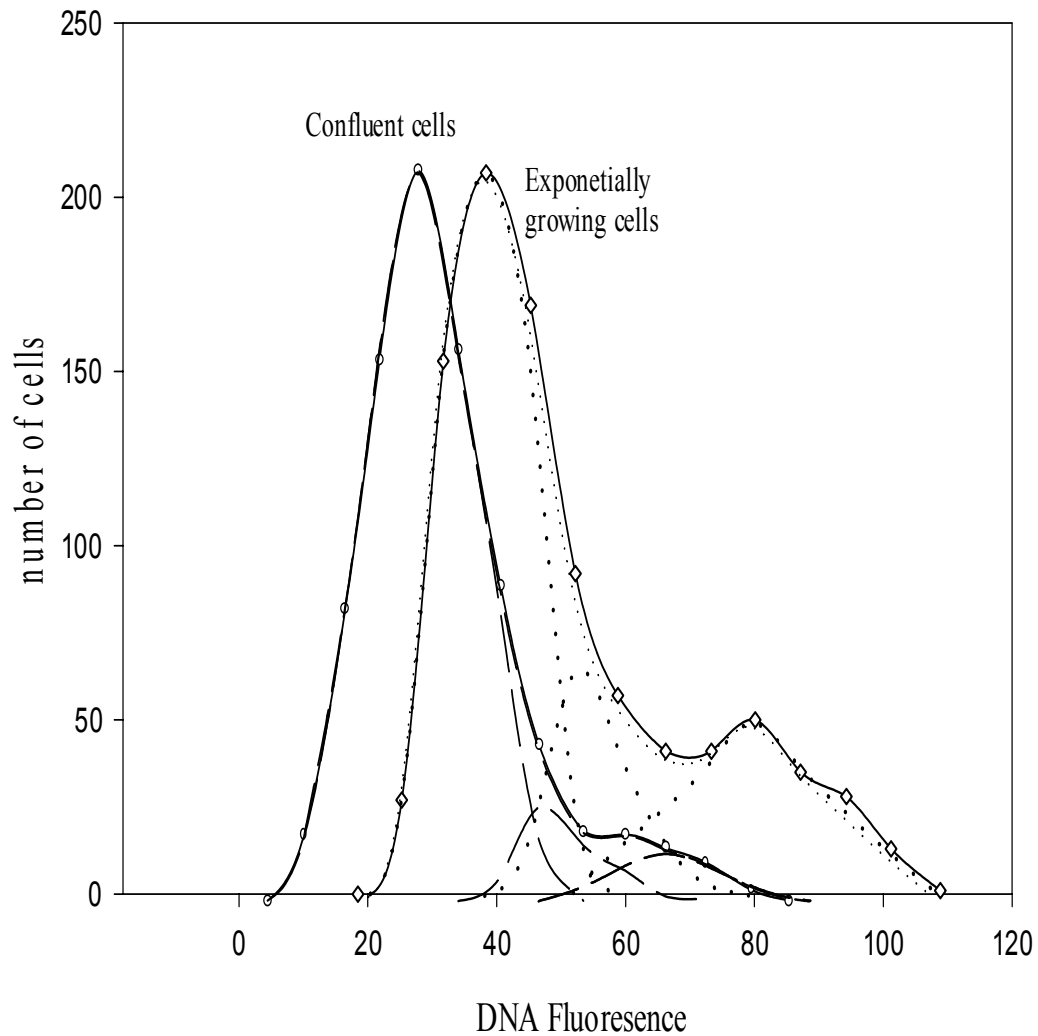


Fig (3.3) DNA- fluorescence histogram of confluent and HSD2- fibroblasts, as compared to that of exponentially growing cells

The broken lines represent the normal fit functions of G1, S and G2/M cells, calculated by the fitting computer program, described in Section (1.1.2)

The solid line represents the total fit function yielding the minimum deviation from the experimental points, obtained by the method of non-linear least squares.



**Table (3.3) Comet geometrical and denistometrical Parameters for different HSD2-fibroblasts, at different stages of the cell cycle.**

<b>Cell population</b>	<b>F</b> (a.u)	<b>A</b> ( $\mu\text{m}^2$ )	<b>F.D</b> (a.u / $\mu\text{m}^2$ )
<b>G0</b> (n=594)	<b>300456</b> $\pm$ 61860 ( $\pm$ 2540)	<b>8374.265</b> $\pm$ 1410 ( $\pm$ 57.853)	<b>36.264</b> $\pm$ 6.995 ( $\pm$ 0.287)
<b>G1</b> (n=451)	<b>333153</b> $\pm$ 44240 ( $\pm$ 2083) <i>(P &lt; 0.00005)</i>	<b>8651.469</b> $\pm$ 1153 ( $\pm$ 54.29) <i>(P &lt; 0.00005)</i>	<b>39.032</b> $\pm$ 6.73 ( $\pm$ 0.317) <i>(P &lt; 0.00005)</i>
<b>S</b> (n=40)	<b>582121</b> $\pm$ 14008 ( $\pm$ 2214,8) <i>(P &lt; 0.00005)</i>	<b>10707</b> $\pm$ 2491 ( $\pm$ 394) <i>(P &lt; 0.00005)</i>	<b>56.798</b> $\pm$ 11.19 ( $\pm$ 1.769) <i>(P &lt; 0.00005)</i>
<b>G2/M</b> (n=80)	<b>814606</b> $\pm$ 53369 ( $\pm$ 5967) <i>(P &lt; 0.00005)</i>	<b>14772</b> $\pm$ 2545 ( $\pm$ 284) <i>(P &lt; 0.00005)</i>	<b>56.986</b> $\pm$ 11.63 ( $\pm$ 1.3) <i>(P &lt; 0.00005)</i>

The values shown represent the mean  $\pm$  SD ( $\pm$ SE) of the nuclear fluorescence (F) . area (A) and the fluorescence density. F.D . (F/A) for. a .number (n) of 40- 594 cells in different phases of the cell cycle. The significance of the difference in the measured parameters between the first and other groups was assessed by the Student's t- test. The difference is considered .significant when  $P < 0.05$  and highly significant when  $p < 0.02$ .

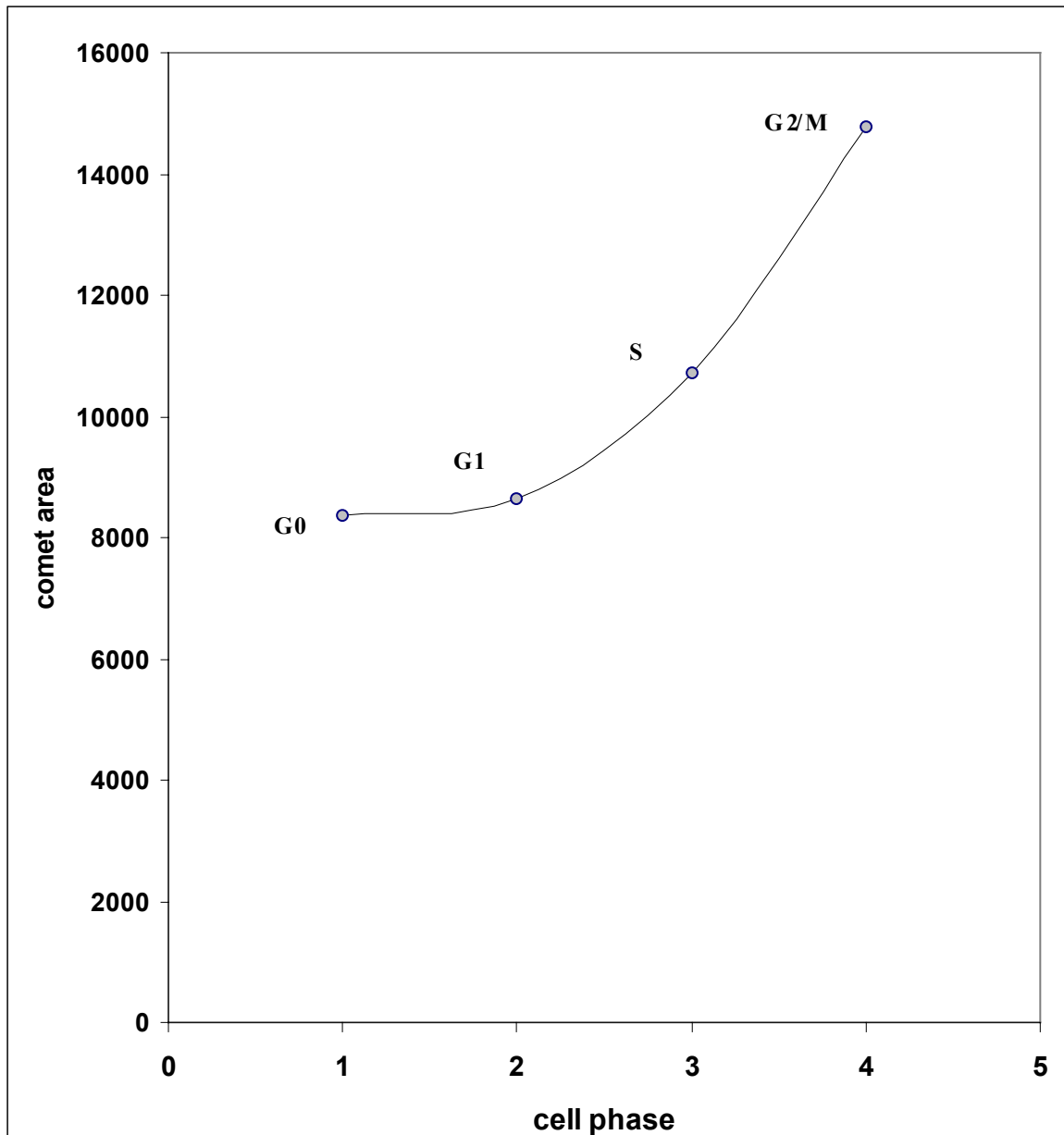


**Fig (3.4) Variation of the comet area (A) with cell cycle position for HSD2- fibroblasts , measured by the neutral comet assay-based cytofluorometry**

The points shown represent the average comet area of 40-594 nucleoids in different phases of the cell cycle obtained from 2 independent experiments , one performed on confluent cells and the other on exponentially growing cells.

**Table (3.4) Relative condensation and molecular size of DNA in HSD2-fibroblasts at different phases, measured comet assay-based cytofluorometry**

<b>Phase</b>	<b>RC</b>	<b>RS</b>
<b>G0</b> (n = 256)	<b>1.00</b>	<b>1.00</b>
<b>G1</b> (n = 451)	<b>0.986±0.143</b> (±0.007)	<b>1.014±0.138</b> (±0.0486)
<b>S</b> (n = 40)	<b>1.013±0.209</b> (±0.033)	<b>0.987±0.240</b> (±0.037)
<b>G2/M</b> (n = 80)	<b>1.174±0.243</b> (±0.027)	<b>0.852±0.152</b> (±0.098)

**The values shown represent the mean ± SD (±SE) of the relative condensation (RC) and the relative molecular size (RS) of DNA in a number (n) of 157-295 cells in different phases obtained from 3 independent experiments.**

concomitant with a significant increase in the relative size (RS), with transition of G<sub>0</sub> cells to G<sub>1</sub> followed by a remarkable recondensation and decrease in RS a further progression of cells through the cell cycle. By comparing the results of DNA-condensation obtained from this study with those of chromatin partially depleted from histones, reported by (*Darzynkiewicz et al., 1980*) (Table 3.5 and Fig. 3.5), we observe a similar course of nuclear DNA condensation through the G<sub>1</sub>-phase and recondensation through the S and G<sub>2</sub>/M-phases in both studies, confirming the succession of the suggested model to predict the various degrees of condensation of nuclear DNA, at different stages of the cell cycle.

#### **3.4) The tail length of unirradiated nucleoids at various stages of the cell cycle**

The results of tail length of unirradiated nucleoids at various stages of the cell cycle are shown in (Table 3.6 and Fig. 3.6). A significant decrease in tail length is observed with transition of G<sub>0</sub> cells to G<sub>1</sub>-phase to reach its minimum at S phase and again increase to some extent when entering the G<sub>2</sub>/M phase.

#### **3.5) The tail intensity of unirradiated nucleoids at various stages of the cell cycle**

The results of tail intensity of unirradiated nucleoids at various stages of the cell cycle are shown in (Table 3.7, Fig. 3.7). Insignificant change in tail intensity is observed with transition of cells from G<sub>0</sub> to G<sub>1</sub> phase. While a significant decrease in tail intensity is observed with transition to S phase and G<sub>2</sub>/M phases of the cell cycle. The results of bivariate analysis of tail intensity versus DNA fluorescence of exponentially growing cells show a remarkable decrease in tail intensity with transition of G<sub>1</sub> cells to S phase which increase once again with transition to G<sub>2</sub>/M phase.

#### **3.6) Effects of the electrophoretic field on the total fluorescence of unirradiated nucleoids at various stages of the cell cycle.**

Variation of the total DNA fluorescence, with the cell cycle position, for HSD2-nucleoids, before and after electrophoresis, is shown in (Table 3.8 and Fig. 3.8). As shown in (Table 3.7), a significant reduction in DNA fluorescence, after electrophoresis, is observed in HSD2-nucleoids, at various stages of the cell cycle. Figure 3.7 confirms these results and shows a remarkable decline in the nuclear fluorescence induced by electrophoresis, at all stages of the cell cycle. The extent of this reduction (-dF<sub>0</sub>) varies with the stage of cell cycle, showing a maximum reduction of the total fluorescence in the G<sub>2</sub>/M phase, as compared to a minimum reduction at the G<sub>0</sub>-phase of cell cycle.

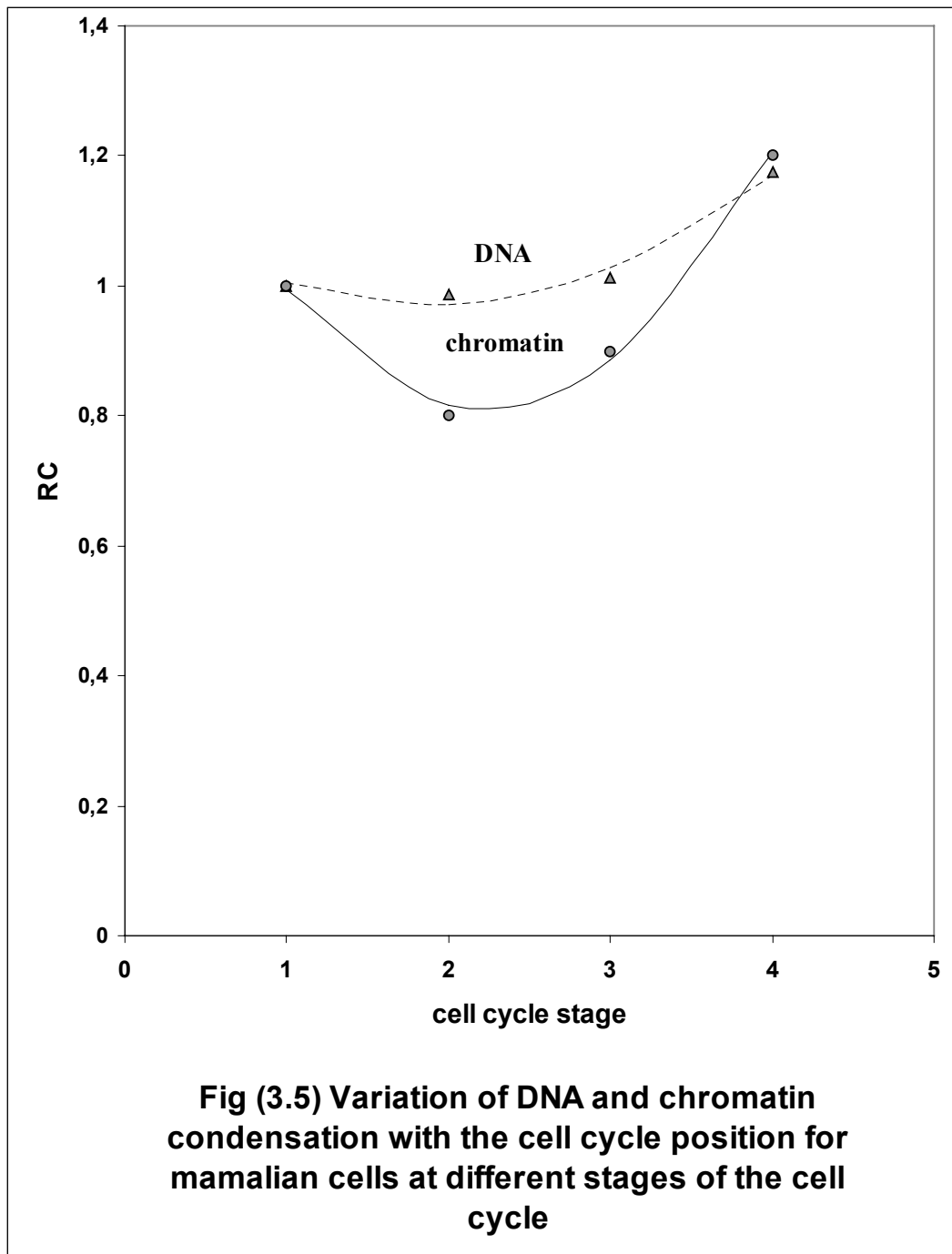
#### **3.7) Effects of ionizing radiation on the DNA-structure and nuclear morphology of HSD2-fibroblasts.**

To study the effects of ionizing radiation on the structure of the nuclear DNA, we have measured the tendency of migration, the relative condensation, the relative size and the total fluorescence of the DNA in individual cells, irradiated with different doses of X-ray. Moreover, the high efficiency of the suggested method to sort cells in different phases, allow examining the effects of ionizing radiation on the DNA in individual cells, at different stages of the cell cycle. On the other hand, the alteration in the nuclear morphology, induced by ionizing radiation, was examined, by measuring the nuclear size of individual nucleoids, at different stages of the cell cycle, before and after irradiation, by using the total area as a comet parameter.

**Table (3.5) Relative condensation of DNA and chromatin in mammalian cells, at different phases, measured by comet assay and FCM method- based cytofluorometry.**

Phase	RC	
	DNA	Chromatin
<b>G0</b> (220)	<b>1</b>	<b>1</b>
<b>G1</b> (n = 447)	<b>0.986 ± 0.137</b>	<b>0.800</b>
<b>S</b> (n = 289)	<b>1.013 ± 0.209</b>	<b>0.900</b>
<b>G2/M</b> (n = 219)	<b>1.174 ± 0.243</b>	<b>1.2</b>

The values shown for DNA represent the mean ± SD of the relative condensation (RC) of DNA in 219-447 nucleoids in different phases, obtained from 3 independent experiments of comet assay- based cytofluorometry. The values shown for chromatin represent the relative condensation of chromatin in nucleoids, partially depleted from histones, by acid treatment and subjected to AO- based flow cytofluorometry (FCM) [Darzynkiewicz, Z. et al, 1980].



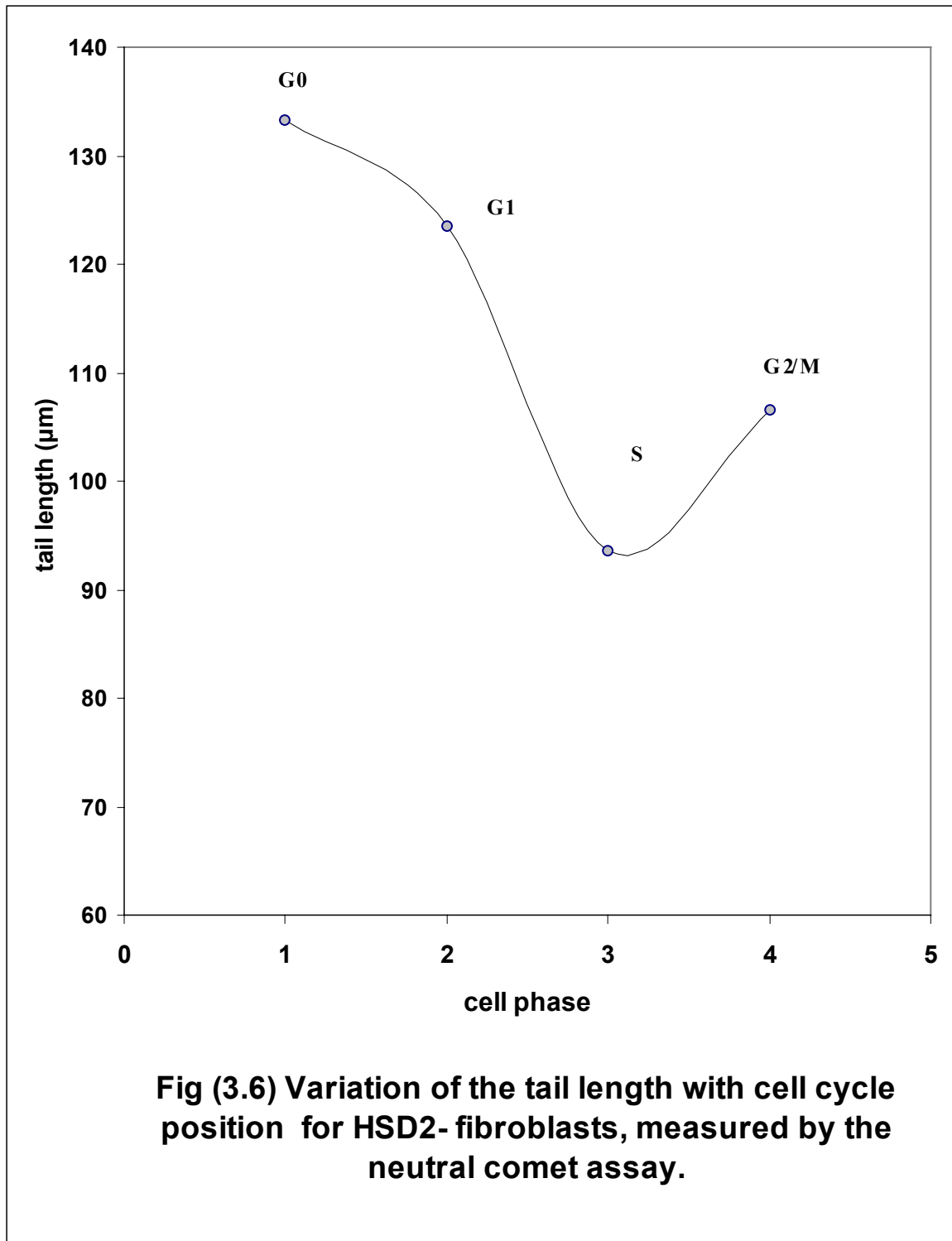
The solid triangles represent the average relative condensation (RC) of DNA in 40 to 594 nucleoids in different phases from two independent experiments. The solid circles represent the relative condensation of chromatin in nucleoids partially depleted from histones by acid treatment and subjected to AO-based cytofluorometry (*Darzynkiewicz et al. 1980*).

Curves shown represent the fit functions calculated by the linear quadratic analysis

**Table (3.6) Variation of the tail length with cell cycle position for unirradiated HSD2 - nucleoids, after neutral electrophoresis, measured by the neutral comet assay**

<b>Phase</b>	<b>Tail length (<math>\mu\text{m}</math>)</b>
<b>G0</b> (n = 506)	<b>133.305<math>\pm</math>42.142 (<math>\pm</math> 1.873)</b>
<b>G1</b> (n = 435)	<b>123.486<math>\pm</math>43.476 (<math>\pm</math> 2.084)</b>  P<0.00005
<b>S</b> (n = 79)	<b>93.589<math>\pm</math>44.834 (<math>\pm</math>5.044)</b>  P<0.00005
<b>G2/M</b> (n = 55)	<b>106.557<math>\pm</math>37.536 (<math>\pm</math>5.061)</b>  P<0.00005

The values shown represent the mean  $\pm$  SD ( $\pm$ SE) of the tail length for 55- 506 cells in different phases obtained from two independent experiments performed on nucleoids after electrophoresis, at an electric field strength (E) of a value (0.6 V/cm).



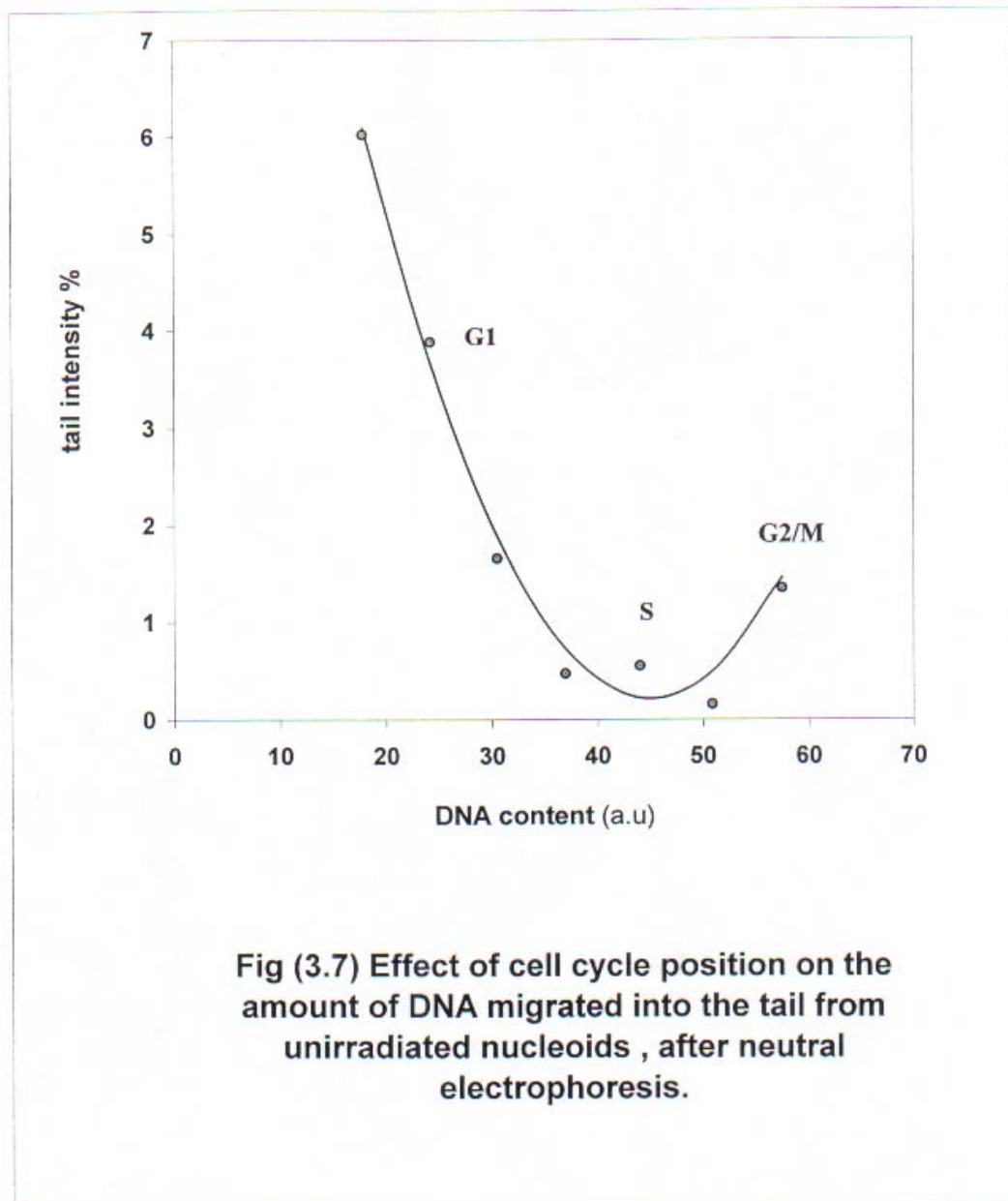
The points shown represent the average tail length of 40-594 nucleoids in different phases of the cell cycle obtained from 2 independent experiments, one performed on confluent cells and the other on exponentially growing cells.



**Table (3.7) Variation of the tail intensity with cell cycle position for unirradiated HSD2 - nucleoids, after neutral electrophoresis, measured by the neutral comet assay**

<b>Phase</b>	<b>Tail intensity %</b>
<b>G0</b> (n = 506)	<b>2.095±8.189 (±0.364)</b>
<b>G1</b> (n = 435)	<b>3.052±7.372 (± 0.353)</b>  p< 0.0005
<b>S</b> (n = 79)	<b>0.150±0.591 (±0.066)</b>  p< 0.00005
<b>G2/M</b> (n = 55)	<b>0.861±2.205 (±0.297)</b>  p< 0.0005

The values shown represent the mean  $\pm$  SD ( $\pm$ SE) of the tail intensity for 55- 506 cells in different phases obtained from two independent experiments performed on nucleoids after electrophoresis, at an electric field strength (E) of a value (0.6 V/cm).



The points shown represent the average tail intensity of 40 to 295 nucleoids in different phases , obtained from a single experiment of comet assay performed on exponentially growing cells , after electrophoresis at an electric field strength ( E ) of a value ( 0,6 v/cm )

The solid curve represent the fit function calculated by the linear quadratic analysis

**Table (3.8) Variation of the nuclear fluorescence with cell cycle position for HSD2-nucleoids, before and after electrophoresis, measured by the neutral comet assay.**

Cell cycle stage	Fluorescence (a.u)		
	0Gy, (E=0V/cm)	0Gy, (E=0.6 V/cm)	-dFo
<b>G0</b> (n = 506)	<b>300456±61860</b> (±2750)	<b>257969±63886</b> (±2840) <i>(P &lt; 0.00005)</i>	<b>42487</b>
<b>G1</b> (n = 435)	<b>333253±44240</b> (±2121)	<b>263463±47413</b> (±2273) <i>(P &lt; 0.00005)</i>	<b>69790</b>
<b>S</b> (n = 79)	<b>582121±14008</b> (±1576)	<b>505700±19872</b> (±2235) <i>(P &lt; 0.00005)</i>	<b>76421</b>
<b>G2/M</b> (n = 55)	<b>814606±53369</b> (±7196)	<b>667944±37892</b> (±5109) <i>(P &lt; 0.00005)</i>	<b>146662</b>

The values shown represent the mean± SD (±SE) of the nuclear fluorescence for 55- 506 cells in different phases, obtained from 2 independent experiments performed on nucleoids, before and after electrophoresis, at an electric field strength ( E ) of a value ( 0.6 V/cm ). dFo represents the fluorescence decrement induced by electrophoresis.

\*The difference in the nuclear fluorescence between unirradiated nucleoids before and after electrophoresis was found significant at all stages of the cell cycle, at the level of (P < 0.00005).

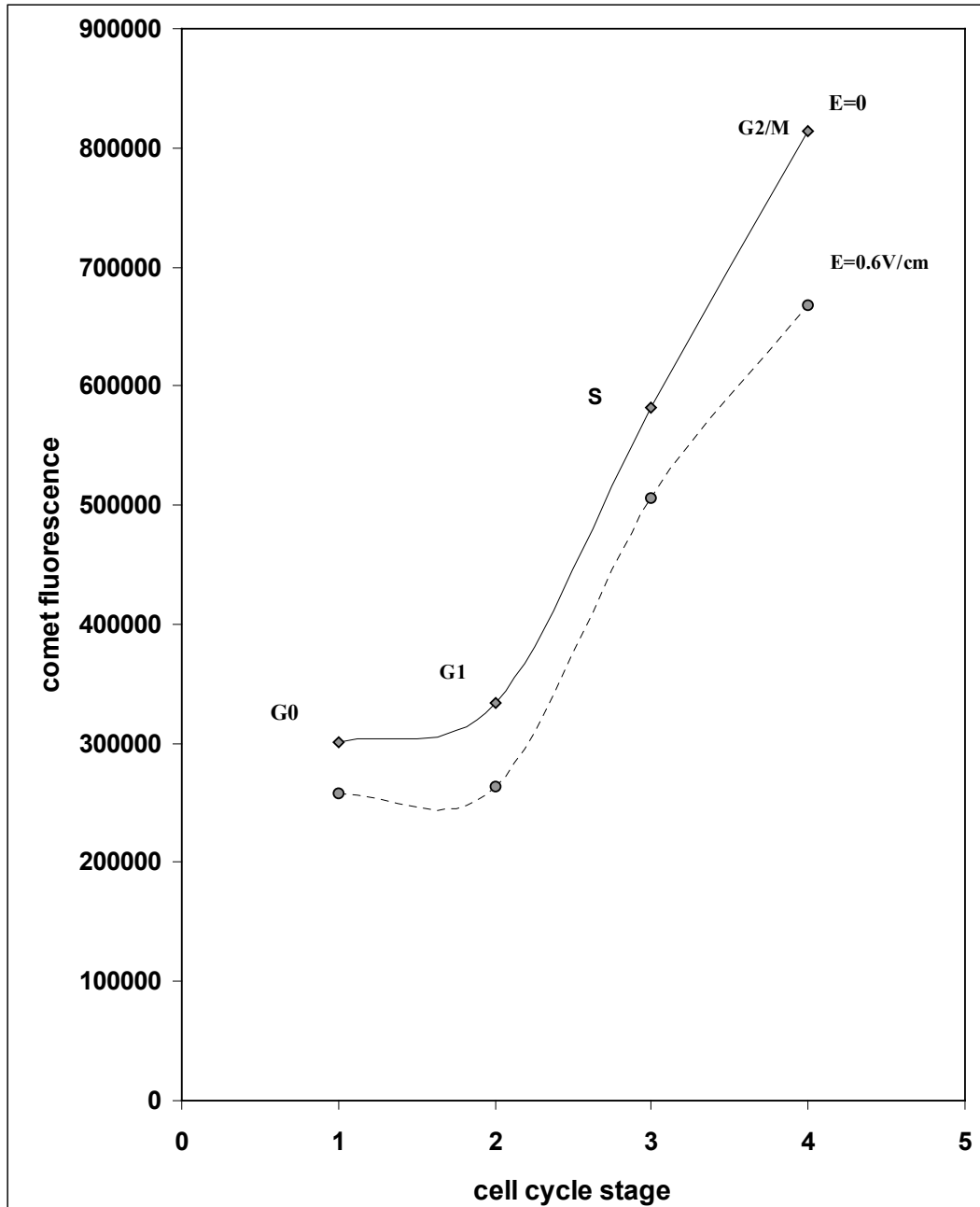


**Fig (3.8) Variation of comet fluorescence with cell cycle position for HSD2- fibroblasts, before and after electrophoresis, measured by the neutral comet assay**

The points shown represent the average comet fluorescence of 55 to 506 nucleoids in different phases of the cell cycle, obtained from 2 independent experiments performed on nucleoids, before (the solid line) and after electrophoresis (the broken line), at an electric field strength (E) of a value (0.6V/cm).

### **3.7.1) Effects of ionizing radiation on the amount of DNA migrated from individual cells, measured by the neutral comet assay.**

Electrophoresis of cells embedded and lysed in agarose on a microscope slide leads to migration of DNA out of the nuclear core into the halo region. After electrophoresis of irradiated cells, the DNA, which is stained with a fluorescent dye, resembles a comet with a head and tail. With increasing dose more damaged DNA migrated out from the head. The amount of DNA migrated into the tail is quantified by the percentage of the total fluorescence of DNA migrated into the tail region, defined as the tail intensity. The results of bivariate analysis of tail intensity versus DNA content (Fig. 3.9) showed a remarkable decrease in tail intensity with transition of cells from G1 to S-phase and increase slightly with transition to G2/M phase. This effect is observed at all doses including unirradiated cells.

The results of tail intensity for cells at various stages of cell cycle before and after irradiation are shown in (Table 3.9 and Fig. 3.10). The increase of tail intensity with X-ray dose is remarkable for G1 and G0 cells, however much less for G2/M cells and not unequivocal for S cells.

By using the tail length as a comet parameter we obtain the results shown in (Table 3.10 and Fig. 3.11). length is observed. For G1 cells only increase with dose up to 5 Gy is observed. Then the tail length remains constant with dose. For G0 cells a decrease in tail length up to 5 Gy is observed. For higher doses the tail length remains more or less constant. For S and G2/M cells an increase in tail length up to 15 Gy is observed, which the decreased at higher doses.

By using the tail moment as a comet parameter we obtain the results shown in (Table 3.11 and Fig. 3.12). Except for G2/M cells the tail moment increases for doses up to 5 Gy. No further increase in tail moment is observed when dose is increased from 5 Gy to 10 Gy except for G1 cells. For doses from 10 Gy to 15 Gy increase of tail moment is observed for G0 and G2/M cells followed by a decrease for doses higher than 15 Gy. For S cells a continuous decrease of the tail moment is obtained for doses higher than 5 Gy. For G1 cells a decrease of the tail moment is observed in the range 10 to 15 Gy, followed by an increase for doses higher than 15 Gy.

### **3.7.2) Effects of ionizing radiation on the fluorescence density of HSD2-nucleoids at various stages of the cell cycle.**

Figure (3.13) and Table (3.12) show the variation in fluorescence density with the cycle stage after exposure of HSD2-fibroblasts, to doses of ionizing radiation. After a decrease in fluorescence density when cells progress from G0 to G1 phase, a strong increase is observed when cells progress from G1 to S phase, being approximately constant during S and G2/M phases. Doses in the range from 5 to 20 Gy do not alter significantly the cell cycle dependence of fluorescence density as observed for the controls (Fig. 3.14).

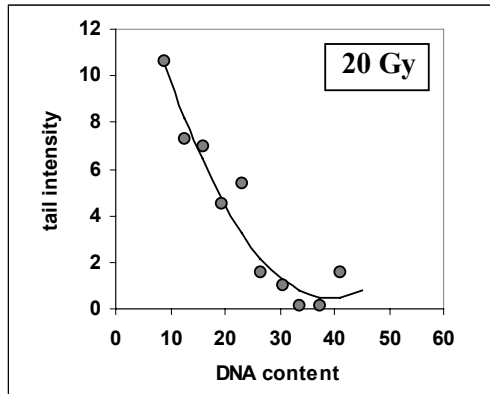
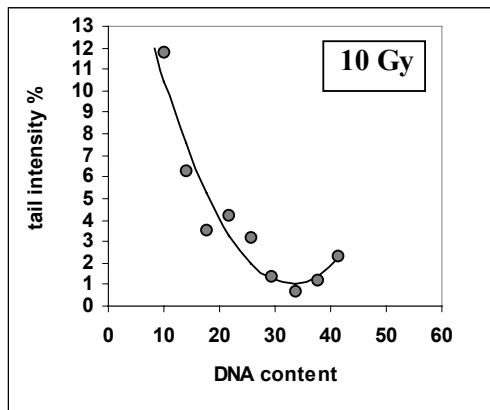
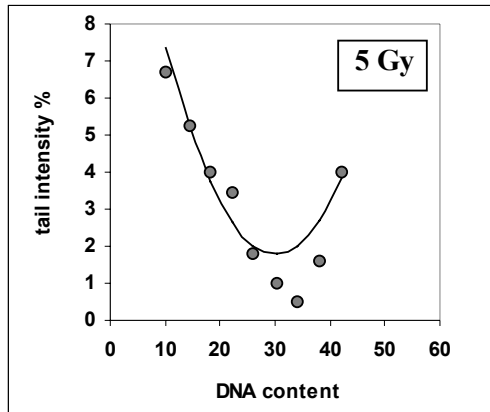
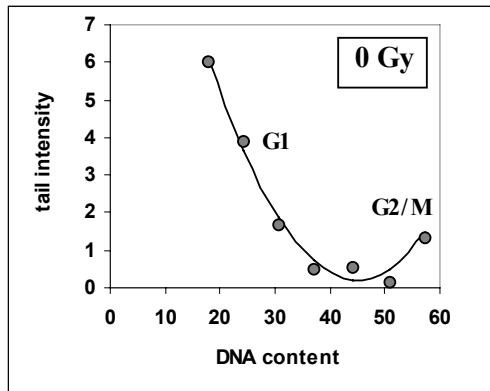


**Fig (3.9) Effect of cell cycle position on DNA damage induced by X-rays irradiation, measured by the neutral comet assay (V-as19)**

**Table (3.9) Changes in the tail intensity induced by X- ray irradiation of HSD2-fibroblasts in different phases of the cell cycle, measured by the neutral comet assay**

Cell phase	tail intensity %				
	0 Gy	5 Gy	10 Gy	15 Gy	20 Gy
<b>G0</b> (n=518)	<b>2.095±8.189</b> (±0.364)	<b>2.701±8.518</b> (±0.361) <i>(P &lt; 0.5)</i>	<b>3.214±10.237</b> (±0.434) <i>(P &lt; 0.1)</i>	<b>5.727±14.465</b> (±0.655) <i>(P &lt; 0.00005)</i>	<b>4.926±12.662</b> (±0.575) <i>(P &lt; 0.0002)</i>
<b>G1</b> (n=449)	<b>3.052±7.37</b> (±0.354)	<b>4.521±10.28</b> (±0.463) <i>(P &lt; 0.0005)</i>	<b>6.019±12.30</b> (±0.559) <i>(P &lt; 0.00005)</i>	<b>5.687±12.622</b> (±0.577) <i>(P &lt; 0.00005)</i>	<b>6.915±13.251</b> (±0.710) <i>(P &lt; 0.00005)</i>
<b>S</b> (n=84)	<b>0.150± 0.591</b> (±0.066)	<b>1.333±4.584</b> (±0.102) <i>(P &lt; 0.00005)</i>	<b>1.096±4.857</b> (±0.546) <i>(P &lt; 0.00005)</i>	<b>1.093-3.223</b> (±0.352) <i>(P &lt; 0.00005)</i>	<b>0.173±0.369</b> (±0.044) <i>(P &lt; 0.5)</i>
<b>G2/M</b> (n=69)	<b>0.861±2.205</b> (±0.297)	<b>1.220±2.205</b> (±0.269) <i>(P &lt; 0.05)</i>	<b>1.264±3.937</b> (±0.517) <i>(P &lt; 0.00005)</i>	<b>1.301±5.714</b> (±0.655) <i>(P &lt; 0.00005)</i>	<b>1.779±5.023</b> (±0.538) <i>(P &lt; 0.00005)</i>

The values shown represent the mean± SD (±SE) of the tail intensity of 69-518 nucleoids on average in the in different phases, obtained from two independent experiments performed on confluent and exponentially growing HSD2-fibroblasts irradiated with different doses of X-ray.

The difference in the tail intensity between irradiated and unirradiated cells is considered significant when  $P < 0.05$  and highly significant when  $P < 0.02$ .

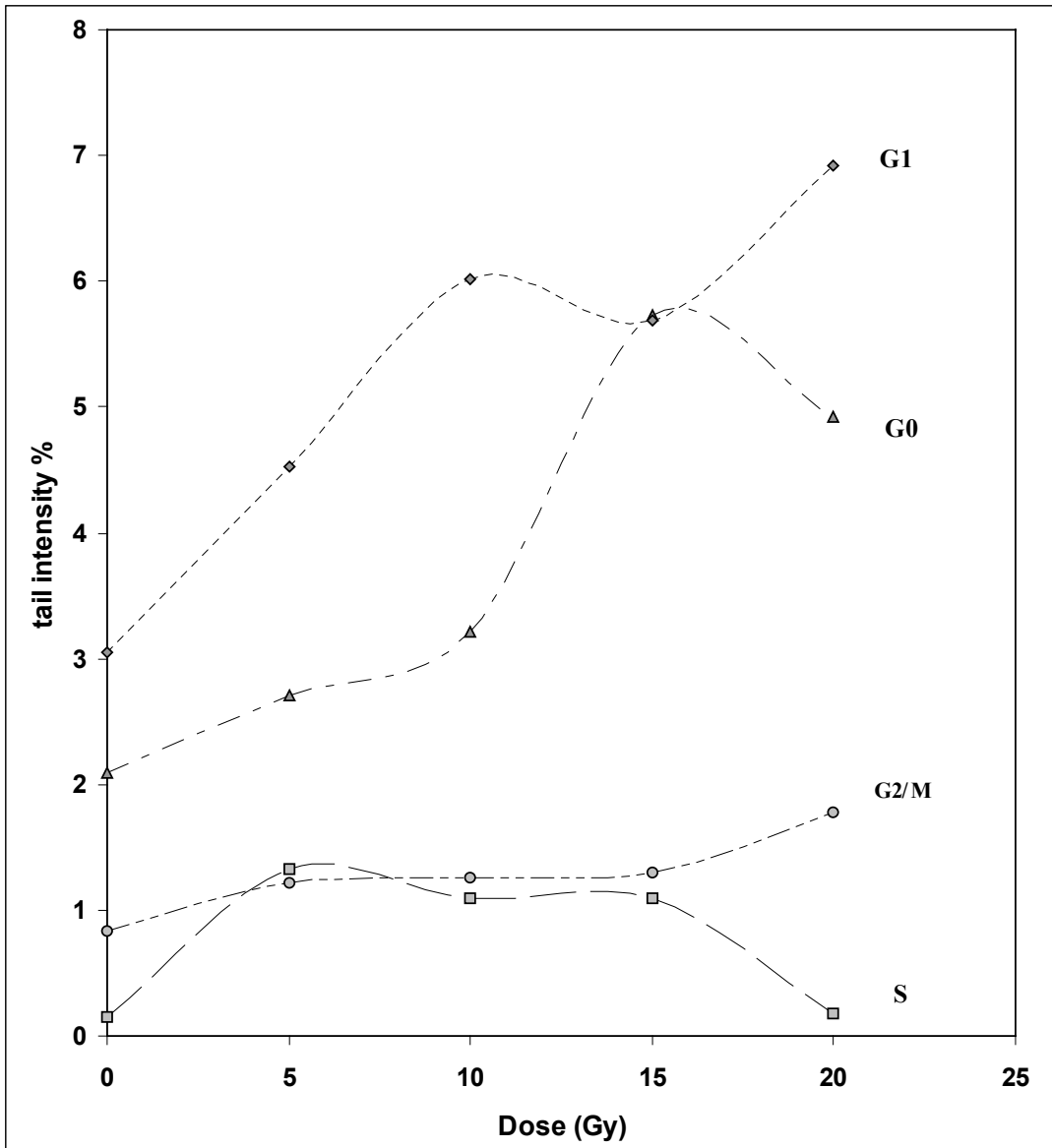


**Fig (3.10) Dose response of the tail intensity to X ray irradiation for HSD2 fibroblasts in different phases, measured by the neutral comet assay**

The points shown represent the average tail intensity of 69 to 518 nucleoids (on average) in different phases, obtained from 2 independent experiments performed on confluent and exponentially growing HSD2- fibroblasts, irradiated with different X-ray doses.



**Table (3.10) Changes in the tail length induced by X- ray irradiation of HSD2-fibroblasts in different phases of the cell cycle, measured by the neutral comet assay**

Cell phase	tail length ( $\mu\text{m}$ )				
	0 Gy	5 Gy	10 Gy	15 Gy	20 Gy
<b>G0</b> (n=518)	<b>133.3</b> $\pm$ 42.142 ( $\pm$ 1.87)	<b>120.815</b> $\pm$ 49.32 ( $\pm$ 2.09) <i>(P &lt; 0.00005)</i>	<b>119.8</b> $\pm$ 50.4 ( $\pm$ 2.137) <i>(P &lt; 0.00005)</i>	<b>127.7</b> $\pm$ 55.6 ( $\pm$ 2.519) <i>(P &lt; 0.0005)</i>	<b>126</b> $\pm$ 51.67 ( $\pm$ 2.346) <i>(P &lt; 0.0005)</i>
<b>G1</b> (n=449)	<b>123.5</b> $\pm$ 43.5 ( $\pm$ 2.085)	<b>144.59</b> $\pm$ 62.16 ( $\pm$ 2.79) <i>(P &lt; 0.00005)</i>	<b>151.9</b> $\pm$ 64.2 ( $\pm$ 2.91) <i>(P &lt; 0.00005)</i>	<b>152.158</b> $\pm$ 68.45 ( $\pm$ 3.12) <i>(P &lt; 0.00005)</i>	<b>146.58</b> $\pm$ 66.3 ( $\pm$ 3.54) <i>(P &lt; 0.00005)</i>
<b>S</b> (n=84)	<b>93.589</b> $\pm$ 44.8 ( $\pm$ 5.04)	<b>102.47</b> $\pm$ 55 ( $\pm$ 5.34) <i>(P &lt; 0.5)</i>	<b>114.30</b> $\pm$ 52.24 ( $\pm$ 5.87) <i>(P &lt; 0.01)</i>	<b>118.32</b> $\pm$ 63.2 ( $\pm$ 6.89) <i>(P &lt; 0.005)</i>	<b>100.7</b> $\pm$ 52.78 ( $\pm$ 6.35) <i>(P &lt; 0.5)</i>
<b>G2/M</b> (n=69)	<b>106.56</b> $\pm$ 37.5 ( $\pm$ 5.05)	<b>102.46</b> $\pm$ 37.5 ( $\pm$ 4.58) <i>(P &lt; 0.5)</i>	<b>115.88</b> $\pm$ 49.49 ( $\pm$ 6.49) <i>(P &lt; 0.5)</i>	<b>123.89</b> $\pm$ 57.25 ( $\pm$ 6.56) <i>(P &lt; 0.001)</i>	<b>110.39</b> $\pm$ 49.7 ( $\pm$ 5.0) <i>(P &lt; 0.5)</i>

The values shown represent the mean $\pm$  SD ( $\pm$ SE) of the tail length of 69-518 nucleoids on average in the in different phases, obtained from two independent experiments performed on confluent and exponentially growing HSD2-fibroblasts irradiated with different doses of X-ray.

The difference in the tail length between irradiated and unirradiated cells is considered significant when  $P < 0.05$  and highly significant when  $P < 0.02$ .

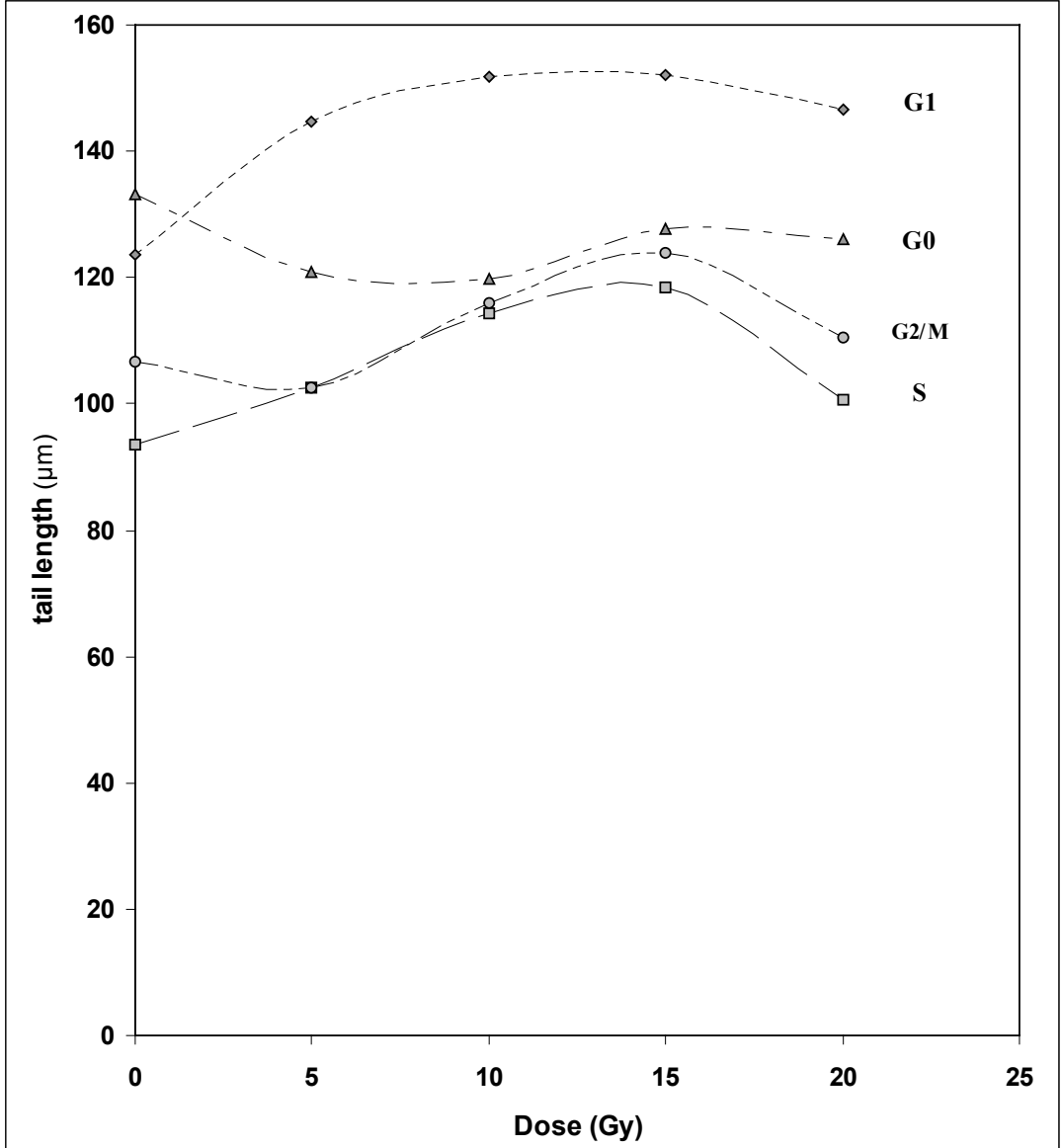


**Fig (3.11) Dose response of the tail length to X ray irradiation for HSD2 fibroblasts in different phases, measured by the neutral comet assay**

The points shown represent the average tail length of 69 to 518 nucleoids (on average) in different phases, obtained from 2 independent experiments performed on confluent and exponentially growing HSD2- fibroblasts, irradiated with different X-ray doses.

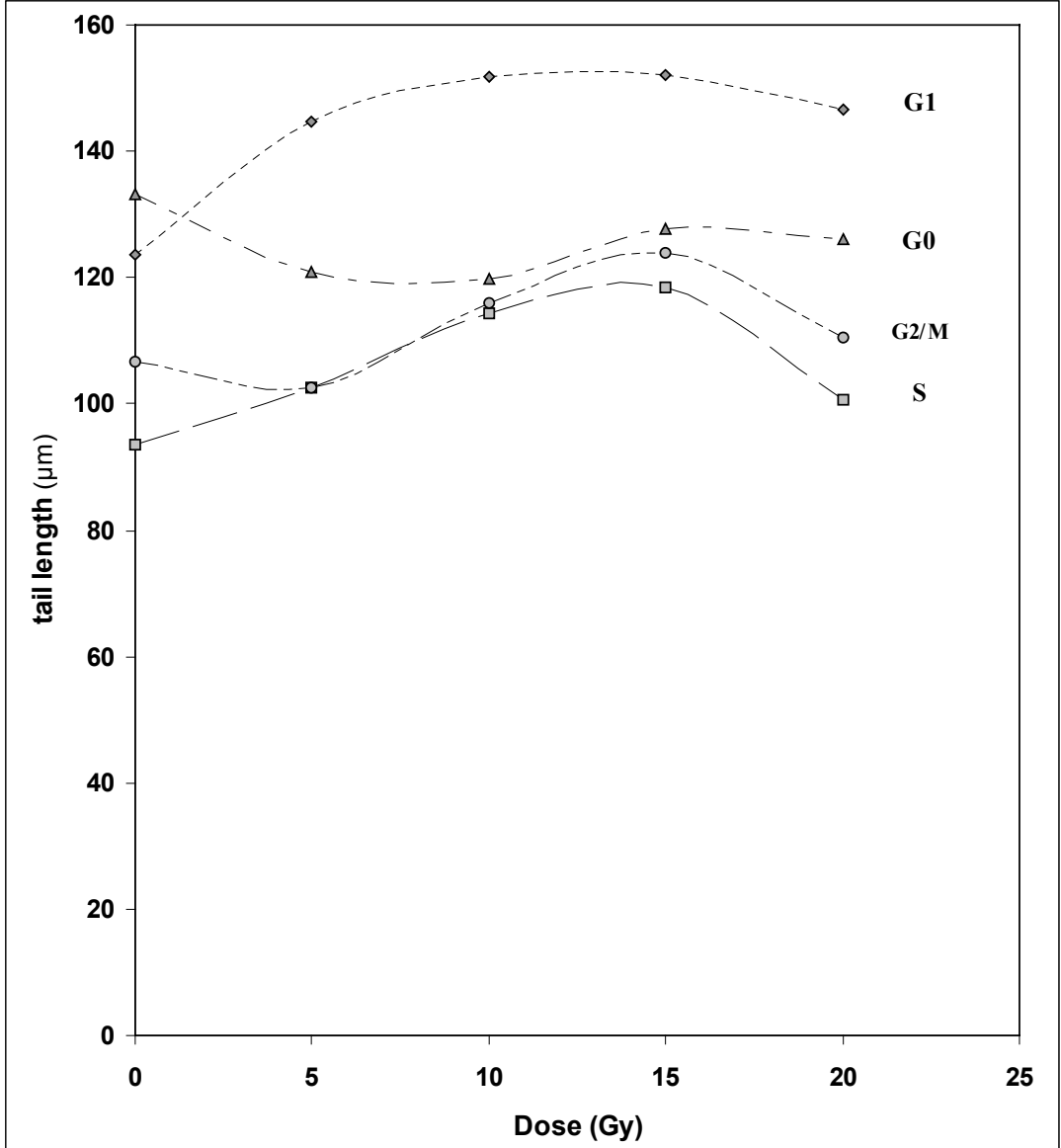


**Fig (3.11) Dose response of the tail length to X ray irradiation for HSD2 fibroblasts in different phases, measured by the neutral comet assay**

The points shown represent the average tail length of 69 to 518 nucleoids (on average) in different phases, obtained from 2 independent experiments performed on confluent and exponentially growing HSD2- fibroblasts, irradiated with different X-ray doses.

**Table (3.11) Changes in the tail moment induced by X- ray irradiation of HSD2-fibroblasts in different phases of the cell cycle, measured by the neutral comet assay**

Cell phase	tail moment				
	0 Gy	5 Gy	10 Gy	15 Gy	20 Gy
<b>G0</b> (n=518)	<b>1.425±5.326</b> (±0.236)	<b>1.683±5.445</b> (±0.231) <i>(P &lt; 0.5)</i>	<b>1.809±5.777</b> (±0.245) <i>(P &lt; 0.5)</i>	<b>3.205±8.395</b> (±0.380) <i>(P &lt; 0.0001)</i>	<b>2.633±6.605</b> (±0.2999) <i>(P &lt; 0.002)</i>
<b>G1</b> (n=449)	<b>1.972±4.74</b> (±0.227)	<b>2.541±5.66</b> (±0.254) <i>(P &lt; 0.1)</i>	<b>3.488±7.015</b> (±0.318) <i>(P &lt; 0.0002)</i>	<b>3.057±6.698</b> (±0.304) <i>(P &lt; 0.005)</i>	<b>3.676±6.839</b> (±0.365) <i>(P &lt; 0.0001)</i>
<b>S</b> (n=84)	<b>0.129±0.535</b> (±0.060)	<b>0.995±3.66</b> (±0.352) <i>(P &lt; 0.02)</i>	<b>0.813±3.756</b> (±0.422) <i>(P &lt; 0.2)</i>	<b>0.588±3.223</b> (±0.351) <i>(P &lt; 0.5)</i>	<b>0.106±0.216</b> (±0.026) <i>(P &lt; 0.5)</i>
<b>G2/M</b> (n=69)	<b>0.692±1.755</b> (±0.236)	<b>0.845±1.755</b> (±0.214) <i>(P &lt; 0.5)</i>	<b>0.930±2.862</b> (±0.375) <i>(P &lt; 0.5)</i>	<b>1.749±4.343</b> (±0.498) <i>(P &lt; 0.1)</i>	<b>1.213±3.599</b> (±0.386) <i>(P &lt; 0.5)</i>

The values shown represent the mean± SD (±SE) of the tail moment of 69-518 nucleoids on average in the in different phases, obtained from two independent experiments performed on confluent and exponentially growing HSD2-fibroblasts irradiated with different doses of X-ray.

The difference in the tail moment between irradiated and unirradiated cells is considered significant when  $P < 0.05$  and highly significant when  $P < 0.02$ .

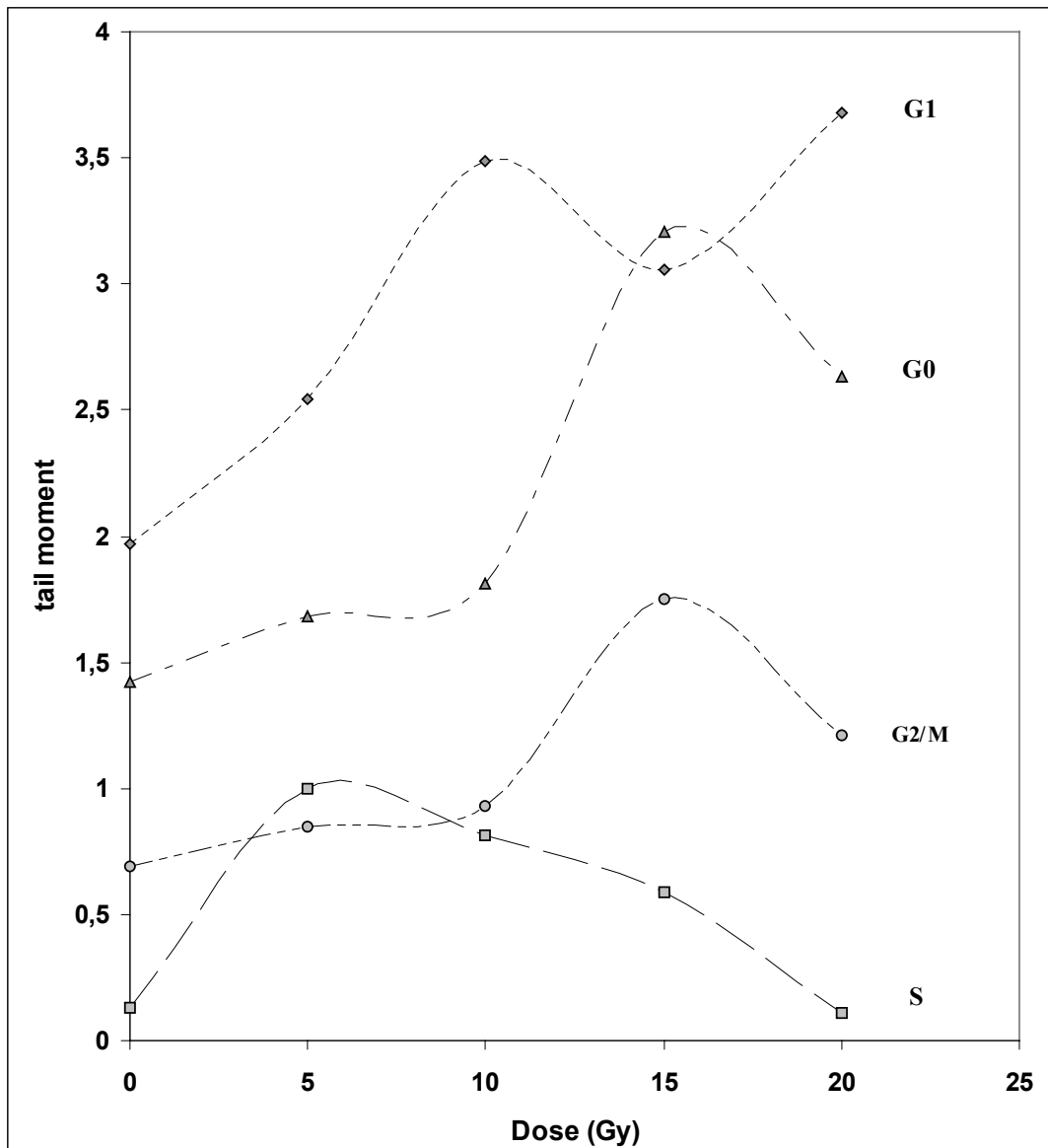


**Fig (3.12) Dose response of the tail moment to X ray irradiation for HSD2 fibroblasts in different phases, measured by the neutral comet assay**

The points shown represent the average tail moment of 69 to 518 nucleoids (on average) in different phases, obtained from 2 independent experiments performed on confluent and exponentially growing HSD2- fibroblasts, irradiated with different X-ray doses.

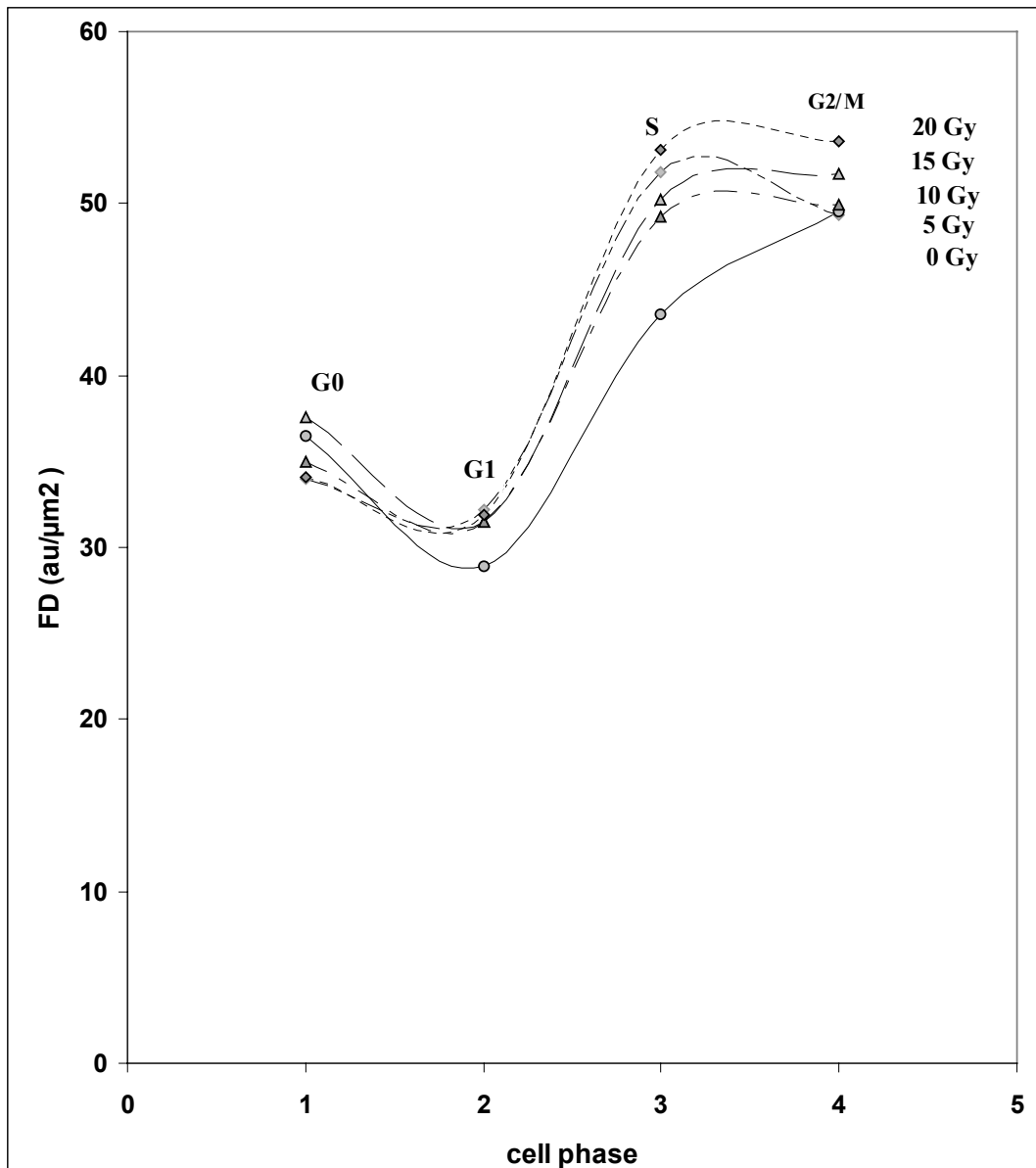


**Fig (3.13) Variation of the comet fluorescence density (FD) with cell cycle position for HSD2-fibroblasts, at different phases, irradiated with different X-ray doses and subjected to neutral microgel electrophoresis**

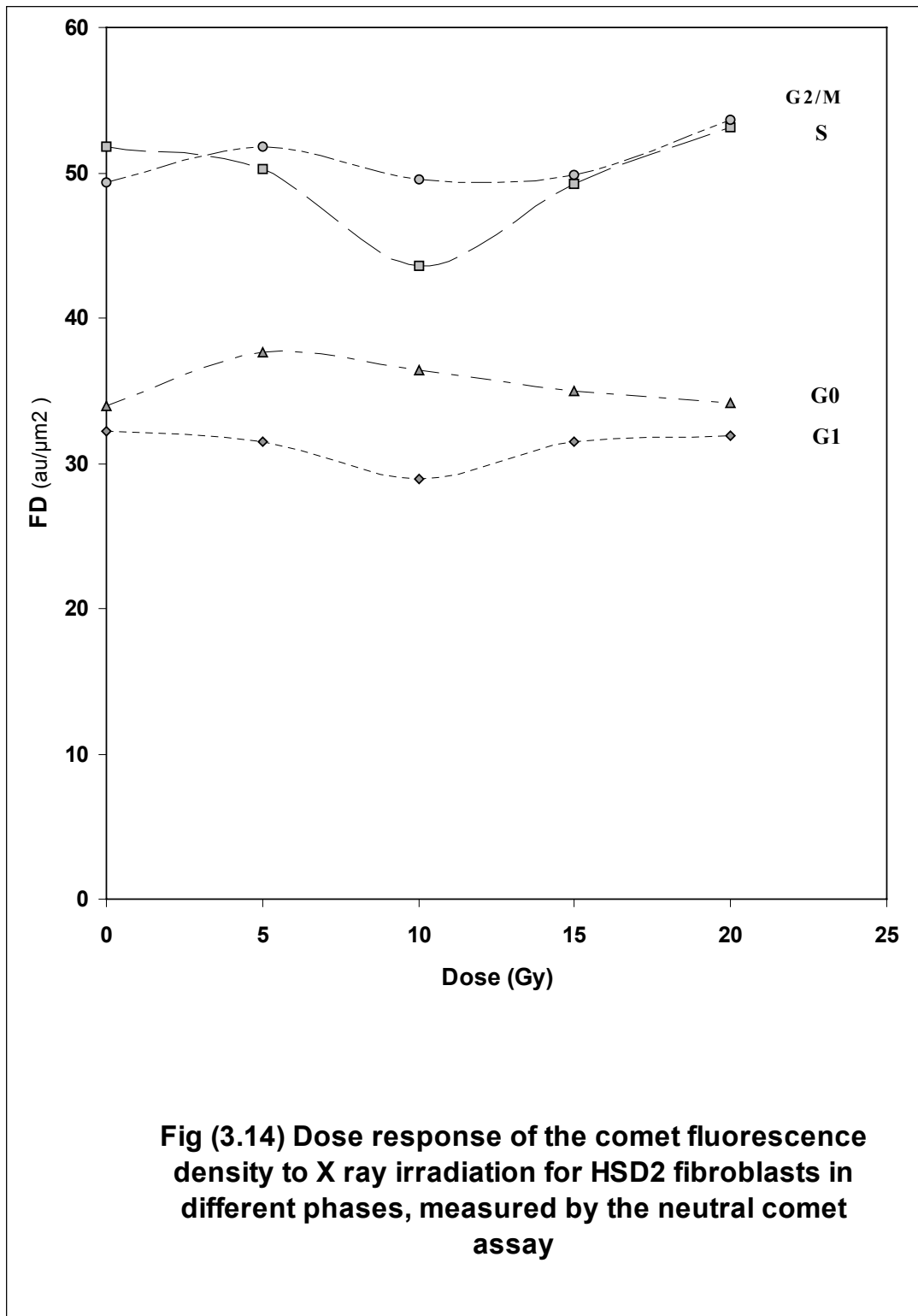
The points shown represent the average fluorescence density (F.D) of 69 to 518 nucleoids (on average) in different phases, obtained from 2 independent experiments performed on confluent and exponentially growing HSD2- fibroblasts, irradiated with different X-ray doses.

**Table (3.12) Changes in the comet fluorescence density induced by X- ray irradiation of HSD2-fibroblasts in different phases of the cell cycle, measured by the neutral comet assay**

Cell phase	F.D (au/μm )				
	0 Gy	5 Gy	10 Gy	15 Gy	20 Gy
<b>G0</b> (n=518)	<b>33.97±6.902</b> (±0.307)	<b>37.59±7.616</b> (±0.323) <i>(P &lt; 0.00005)</i>	<b>36.456±9.385</b> (±0.398) <i>(P &lt; 0.00005)</i>	<b>34.96±9.681</b> (±0.439) <i>(P &lt; 0.1)</i>	<b>34.121±9.787</b> (±0.444) <i>(P &lt; 0.5)</i>
<b>G1</b> (n=449)	<b>32.174±6.313</b> (±0.302)	<b>31.477±7.472</b> (±0.336) <i>(P &lt; 0.5)</i>	<b>28.882±7.458</b> (±0.338) <i>(P &lt; 0.01)</i>	<b>31.479±8.021</b> (±0.366) <i>(P &lt; 0.5)</i>	<b>31.862±10.028</b> (±0.536) <i>(P &lt; 0.5)</i>
<b>S</b> (n=84)	<b>51.841±8.922</b> (±1.00)	<b>50.236±8.555</b> (±0.823) <i>(P &lt; 0.5)</i>	<b>43.543±7.250</b> (±0.815) <i>(P &lt; 0.00005)</i>	<b>49.279-8.061</b> (±0.879) <i>(P &lt; 0.005)</i>	<b>53.114±7.763</b> (±0.934) <i>(P &lt; 0.002)</i>
<b>G2/M</b> (n=69)	<b>49.362±9.797</b> (±1.321)	<b>51.761±9.797</b> (±1.197) <i>(P &lt; 0.5)</i>	<b>49.552±9.23</b> (±1.212) <i>(P &lt; 0.5)</i>	<b>49.897±11.727</b> (±1.328) <i>(P &lt; 0.5)</i>	<b>53.671±10.750</b> (±1.152) <i>(P &lt; 0.5)</i>

The values shown represent the mean± SD (±SE) of the fluorescence density of 69-518 nucleoids on average in the in different phases, obtained from two independent experiments performed on confluent and exponentially growing HSD2-fibroblasts irradiated with different doses of X-ray.

The difference in the fluorescence density between irradiated and unirradiated cells is considered significant when  $P < 0.05$  and highly significant when  $P < 0.02$ .



The points shown represent the average fluorescence density of 69 to 518 nucleoids (on average) in different phases, obtained from 2 independent experiments performed on confluent and exponentially growing HSD2- fibroblasts, irradiated with different X-ray doses.



### **3.7.3) Effects of ionizing radiation on the comet area of individual cells at various stages of the cell cycle.**

(Table 3.13 and Fig. 3.15) show a significant decrease in the comet area of HSD2-nucleoids at all stages of the cell cycle after exposure to 5 Gy when compared to unirradiated nucleoids. Whereas for G0 and G1 phase cells a further decrease is observed with increasing dose, the comet area for G2/M and S- phase cells increases for higher doses up to 10 Gy followed by a decrease for doses higher than 10 Gy.

### **3.7.4) Effects of ionizing radiation on the comet fluorescence of individual cells at various stages of the cell cycle.**

The results of comet fluorescence for HSD2 fibroblasts at various stages of the cell cycle before and after irradiation are shown in (Table 3.14 and Fig. 3.16). A significant decrease in comet fluorescence is observed at all doses. An approximately linear decrease is observed for G2/M and G1 cells. For S cells a step decrease up to a dose of 5 Gy is followed by a linear decrease at a much smaller slope up to 20 Gy. Similarly, for G0 cells a significant decrease up to 5 Gy is followed by no change in comet fluorescence up to 20 Gy.

### **3.7.5) Effects of ionizing radiation on the degree of condensation of DNA in individual cells at various stages of the cell cycle.**

The results of relative DNA condensation of HSD2- nucleoids at various stages of the cell cycle before and after X-irradiation are shown in (Table 3.15 and Fig. 3.17). Except for G2/M cells a significant increase in DNA condensation is observed after irradiation with 5 Gy. This increase is followed by a significant decrease after irradiation with 10 Gy. For doses higher than 10 Gy a gradual increase is observed in the dose range 10 to 20 Gy.

### **3.7.6) Effects of ionizing radiation on the relative size of DNA in individual cells at various stages of the cell cycle.**

Since the relative DNA size is the inverse of the relative condensation RC , the increase dependencies on dose are seen in Fig. 3.18 and Table 3.16.

### **3.7.7) Effects of ionizing radiation on the fluorescence-decrement of HSD2-fibroblasts at different stages of the cell cycle.**

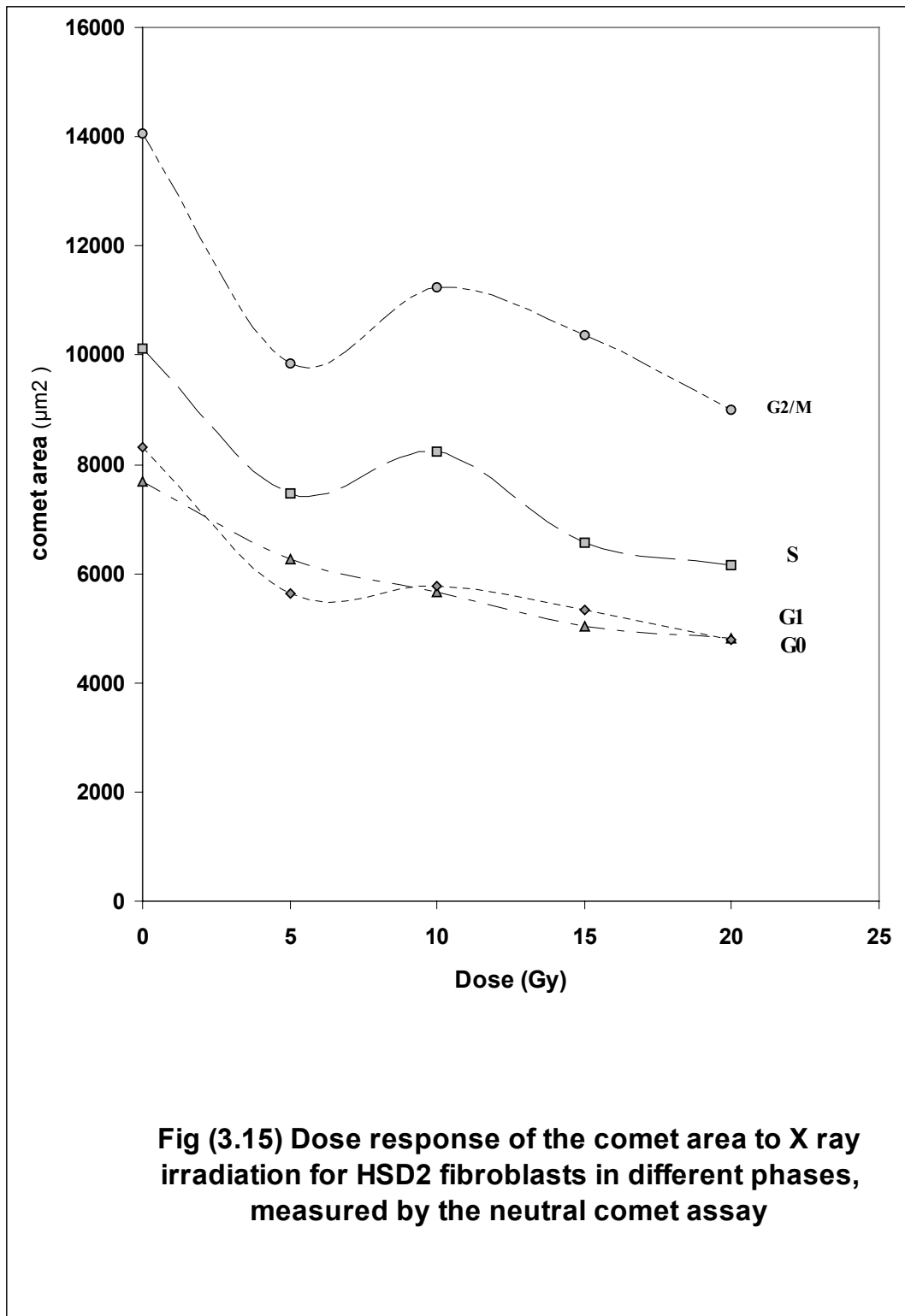
The fluorescence decrement (dF) induced by electrophoresis of HSF2 fibroblasts can be calculated as a function of dose for the different cell cycle phases using Table 3.17. As seen in Table 3.17 and Fig. 3.19, a steep increase in fluorescence decrement is observed after irradiation with 5 Gy followed by an increase with a slower slope at higher doses. This effect is observed at G0 G1 and S phases. While a further remarkable decline in the fluorescence decrement of G2/M cells is observed after irradiation with 10 Gy followed by a remarkable increase at higher doses.

**Table (3.13) Changes in the comet area induced by X- ray irradiation of HSD2-fibroblasts in different phases of the cell cycle, measured by the neutral comet assay**

Cell phase	Comet area ( $\mu\text{m}^2$ )				
	0 Gy	5 Gy	10 Gy	15 Gy	20 Gy
<b>G0</b> (n=518)	<b>7679</b> $\pm$ 1604 ( $\pm$ 71.3)	<b>6271</b> $\pm$ 1310 ( $\pm$ 55.5) <i>(P &lt; 0.00005)</i>	<b>5667</b> $\pm$ 1251 ( $\pm$ 53.05) <i>(P &lt; 0.00005)</i>	<b>5044</b> $\pm$ 1144 ( $\pm$ 51.84) <i>(P &lt; 0.00005)</i>	<b>4818</b> $\pm$ 1245 ( $\pm$ 56.53) <i>(P &lt; 0.00005)</i>
<b>G1</b> (n=449)	<b>8306</b> $\pm$ 1271 ( $\pm$ 60.89)	<b>5633</b> $\pm$ 1243 ( $\pm$ 55.925) <i>(P &lt; 0.00005)</i>	<b>5775</b> $\pm$ 1285 ( $\pm$ 58.288) <i>(P &lt; 0.00005)</i>	<b>5340</b> $\pm$ 1079 ( $\pm$ 49.249) <i>(P &lt; 0.00005)</i>	<b>4790</b> $\pm$ 1202 ( $\pm$ 64.249) <i>(P &lt; 0.00005)</i>
<b>S</b> (n=84)	<b>10116</b> $\pm$ 2259 ( $\pm$ 254)	<b>7458</b> $\pm$ 1466 ( $\pm$ 0.823) <i>(P &lt; 0.00005)</i>	<b>8227</b> $\pm$ 1549 ( $\pm$ 0.815) <i>(P &lt; 0.00005)</i>	<b>6553</b> $\pm$ 1096 ( $\pm$ 0.879) <i>(P &lt; 0.00005)</i>	<b>6157</b> $\pm$ 953 ( $\pm$ 0.934) <i>(P &lt; 0.00005)</i>
<b>G2/M</b> (n=69)	<b>14057</b> $\pm$ 2852 ( $\pm$ 1.321)	<b>9856</b> $\pm$ 2852 ( $\pm$ 274) <i>(P &lt; 0.00005)</i>	<b>11243</b> $\pm$ 2225 ( $\pm$ 250) <i>(P &lt; 0.00005)</i>	<b>10379</b> $\pm$ 2351 ( $\pm$ 256) <i>(P &lt; 0.00005)</i>	<b>8998</b> $\pm$ 2126 ( $\pm$ 256) <i>(P &lt; 0.00005)</i>

The values shown represent the mean $\pm$  SD ( $\pm$ SE) of the comet area of 69-518 nucleoids on average in the in different phases, obtained from two independent experiments performed on confluent and exponentially growing HSD2-fibroblasts irradiated with different doses of X-ray.

The difference in the comet area between irradiated and unirradiated cells is considered significant when  $P < 0.05$  and highly significant when  $P < 0.02$ .



The points shown represent the average comet area of 69 to 518 nucleoids (on average) in different phases, obtained from 2 independent experiments performed on confluent and exponentially growing HSD2- fibroblasts, irradiated with different X-ray doses

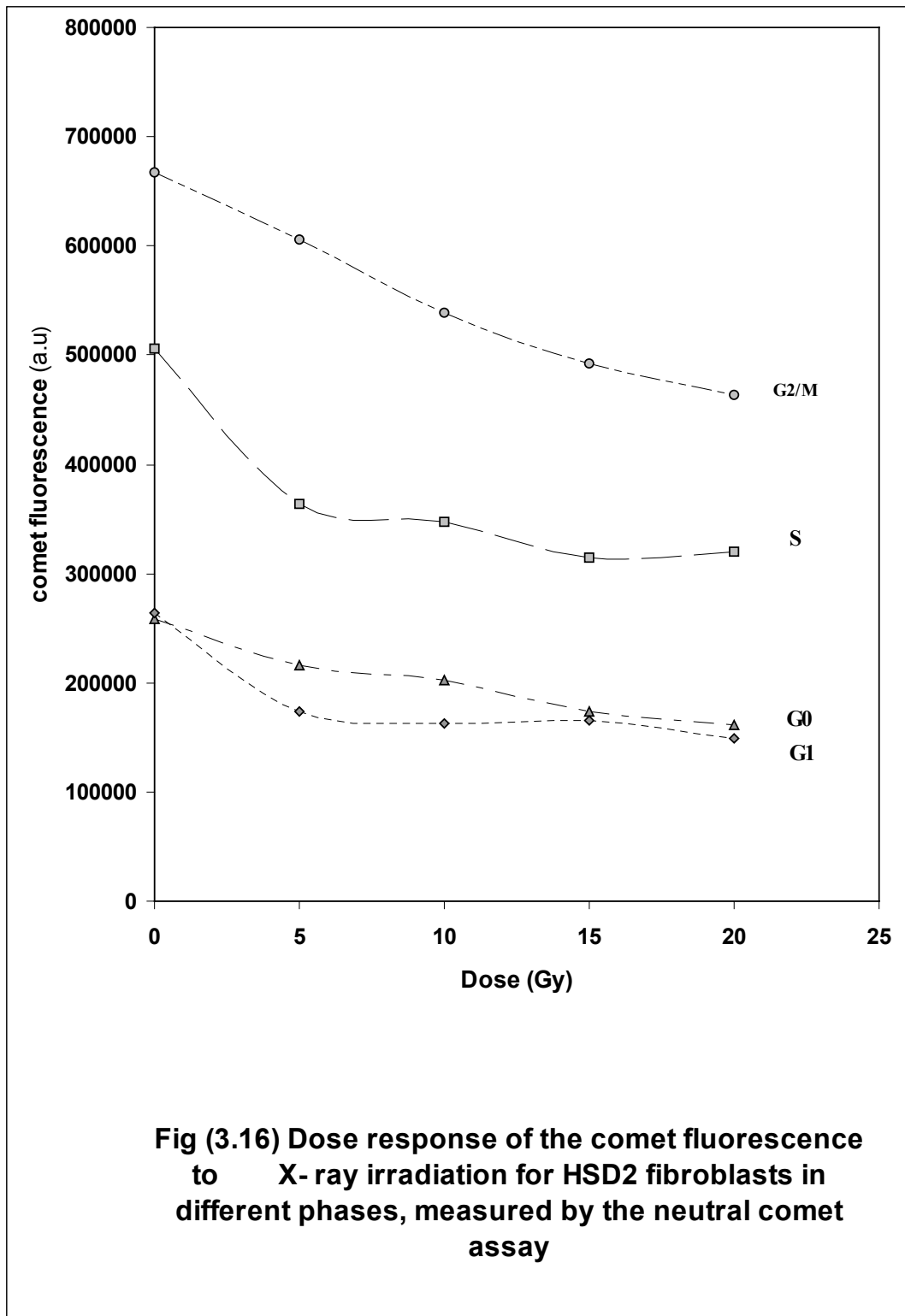
**Table (3.14) Changes in the comet fluorescence induced by X- ray irradiation of HSD2-fibroblasts in different phases of the cell cycle, measured by the neutral comet assay**

Cell phase	Comet fluorescence				
	0 Gy	5 Gy	10 Gy	15 Gy	20 Gy
<b>G0</b> (n=518)	<b>257969±63886</b> (±2840) (237363)	<b>216483±4988</b> 7 (±2115) ( <i>P</i> < 0.00005)	<b>202772±54579</b> (±2314) ( <i>P</i> < 0.00005)	<b>173922±5342</b> (±2421) ( <i>P</i> < 0.00005)	<b>161011±5049</b> (±2293) ( <i>P</i> < 0.00005)
<b>G1</b> (n=449)	<b>263462+</b> 47413 (±2273) (180985)	<b>173708±4275</b> 5 (±1923) ( <i>P</i> < 0.00005)	<b>163012±41882</b> (±1899) ( <i>P</i> < 0.00005)	<b>165895±4450</b> (±2031) ( <i>P</i> < 0.00005)	<b>148458±4315</b> (±2306) ( <i>P</i> < 0.00005)
<b>S</b> (n=84)	<b>505700±1400</b> (±1576) (377065)	<b>363225±1488</b> 8 (±1432) ( <i>P</i> < 0.00005)	<b>347833±12838</b> (±1444) ( <i>P</i> < 0.00005)	<b>314531±8217</b> (±896) ( <i>P</i> < 0.00005)	<b>320153±1188</b> (±1431) ( <i>P</i> < 0.00005)
<b>G2/M</b> (n=69)	<b>667944±3789</b> (±5109) (641116)	<b>605945±3789</b> 2 (±4629) ( <i>P</i> < 0.00005)	<b>538544±35138</b> (±4613) ( <i>P</i> < 0.00005)	<b>492751±4530</b> (±5197) ( <i>P</i> < 0.00005)	<b>463975±5881</b> (±6305) ( <i>P</i> < 0.00005)

The values shown represent the mean± SD (±SE) of the comet fluorescence of 69-518 nucleoids on average in the in different phases, obtained from two independent experiments performed on confluent and exponentially growing HSD2-fibroblasts irradiated with different doses of X-ray.

The values between parantheses are the intercept of the comet fluorescence- dose relationship in the dose range (5-20Gy) calculated by the linear regression analysis.

The difference in the comet fluorescence between irradiated and unirradiated cells is considered significant when  $P < 0.05$  and highly significant when  $P < 0.02$ .



The points shown represent the average comet fluorescence of 69 to 518 nucleoids (on average) in different phases, obtained from 2 independent experiments performed on confluent and exponentially growing HSD2- fibroblasts, irradiated with different X-ray doses.

**Table (3.15) Changes in DNA condensation induced by X- ray irradiation of HSD2-fibroblasts in different phases of the cell cycle, measured by the neutral comet assay**

Cell phase	relative DNA condensation				
	0 Gy	5 Gy	10 Gy	15 Gy	20 Gy
<b>G1</b> (n=449)	<b>0.949</b> ±0.162 (±0.008)	<b>1.175</b> ±0.294 (±0.013) <i>(P &lt; 0.00005)</i>	<b>1.031</b> ±0.236 (±0.0107) <i>(P &lt; 0.0005)</i>	<b>0.988</b> ±0.223 (±0.0102) <i>(P &lt; 0.5)</i>	<b>1.080</b> ±0.322 (±0.017) <i>(P &lt; 0.00005)</i>
<b>S</b> (n=84)	<b>0.97</b> ±0.170 (±0.019)	<b>1.067</b> ±0.180 (±0.017) <i>(P &lt; 0.0005)</i>	<b>0.873</b> ±0.143 (±0.016) <i>(P &lt; 0.00005)</i>	<b>0.973</b> ±0.165 (±0.018) <i>(P &lt; 0.5)</i>	<b>0.983</b> ±0.140 (±0.017) <i>(P &lt; 0.5)</i>
<b>G2/M</b> (n=69)	<b>1.14</b> ±0.246 (±0.033)	<b>1.333</b> ±0.246 (±0.03) <i>(P &lt; 0.5)</i>	<b>1.047</b> ±0.208 (±0.027) <i>(P &lt; 0.5)</i>	<b>1.030</b> ±0.269 (±0.0308) <i>(P &lt; 0.5)</i>	<b>1.130</b> ±0.261 (±0.028) <i>(P &lt; 0.5)</i>

The values shown represent the mean± SD (±SE) of the relative DNA condensation of 69-518 nucleoids on average in the in different phases, obtained from two independent experiments performed on confluent and exponentially growing HSD2- fibroblasts irradiated with different doses of X-ray.

The difference in the DNA condensation between irradiated and unirradiated cells is considered significant when  $P < 0.05$  and highly significant when  $P < 0.02$ .

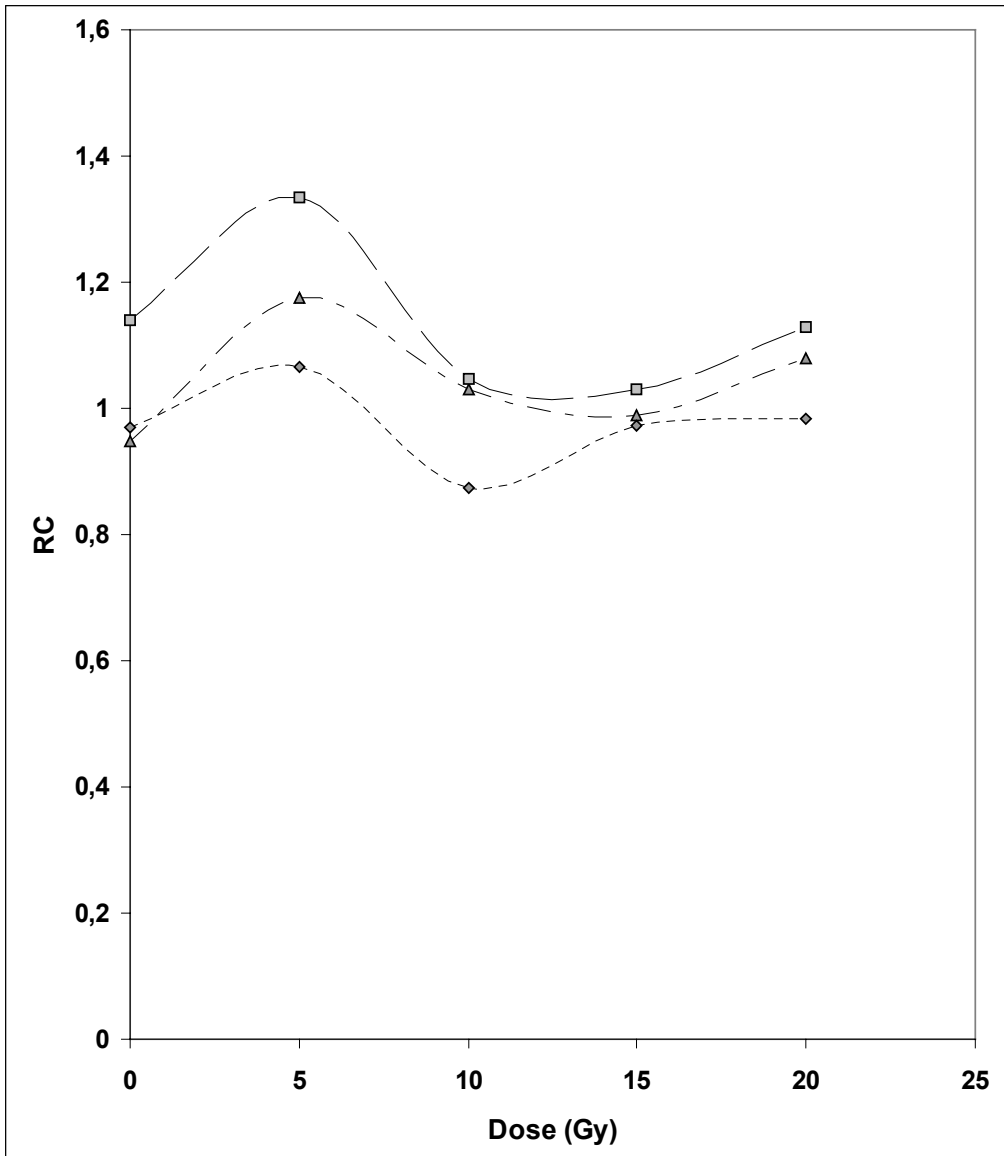


**Fig (3.17) Dose response of the relative DNA condensation (RC) to X ray irradiation for HSD2 fibroblasts in different phases, measured by the neutral comet assay**

The points shown represent the average relative DNA condensation (RC) of 69 to 518 nucleoids (on average) in different phases, obtained from 2 independent experiments performed on confluent and exponentially growing HSD2- fibroblasts, irradiated with different X-ray doses.

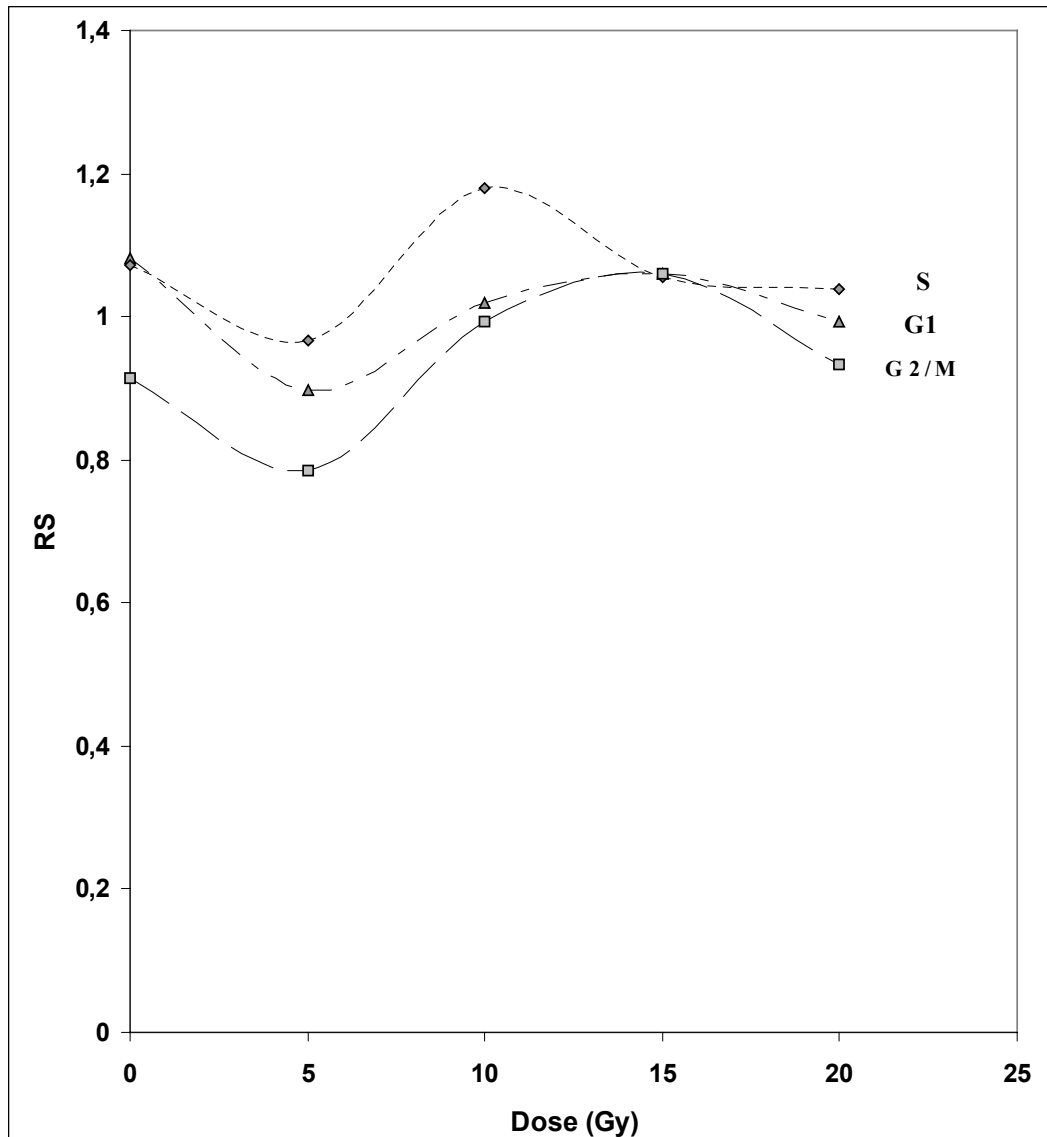


**Fig (3.18) Dose response of the relative DNA size (RS) to X ray irradiation for HSD2 fibroblasts in different phases, measured by the neutral comet assay**

The points shown represent the average relative DNA size (RS) of 69 to 518 nucleoids (on average) in different phases, obtained from 2 independent experiments performed on confluent and exponentially growing HSD2- fibroblasts, irradiated with different X-ray doses.



**Table (3.16) Changes in relative DNA size induced by X- ray irradiation of HSD2- fibroblasts in different phases of the cell cycle, measured by the neutral comet assay**

Cell phase	relative DNA size				
	0 Gy	5 Gy	10 Gy	15 Gy	20 Gy
<b>G1</b> (n=449)	<b>1.082±0.166</b> (±0.0079)	<b>0.898±0.198</b> (±0.0089) <i>(P &lt; 0.00005)</i>	<b>1.019±0.227</b> (±0.0102) <i>(P &lt; 0.00005)</i>	<b>1.059±0.214</b> (±0.0103) <i>(P &lt; 0.5)</i>	<b>0.994±0.250</b> (±0.013) <i>(P &lt; 0.0005)</i>
<b>S</b> (n=84)	<b>1.071±0.239</b> (±0.0268)	<b>0.967±0.190</b> (±0.0182) <i>(P &lt; 0.0005)</i>	<b>1.180±0.222</b> (±0.0249) <i>(P &lt; 0.0005)</i>	<b>1.056±0.177</b> (±0.019) <i>(P &lt; 0.5)</i>	<b>1.039±0.161</b> (±0.019) <i>(P &lt; 0.5)</i>
<b>G2/M</b> (n=69)	<b>0.915±0.186</b> (±0.025)	<b>0.786±0.186</b> (±0.0227) <i>(P &lt; 0.0001)</i>	<b>0.992±0.196</b> (±0.0257) <i>(P &lt; 0.05)</i>	<b>1.029±0.233</b> (±0.0267) <i>(P &lt; 0.002)</i>	<b>0.934±0.221</b> (±0.0236) <i>(P &lt; 0.5)</i>

The values shown represent the mean± SD (±SE) of the relative DNA size of 69-518 nucleoids on average in the in different phases . obtained from two independent experiments performed on confluent and exponentially growing HSD2- fibroblasts irradiated with different doses of X-ray.

The difference in the relative DNA size between irradiated and unirradiated cells is considered significant when  $P < 0.05$  and highly significant when  $P < 0.02$ .

**Table (3.17) Variation of the comet fluorescence decrement. with respect to unirradiated nucleoids after electrophoresis for G1, S and G2/M HSD2 fibroblasts at different doses. measured by the neutral comet assay**

Cell phase	$\Delta F$ (a.u)				
	0 Gy	5 Gy	10 Gy	15 Gy	20 Gy
<b>G0</b> (n=518)	<b>0</b>	<b>41486</b>	<b>55197</b>	<b>84047</b>	<b>96958</b>
<b>G1</b> (n=449)	<b>0</b>	<b>89754</b>	<b>100450</b>	<b>97567</b>	<b>115004</b>
<b>S</b> (n=84)	<b>0</b>	<b>142475</b>	<b>157867</b>	<b>191169</b>	<b>185547</b>
<b>G2/M</b> (n=69)	<b>0</b>	<b>61999</b>	<b>129400</b>	<b>175193</b>	<b>203970</b>

The values shown represent the fluorescence decrement ( $\Delta F$ ). with respect to unirradiated nucleoids after electrophoresis. calculated as  $\Delta F = F - F_0$ . where.  $F$  is the total fluorescence of irradiated nucleoids.  $F_0$  is the total fluorescence of unirradiated nucleoids (the intercept value of the fluorescence-dose response relationship calculated in the dose range (5-20 Gy) (Table 3.14).

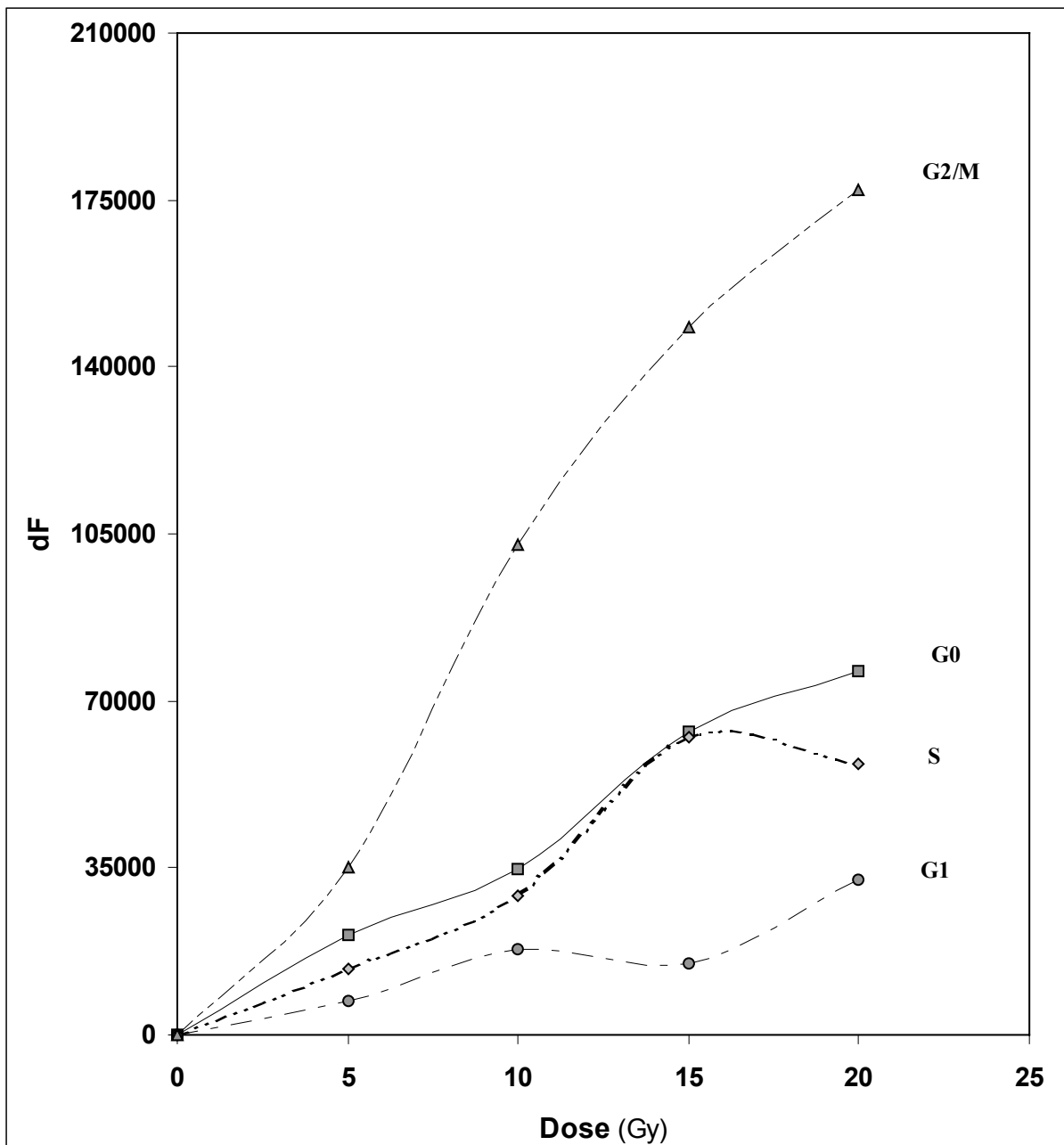
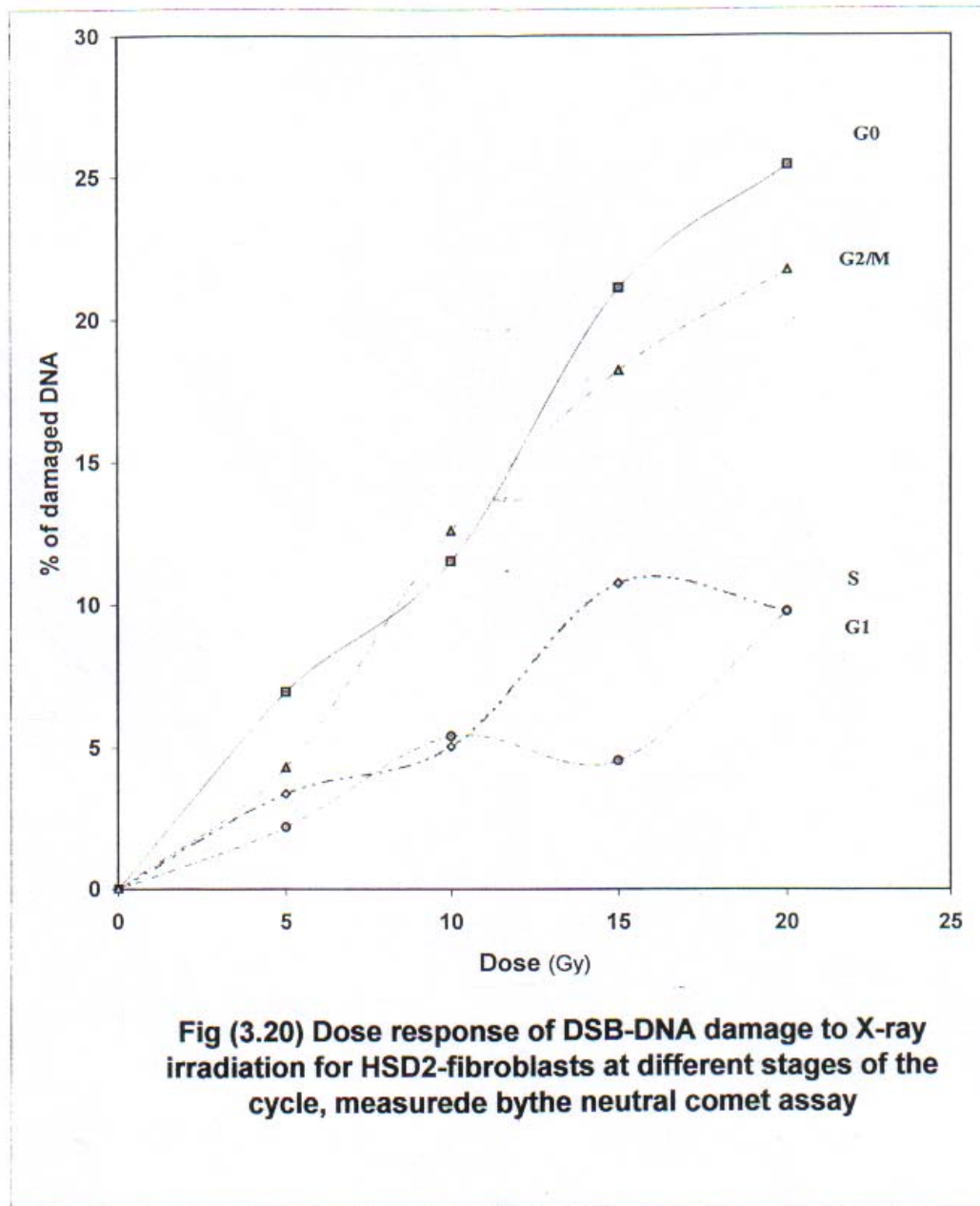


**Fig (3.19)** Radiation dose-response of the comet fluorescence decrement (df) to X-ray irradiation for HSD2 fibroblasts, at different phases measured by the neutral comet assay

The points shown represent the fluorescence decrement (df), with respect to unirradiated nucleoids after electrophoresis for cells at different stages of the cell cycle.

**Table (3.18) DNA damage induced by X-ray irradiation in HSD2 fibroblasts at different stages of the cell cycle. measured by the neutral comet assay**

Cell phase	% of damaged DNA				
	0 Gy	5 Gy	10 Gy	15 Gy	20 Gy
<b>G0</b> (n=518)	0	6.949	11.513	21.111	25.412
<b>G1</b> (n=449)	0	2.183	5.393	4.528	9.760
<b>S</b> (n=84)	0	2.377	5.022	10.742	9.777
<b>G2/M</b> (n=69)	0	4.318	12.591	18.213	21.745



The points shown represent the percentage of DSB- damaged DNA in HSD2- fibroblasts in different stages of the cell cycle irradiated with different doses.

**Table (3.19) Rates of radiation-induced DSB damage of DNA in HSD2 fibroblasts. at different stages of the cell cycle. measured by the neutral comet assay.**

<b>Cell cycle stage</b>	<b>DNA Damage rate (%DNA/Gy)</b>
<b>G0</b>	<b>1.880</b>
<b>G1</b>	<b>2.18</b>
<b>S</b>	<b>1.83</b>
<b>G2/M</b>	<b>1.52</b>

The values shown represent the rates of radiation induced DNA damage. which represent the slope of the DNA damage versus dose relationship calculated by linear regression analysis.

**Table (3.20) Rates of DNA-DSB induction by ionizing radiation in HSD2 fibroblasts. at different stages of the cell cycle. measured by the neutral comet assay.**

<b>Cell cycle stage</b>	<b>DSB-induction rate (DSB/Gy cell)</b>
<b>G0</b>	<b>18.1</b>
<b>G1</b>	<b>21.0</b>
<b>S</b>	<b>17.6</b>
<b>G2/M</b>	<b>14.6</b>

### **3.7.8) Effects of ionizing radiation on the DNA damage in HSD2-fibroblasts at different stages of the cell cycle.**

The fluorescence decrement induced by ionizing radiation is attributed mainly to extensive breakage of DNA induced by ionizing radiation (*Olive et al., 1994*). Conversion of double stranded DNA to single stranded damaged DNA during the short period of alkaline treatment, after neutral electrophoresis, leads to a decrease in the total fluorescence (F590) with an extent proportional to the extent or degree of DNA damage. Since the major quantity of single stranded denatured DNA is induced at the SSB-sites of the broken loops made accessible to the alkaline action via DSB-induction and the consequent relaxation during neutral electrophoresis, the fluorescence decrement induced by X-rays observed under the suggested conditions of neutral lysis and electrophoresis is caused mainly by DSB-induction. Therefore, extent of DSB-damage of DNA induced by ionizing radiation can be calculated as the fractional decrement of the total fluorescence induced by ionizing radiation, by using equation 1 in chapter 2.7.3.

The results of DNA damage calculated by this method are shown in (Table 3.18). A general increase in the fraction of damaged DNA with dose is observed, at all stages of the cell cycle. By plotting a relationship between the percentage damaged DNA and the dose of X-ray, we obtain the results shown in (Fig. 3.20). The slopes of this increase, calculated by linear regression analysis, which represents the rate of DNA damage induced by ionizing radiation, are shown in (Table 3.19). As shown in this table, the rate of DNA damage varies in the following order  $G_0 > G_2/M > S > G_1$ .

### **3.7.9) Effects of ionizing radiation on DSB-induction in individual cells at various stages of the cell cycle.**

By calibrating the rates of DNA damage (Table 3.19), using the rate of DSB-induction in G1-phase cells (21 DSBs/Gy.cell) (*Iliakis et al., 1991b*), as a reference value, we obtain the rate values of DSB induction, at various stages of the cell cycle, shown in (Table 3.20). The induction rate of DSB varies in the following order  $G_0 > G_2/M > S > G_1$ .



# ***DISCUSSION***

## **Discussion**

DNA double strand breaks (DSBs) are considered as the most important initial DNA lesions leading to the mutagenic, carcinogenic and lethal effects of radiation. In 1984 *Ostling and Johanson* described a method to measure DNA damage in individual cells based on migration of DNA in an electric field called single cell gel electrophoresis (or comet assay).

*Olive et al.* (1993) have modified the neutral comet assay to incorporate more vigorous lysis and elevated temperature (50°C), aiming to bias DNA damage detection towards (DSBs). *Ross et al.* (1995) found this system too aggressive for some human cell lines, with unacceptable background damage. To overcome this problem, we have developed the neutral comet assay experimentally, by lysing the cells at the physiological temperature (37°C), in presence of Proteinase-K to remove most of DNA-bound proteins, which would retard DNA migration.

In 1993, *Olive and Banath* have introduced a new technique for analysis of DNA damage as a function of the cell cycle position, utilizing the potential of comet assay for simultaneous measurements of DNA content (total fluorescence) and DNA damage for each single cell. The method is based on measuring DNA-damage as a function of DNA-content. By means of this bivariate analysis, the DNA damage can be measured at different positions of the cell cycle. However, this analytical method has many back draws, which were described previously in Section (1.3). To overcome these back draws, an analytical method for sorting cells in different phases (sections 1.2 and 1.3) was developed by which DNA-damage at different stages of the cell cycle could be measured. This method has several advantages:

- 1) It is based on quantitative measurement of fractions of cells at different phases, in 20 channels, representing the whole range of DNA-content, which permits accurate estimation of the exact border values of DNA content separating different phases and the sorting windows for each of the three populations. Therefore, it yields more accurate and reliable results for the mean DNA damage of individual cells at the three phases of cell cycle.
- 2) Sorting of cells into different phases can be achieved by using a computer program-based mathematical analysis of the comet fluorescence (DNA)-histograms, without the need to use any other accessory methods like flow-cytofluorometry.
- 3) The analytical method in conjunction with the software-programs, can be used successfully (with a high reproducibility) to measure the fraction of cells in G1, S and G2/M phases of the cell cycle.
- 4) 800-1100 cells are scored on each slide, which is statistically enough to get reproducible results and a reliable conclusion about the effect of cell cycle position on DNA-damage in individual cells.

The developed method has also several experimental advantages over the previous methods described in section (1.3), which makes it more sensitive, reliable and accurate for measuring the nuclear DNA content and analysis of DNA histograms and the cell cycle distribution namely:

1) Treatment of cells with RNase (10  $\mu\text{g/ml}$ ) for 2 h followed by alkaline shock treatment with 0.15 M NaOH for 1 min removes the major quantity of RNA from the cell nuclei resulting in a higher accuracy and reliability of the nuclear DNA-content. Therefore this method is more applicable for analysis of DNA histograms and the cell cycle distribution, as compared to the Olive's protocol (see section 1.3).

2) Lysing is conducted in a lysing solution at 4°C for 1 hr and then in the same solution without Triton in presence of RNase for 2 hrs and finally in presence of proteinase-K at 37°C for half an hour. This system is not too aggressive for DNA in human cell lines, yielding measurements without any appreciable background damage, which represents a technical advantage of the developed technique over Olive's method.

3) Partial unwinding of the nuclear DNA, by using mild alkaline conditions (0.15 M NaOH for 1 min) enhances the difference in the DNA structure between cells in different phases of the cell cycle, required for defining more sub-compartments of cells in different phases of the cell cycle and for analysis of DNA condensation at these phases. Thus, this method is more accurate and reliable for measuring the DNA content in individual cells and more applicable for analysis of DNA histograms and the cell cycle distribution, as compared to the Singh's method (section 1.3).

The comet assay has the advantage of being applicable for measuring simultaneously the nuclear DNA-content (the total comet fluorescence) and DNA-damage in individual cells, providing the possibility to measure the fraction of cells in different phases of the cell cycle.

800-1100 cells (comets) stained with (EB), visualized by an epi-fluorescence microscope supplied with a CCD-camera and an image analysis system, were analyzed for DNA damage and DNA-content (represented by the total fluorescence), simultaneously. The cells then were sorted according to the DNA-content (DNA-histograms). Analysis of these histograms by the developed computer program-based mathematical technique was described previously in detail in Section (1.1).

As shown in the histograms (Figs 3.1 and 3.2), representing the data, all cells in the G1-phase of the cell cycle would have diploid (2C)-DNA content, those in G2/M would have tetraploid (4C)-DNA content, and those in S-phase would have intermediate DNA contents between the two peaks. If the staining procedure was perfectly uniform and cells were measured in a system that introduced no instrumental dispersion (broadening due to electronic noise, light scattering, etc.), the distribution of the cells in (Fig 1.1.b) would appear as shown in (Fig 1.1.a). The difference between (Fig 1.1.a) and (Fig 1.1.b), which are different kinds of plots of the same data, is due to the broadening effects mentioned above. If the broadening is random from cell to cell, then the G1 and G2/M-cells, which have diploid and tetraploid DNA-content, respectively, could be described by normal curves. In fact the DNA-histograms obtained in this study could be described to a high extent by normal distribution functions, as indicated by the small sum of squared errors of the fit lines (Table 3.1) and as shown by the small deviation of the fit line from the experimental data in most histograms shown in this study.

By comparing the DNA-histograms of the stimulated confluent cells with that of the exponentially growing cells, we observed a considerable shift of the distribution after releasing of cells from contact inhibition by trypsinization and replating at lower density. These results are consistent with

those reported by *Smets* (1973), who observed that the nuclear chromatin from contact-inhibited confluent 3T3-fibroblasts bound 50-70 % less acridine orange dye than did exponentially growing cells. As shown in (Fig 3.3), we observed a remarkable shift of the G1-peak of the exponentially growing cells to a higher fluorescence, when compared to that of contact inhibited (confluent) cells. Similar results were obtained, in 1975, by *Chiu and Baserga*, who observed an increase in template activity, circular dichroism spectra, ability to bind EB in the nuclei isolated from the G1 WI-38 fibroblasts released from contact inhibition by trypsinization and replating at lower density, when compared to G0-cells.

With respect to the alteration in the nuclear morphology and DNA fluorescence accompanying transition of cells through various phases of the cell cycle, the results of comet area versus cell cycle stage, (Fig 3.4), showed a general increase in the nuclear size with progression of cells through the cell cycle, with four distinct phases; the first one occurs with transition of G0 cells through the G1 phase of cell cycle, which is characterized by a remarkable and significant increase ( $p < 0.00005$ ) in nuclear size (Table 3.2): These results are consistent with previous studies indicating a significant increase in the nuclear size (area and projection), with transition of cells from G0 to G1-phases of the cell cycle (*Kendall et al., 1977; Nicolini et al., 1977c*). This increase in nuclear size with G0-G1 transition was established in another study, by using the FCN- pulse width as a measure of the nuclear diameter (*Darzynkiewicz, 1977d*).

The developed technique defines compartments of cells in different phases, and measures simultaneously comet parameters related to DNA structure and nuclear morphology, like (the total fluorescence and comet area), allowing the development of a biophysical model for the analysis of the degree of condensation and relative molecular size of DNA in single cells at different stages of the cell cycle (section 1.2).

The results obtained (Figures 3.5 and Table 3.4) showed a remarkable decondensation of the nuclear DNA, concomitant with a considerable increase in the relative molecular size of DNA (DNA dispersion), with progression of cells through the G1-phase of the cell cycle. These results are in accordance with results reported by (*Baserga and Nicolini 1976*) on chromatin isolated from WI-38 cells, which revealed an increase in the intrinsic viscosity of chromatin from G0-cells, 3 hrs after stimulation; this increase correlates with an increase in the chromatin template activity, indicating an increase in the effective molecular size of nuclear chromatin during the course of DNA activation for transcription in the pre-replication phase of the cell cycle. Similar changes in nuclear chromatin structure were observed in cells stimulated to proliferate through the G1-phase, from a decreased thermal stability (*Rigler et al., 1969*) to an increased binding of EB (*Ringertz and Bolund, 1969; Chiu and Baserga, 1975; Nicolini and Baserga, 1975 a, b*) and increase in positive ellipticity in the 250-300 nm region of CD spectra (*Nicolini and Baserga 1975 a, b*). Moreover, an increased sensitivity to DNase in chromatin from cells in the late-G1/early-S period was observed by *Pederson (1972)*, indicating a high degree of chromatin dispersion during these stages of cell cycle, as observed in this study.

This agreement of the results of this study on nuclear DNA with the results obtained on intact chromatin in (or isolated from) nuclear systems, indicate that the comets (nucleoids) prepared by the developed method retain significant features of the DNA structure of the intact chromatin in mammalian cells.

With transition of cells from the G1-phase to the S stage of cell cycle, a slight increase in DNA condensation is observed. However, the nuclear DNA during this early stage of replication retain the highly active dispersed DNA structure of G1-phase, as indicated by the high relative size of DNA during this stage of cell cycle (Table 3.4). These results are consistent with those obtained by *Darzynkiewicz et al.*, 1980, based on the sensitivity of chromatin to acid denaturation or those obtained by *Sawicki et al.* (1974), by means of automated image analysis of Feulgen stained mouse fibroblasts.

Agreement of the results in this study with those reported by (*Darzynkiewicz et al.*, 1980) on nucleoids partially depleted from histone or by on DNA isolated from iris's cells (*Collins, 1974*) and on isolated intact chromatin (*Nicolini et al.*, 1977 a, b and *Pederson, 1972*) indicates that the histone depleted nucleoids, prepared by the developed method retain significant features of DNA structure and supercoiling of the chromatin in intact cells.

The results of relative DNA-condensation obtained by the developed method (Fig 3.5 and Table 3.4) showed a complete agreement, at all phases of cell cycle with those obtained by (*Darzynkiewicz et al.*, 1980) by using flow cytofluorometry. This observation confirms the succession of the developed model to predict the different degree of DNA condensation in individual cells, at various stages of the cell cycle.

Our technique has the advantages over all FCM-methods, mentioned above, in that:

- 1) It utilizes physiological non-denaturing conditions for histone extraction and depletion of nuclei from DNA bound proteins (the high salt extraction and proteinase K treatment at 37 C, as compared to the acid or thermal extraction used in other methods, which is usually accompanied by a high background DNA damage (*Ross et al.*, 1995). Therefore our technique permits examination of nuclear DNA condensation and the degree of supercoiling, under physiological non-denaturing conditions, allowing it to be used further in investigating the effects of ionizing radiation and other DNA-damaging agents on the degree of DNA condensation in individual cells, by using comet assay.
- 2) Mild alkaline conditions (alkaline shock treatment in 0.15 M NaOH for 1 min) was used in our method for partial unwinding of DNA, allowing the nuclear DNA in single cells to retain significant features of the secondary and higher order structures of the intact chromatin in the untreated intact cells. Partial unwinding and denaturation of nuclear DNA has been established as an essential step in our method, as in other FCM- methods to enhance the differences in DNA structure between cells in various phases and to distinguish them according to the DNA condensation.
- 3) The treatment used in our method appears to enhance the difference in chromatin structure among different phases of the cell cycle to the extent that cells could be separated on the basis of DNA condensation. By this treatment the sensitivity of the method increases to the extent that it be able to detect the small difference in DNA condensation among cells in the various phases of the cell cycle.

- 4) Using cells embedded in agarose reduces chromatin- degradation induced by shearing during the cell preparation, which could not be avoided by the other methods, which based on the fluorescence measurements of cells suspended and treated in solution. This advantage reduce the problems of cell clumping and loss of cells, with the consequent high error and uncertainty of the measured data.

The most interesting advantage of the developed technique, besides its potential to measure the DNA damage in single cells, is the ability to measure with a high sensitivity the effects of ionizing radiation on the degree of supercoiling and condensation of DNA in individual cells at different stages of the cell cycle. Several methods have been used for this purpose. One of these methods is the fluorescence halo assay described previously in (1.1.2.3).

The results of bivariate analysis of tail intensity versus DNA content (Fig 3.6) showed that G1 cells approaching the S-phase have the same low tendency of DNA migration like S- cells. These results

Can be explained by a model proposed recently by (*Blow, 1992*) for initiation of DNA replication. In this model, the initiation occurs in the G1-phase by assembly of an initiation complex

at the origin of replication. One of the earliest events for the initiation of DNA replication during the G1-phase is site specific binding of an initiator protein to the replication origin, followed by unwinding

of the origin DNA by a helicase (*Stahl et al., 1986; Dean et al., 1987; Dodson et al., 1987; Wold et al., 1987; Roberts and D' Urso, 1988; Kornberg, 1988*). The binding of this initiation complex leads ultimately to unwinding of the DNA duplex. The single stranded DNA exposed by this activity is stabilized by a single- stranded DNA binding protein (RF.A). The result of this action is to produce a stretch of unwounded, single stranded DNA around the origin of replication, onto which the other proteins of replication fork can be loaded. These partially unwounded DNA segments induced at these active initiation sites highly entangle with other DNA molecules during lysis (*Klaude et al., 1996*). Partial alkaline unwinding followed by neutralization lead to further tangling of DNA molecules at these active initiation sites (*Olive and Banath, 1993*). This tangling may lead to further increase the effective molecular size of DNA (Table 3.4), with a consequent retardation of DNA migration from cells during the mid and late stages of pre-replication (Fig 3.6).

With progression of cells from G1 to S-phase of the cell cycle, further decrease in DNA migration from individual cells is observed (Fig 3.6). DNA from unirradiated cells in the DNA synthetic (S) phase of the cell cycle generally show lower tendency to migrate from the nuclear core. The results are consistent with those reported recently by *Olive (1999)* confirming that the problem is intrinsic to S-phase cells. This low tendency of DNA migration from S-phase cells may be attributed to factors related to the transcribing and replicating DNA structures, which have larger effective size and therefore migrate less effectively in the electric field.

Dispersion and unwinding of DNA associated with activation of chromatin for transcription lead to a gradual increase in the relative size of DNA, and in turn to a remarkable decline in DNA migration; with transition of cells from G0 to G1 phase of cell cycle (Table 3.5 and Fig 3.5). During S phase the forked structures, associated with DNA replication, lead to a further retardation of DNA migration from S cells. During G2/M phase association of DNA with

nuclear matrix fibrillar proteins leads to a remarkable retardation of DNA migration from G2/M cells, as compared to G0 cells, which can be recorded by the developed method.

A striking observation was that although the G0 and G2/M cells have a relatively condensed DNA they exhibit different behavior of DNA migration (Table 3.5 and Fig 3.6). G0 cells show a higher tendency of DNA migration, as compared to G2/M phase cells. To explain this phenomenon, it should be taken into account that the two populations have condensed DNA and chromatin structure and therefore they have the lowest template and transcriptive activities with respect to the interphase cells. Therefore, the difference in DNA migration between the two populations can not be attributed to differences in DNA unwinding involved in transcription and replication processes as in G1 and S cells. Also this retardation of DNA migration during G2/M phase can not be attributed to the presence of any replicating structures, which completely disappear at the end of S-phase of cell cycle. This indicates that other factors play a role in reducing the DNA migration from G2/M cells, as compared to cells in the G0-phase of cell cycle.

It is believed that the difference in DNA migration between the two populations of cells is due to differences in the extent of binding of DNA to the tightly bound components of the nuclear proteins. These tightly bound proteins could then play a critical role in preventing DNA from migrating in an electric field.

The results of comet fluorescence (Fig 3.7 and Table 3.7) showed a significant decrease in the DNA fluorescence in unirradiated nucleoids, after electrophoresis. This decrease in fluorescence can be attributed to partial unwinding of DNA, at the alkaline labile sites, made accessible to the action of alkali by electro stretching of DNA loops, at the solenoidal level, during electrophoresis. Therefore, this reduction in DNA fluorescence reflects a relaxation of DNA at the level of the solenoid fiber, which leads to an increase in the accessibility of alkali labile sites to the alkaline action, with a consequent increase in the amount of single stranded DNA and consequently to a reduction in the nuclear fluorescence, after electrophoresis.

The decrease in the DNA fluorescence induced by partial alkaline unwinding is attributed to the metachromatic properties of EB, which emit fluorescence in the 590 nm region, with a less quantum efficiency, on binding to single stranded DNA, than on binding to double stranded DNA (*LE Pecq and Paolett, 1966, 1967; Darzynkiewicz et al., 1987; Olive and Banath, 1995*).

As shown in (Table 3.7), a remarkable decrease in the nuclear fluorescence after electrophoresis is observed, with various degrees, at different stages of the cell cycle, indicating the presence of alkali labile sites in all cell populations studied. The decrease in the DNA fluorescence induced by partial alkaline unwinding is attributed to the metachromatic properties of EB, which emit fluorescence in the 590 nm region, with a less quantum efficiency, on binding to single stranded DNA, than on binding to double stranded DNA (*LE Pecq and Paolett, 1966, 1967; Darzynkiewicz et al., 1987; Olive and Banath, 1995*). As shown in (Table 3.7), a remarkable decrease in the nuclear fluorescence after electrophoresis is observed, with various degrees, at different stages of the cell cycle, indicating the presence of alkali labile sites in all populations studied.

During G1-phase, DNA must undergo a change from the chromosomal or ``inactivated`` state to the ``activated`` state in order for replication to proceed. On this basis, the alkaline labile sites in G1- cells may arise from the nicking process of DNA involved in DNA activation for transcription and initiation of replication. For initiation of DNA replication and activation of DNA for transcription during G1-phase, the DNA at the origin of replication must be unwound and the superhelical twist must be resolved by nicking DNA at certain initiation sites by excision enzymes and nicking closing enzymes (topoisomerases) (*Blow, 1992*). Subtle changes occur in native DNA prior to replication. These changes result in an activated DNA, which contains nicks (in early-G1) and then gaps or runs of removed excised nucleotides during the late stages of pre-replication. (*Collins, 1974*). Therefore a steady state of strand breaks is generated by DNA activation during this phase of cell cycle. An additional number of strand breaks is generated in this phase by the incision and rejoining processes involved in DNA repair (*Salganik et al., 1992*), which showed the maximum rate of DNA repair among all phases of the cell cycle (*Olive and Banath, 1993*).

During S-phase, cells contain replication forks or „bubbles“. Each replication fork behaves as a single strand break, when exposed to alkali, increasing the background DNA single strand breaks in S- cells. There are more than 10000 replicons per cell and the number of active replicons varies through S phase (*Collins et al., 1980; Blow, 1992*). By means of Bromodeoxyuridine (Brd-Urd) labeling in conjunction with confocal laser microscopy and anti Brd Urd staining (*Fox et al., 1991*) were able to resolve at least 250 separate replicon complexes in early-S phase, which were reduced to less than 80 at mid-S. If each of these active complexes were responsible for two single stand breaks, when DNA is denatured in alkali, then we might expect 500 background SSBs in early-S stage of cell cycle. In another study, *Graubmann and Dikomey (1983)*, have estimated from 600 to 2000 stand breaks per unirradiated S-cells. Moreover, a high proportion of single stranded DNA molecules have been observed by electron microscopy in DNA preparations from S-phase cells (*Carnevali and Filetici, 1981*).

After replication is completed the DNA would presumably be converted back to the chromosomal (native) state by DNA repair ligation mechanisms. However, a large number of alkali labile sites are observed in the G2/M-cells, as indicated by the high fluorescence decrement (dFo) (Table 3.7). These sites may be the nuclear matrix anchorage points involved in the supercoiling of DNA through the nucleoprotein (topoisomerase II), which leads to extensive condensation of the chromatin in M-phase cells. The previous suggestion based on previous results reported by *Singh and Stephens (1997)*, which revealed an extensive breakage at the alkali labile sites in human lymphocytes, lysed under the alkaline conditions and subjected to alkaline single cell gel electrophoresis (comet assay). Under these alkaline conditions, the DNA molecules in the tail region break down into small pieces of relatively uniform size, indicating that DNA is periodically associated and firmly attached to tightly bound proteins, which are stable and indigestible by proteinase-K treatment, under the neutral lysis conditions. This configuration of DNA structure resembles the higher order supercoiled structure, basing on the DNA loop domains, discussed previously in this chapter.



Briefly, in this model, the chromosomal DNA is associated periodically to certain nuclear matrix anchorage sites, through the nucleoprotein (topoisomerase II) (*Van Der Velden and Wanka, 1987; Roti Roti et al., 1992, 1993*). These nuclear matrix anchor sites are stable, under the neutral conditions of lysis, whereas they are dissociated, under the alkaline conditions, with a consequent extensive breakage of DNA into single stranded segments, which fluorescence less intensively on binding to EB. The large proportion of these topoisomerase II-binding sites are formed during the G2/M phase (*Earnshaw and Heck, 1988; Goswami et al., 1992*) which may account for the high fluorescence decrement observed in G2/M cells, as compared to cells in other phases of the cell cycle (Table 3.7). A high frequency of these sites is essential for chromosome condensation during mitosis and protects the integrity of the DNA in somatic cells. However, a high frequency of these sites of tightly bound proteins was observed also in sexual (human sperm) cells (*Singh et al., 1989*) to indicate that the high frequency of alkali labile sites is a general feature of the condensed chromatin.

The minimum fluorescence decrement (dFo) was observed in Go-cells (Table 3.7), which indicates a lower number of alkali labile sites formed during Go-phase of cell cycle. These results are consistent with a previous study performed by *Collins (1974)* which revealed a lower number of single strand breaks and/or alkali labile sites in Go cells, by using the alkaline sucrose gradient centrifugation method. More recently, a lower number of single strand breaks and/or labile sites was observed in Go-human lymphocytes, subjected to comet assay and agarose gel electrophoresis (*Singh et al., 1989*).

Since the original neutral comet protocol of *Östling (1984)*, several protocols have been developed and utilized (*Östling and Johanson, 1987; Olive, 1990, 1992; Olive and Banath et al., 1998*). However, these protocols have several back draws and disadvantages mentioned previously in Section (1.3). In this study, we have developed the neutral comet assay by optimizing the chemical and enzymatic treatments, the electrophoretic conditions (either the buffer or the time of electrophoresis) to overcome the back draws of the previous methods, to be applicable for accurate analysis of DNA histograms and the cell cycle distribution and to increase the sensitivity of the method for detecting DNA damage in the higher dose range (0-20Gy).

Concerning the DNA damage, the most important feature recognized is the tail length, which is proportional to the size of DNA loops migrated into the tail and the tail intensity, which is related to the number of DNA loops migrated into the tail.

The non-irradiated nucleoid showed a fluorescent sun with a halo of supercoiled loops around it. Irradiation caused strand breaks and releases DNA supercoiling, as the cells accumulate more damage. The electric field is more effective in drawing broken / relaxed DNA away from the nucleus. Not only does the tail appear longer, but also more DNA is found within the tail. The distance the DNA moves is likely to be related to the size of free or relaxed pieces that can migrate, while the tail intensity represents the number of DNA loops relaxed into the tail region.

By using the tail intensity as a comet parameter, the developed method was able to detect DNA damage in confluent cells induced by so low doses of X-rays as 5 Gy

Irradiation induces SSBs and DSBs in the DNA of irradiated cells. SSBs reduce DNA loop supercoiling, increasing the loop size. However, the DNA still retains the looped (circular)

configuration, which determines its mobility during neutral electrophoresis (*Salganik and Dianov, 1992*), excluding the possibility of contribution of SSBs to the increased tail intensity in irradiated nucleoids, as observed in this study.

On the other hand, DSBs relax the DNA loop completely from the supercoiling, which leads to conversion of DNA from the looped configuration to the linear configuration of a higher electrophoretic mobility (*Salganik and Dianov, 1992*), which can account for the increased amount of DNA migrated into the tail from irradiated nucleoids. However, the broken DNA loops relaxed into the tail appear to be attached to certain anchorage sites in the nuclear core matrix. Therefore, the increased tail intensity in irradiated nucleoids is induced mainly by DNA double strand breaks.

As shown in (Table 3.8), DNA migrates into the tail with different extents depending on the cell phase of irradiated populations. As compared to Go cells, we observed a significant decrease in the amount of DNA migrated into the tail from S and G2/M-phase cells, when compared to Go cells.

The newly developed analytical method for cell sorting as discussed previously in Section (3.1) provided the possibility to examine the effects of ionizing radiation on DNA migration from single cells, at different stages of the cell cycle. The results of bivariate analysis of tail intensity versus DNA content (Fig 3.8) showed a gradual decrease in the tendency of DNA migration with progression of cells from G1 to S phase, which increases again with transition to G2/M phase. Among all populations studied S-phase cells show the lowest tendency of DNA migration. The effect is observed at all doses including unirradiated cells, indicating that the effect is inherent to DNA structure and not caused by DSBs.

The results of the fluorescence density-dose response curves (Fig. 3.12) showed insignificant changes in the fluorescence density with dose, in the majority of cell populations examined. These results indicate the small effect of ionizing radiation on the fluorescence density as a comet parameter.

The results of comet area-dose response curves for cells, at different stages of the cell cycle (Table 3.10) showed a significant decrease in the comet area, at all doses, when compared to the control cells. The results of dose-response curves (Fig 3.13) showed a linear decrease in comet area with dose, for all cell populations studied. This decrease in comet area with dose is consistent with previous results reported by *Tempel* (1990) which revealed a linear decline in nuclear size, after X-ray irradiation in the dose range (0.5-19 Gy), by measuring the relative viscosity of thymic nucleoids at different doses.

It appears that tangling of DNA during alkaline shock treatment and neutralization reduces the effective volume of the nucleoids, with a consequent decrease in the comet area. The extent of this tangling and the consequent reduction in comet area increases with dose of ionizing radiation. The extent of these tangling increases with increasing the number of single stranded DNA segments in irradiated nucleoids. DSBs leads to a relaxation of DNA loops from supercoiling and exposing more number of alkali labile sites to the action of alkali, during the short period of the alkaline treatment, which leads consequently to increasing the number of

single stranded DNA segments and, in turn, the extent of DNA tangling and reduction in the comet area with the dose of X-rays.

A striking observation is the tendency of saturation of the comet area in the dose range (5-20 Gy). SSBs induced by a dose of 5 Gy leads to a maximum relaxation of the solenoid fiber in all DNA loops in irradiated nucleoids from supercoiling, with a consequent maximum exposure of alkali labile and SSB-sites to the action of alkali and in turn to a high extent of DNA tangling and reduction in the comet area. Further increase in the dose of X-rays leads to no further increase in the relaxation of the solenoid fiber, and consequently in the extent of DNA tangling. However, a remarkable decline in the comet area is observed at a lower rate for doses higher than 5 Gy, which may be attributed to tangling of single stranded DNA fully relaxed from the supercoiling, via DSB-induction, which leads to a consequent reduction in the comet area.

The results shown in (Tables 3.12) revealed a significant decrease in the comet fluorescence of cells at different stages of the cell cycle with increasing dose. These results contradict with a previous study performed by *Olive and Banath* (1994) which showed constant comet fluorescence over the dose range (0-50 Gy) for cells lysed and electrophoresed under the neutral conditions. It seems that the alkaline shock treatment of cell nucleoids subjected to neutral electrophoresis leads to a partial unwinding of double stranded DNA to single stranded DNA of a lower EB-stainability and decreased fluorescence. This partial unwinding of DNA is stabilized by the renaturation (neutralization) of DNA with 0.4 M Tris, since a large proportion of DNA from (2-37 %) in the dose range (5-20 Gy) no longer resembles the duplex DNA molecules in unirradiated nucleoids, a structure that these dyes must be able to recognize in order to bind efficiently.

An interesting observation in the fluorescence-dose response curves (Fig 3.15) is the deviation of the 0 Gy-point from the linearity observed in the dose range (5-20 Gy) and the approach to saturation observed in this dose range. This deviation from the linearity is attributed to a higher reduction in the comet fluorescence after irradiation with 5 Gy X-ray dose, which can not be attributed only to DSBs measured under the neutral conditions of the developed protocol, because of the low number of DSBs induced by X-rays, relative to the number of SSBs and superstructure (DNA-loop) units in irradiated cells.

Irradiation of diploid cells with 1 Gy induces 500 SSBs (*Olive et al., 1998*) and 20-30 DSBs (*Iliakis et al., 1991a; Olive and Banath, 1993*).

Based on a value of 500 SSBs/cell.Gy, a 5Gy-dose of X-ray induces about 2500 SSBs, as compared to only 150 DSBs in the DNA of diploid cells. There are about 1500 superstructure units or DNA loop domains attached to the nuclear matrix / membrane in the mammalian cell (*Östling and Johanson, 1987*). Basing on the assumption that a single DSB leads to a full relaxation of a single DNA loop from the supercoiling, a 5 Gy will lead to a complete relaxation of only 150 DNA loop domains (about 10 % of all looped superstructure units). If the whole fluorescence decrement at 5 Gy is induced by DSBs, measured under the neutral conditions of the developed protocol, then the 10 Gy-dose will lead to two fold decrease in the comet fluorescence, which was not observed in this study. Otherwise, we observed only about 1.1 fold decrease in the comet fluorescence in 10 Gy irradiated nucleoids, which indicate that a significant fraction of the fluorescence decrement in irradiated cells is induced by SSBs, which appear in DNA during the alkaline shock treatment, after (neutral) electrophoresis.

If the fluorescence decrement in the 5 Gy-irradiated nucleoids is induced by SSBs, it would be expected that two fold decrease in the comet fluorescence occurs in 10 Gy-irradiated nucleoids. However this was not observed, since irradiation with 10 Gy leads to a reduction in comet fluorescence of only 1.1 times that induced by 5 Gy. This finding indicates that a saturation of the reduction in comet fluorescence induced by SSBs occurs after irradiation with 5 Gy and another breakage process besides SSB-induction is responsible for the further reduction in comet fluorescence at higher doses of X-rays. It appears that the 5 Gy-dose leads to a maximum unwinding of all DNA loops in the irradiated cell. On this basis, it appears that 1 SSB can lead to approximately maximum unwinding of a single DNA loop. Since 1Gy of X-rays induces about 500 SSBs/ cells and there are about 1500 superstructure (DNA-loop) units in each cell, supposing a random poissonian distribution of SSBs among these units, a dose of 3 Gy can induce a SSB in each DNA loop and unwind all the superstructure units in the cell nucleoid. 3 Gy is close to the dose (5 Gy) required to reach the near-plateau-fluorescence decrement observed in this study (Fig 3.15), and is also close to the dose required to reach the plateau level found in the ( $F_{50}/F_0$ )-dose response curves, observed by *Östling and Johanson* (1984, 1987). Therefore, the 5 Gy-dose leads to maximum unwinding of the solenoid fiber in all DNA loops in interphase cells, with a consequent remarkable drop in the comet fluorescence at this dose. However, this effect was not observed in Go and G2/M cells. This may be due to the highly condensed supercoiled DNA in these cells reducing the accessibility of SSB-sites to the action of alkali during the short period (1 min) of alkaline treatment, with a consequent slight reduction in the comet fluorescence induced by SSBs in these cells, at the 5 Gy-dose of ionizing radiation. Therefore, the 5 Gy dose leads to a maximum unwinding in all DNA loops in interphase cells, as compared to a minimum unwinding in Go and late-G2/M cells.

If a complete unwinding induced by SSBs occur in irradiated interphase nucleoids, then a considerable reduction in comet fluorescence (at least 80 %) would occur, which was not observed in this study, which showed only (8-34 %) decrease in comet fluorescence at the 5 Gy dose of X-rays. This finding indicates a partial and incomplete unwinding of DNA induced by SSBs in irradiated interphase cells. It appears that tangling and renaturation of unwinded DNA loops, particularly those highly packaged and concentrated in the nuclear core, during neutralization reduce the extent of this unwinding, increase the proportion of double stranded DNA segments of a higher EB-stainability and fluorescence efficiency, and therefore reduce the extent of fluorescence decrement induced by ionizing radiation.

Doses up to 5 Gy lead to a maximum relaxation of the solenoid fiber and unwinding of DNA in all nuclear superstructure units. Further increase in the dose of ionizing radiation leads only to slight decrease in comet fluorescence. This reduction in comet fluorescence at higher doses indicates that a second process of DNA unwinding measured by the neutral protocol of comet assay (i.e. DSBs) occur, simultaneously, with the first process in irradiated nucleoids. Under these conditions, the DSB-broken loops, either those relaxed into the tail or remained in the head, become more accessible to alkaline action, which leads consequently to a detectable unwinding of DNA, with a consequent reduction in EB-stainability and comet fluorescence in irradiated nucleoids.

With increasing X-ray dose the number of broken, relaxed DNA loops and consequently the number of single stranded DNA segments increase. This increase in the number of unwinded DNA segments in irradiated nucleoids leads ultimately to a decrease in the comet fluorescence, with

increasing dose of ionizing radiation. The extent of this fluorescence decrement is proportional to the DNA damage and number of DSBs induced by ionizing radiation. Most of the radiation induced fluorescence decrement in G<sub>0</sub> and G<sub>2</sub>/M cells is induced by this process. This suggestion based on the observation of a slight reduction in comet fluorescence at the 5 Gy-dose, with respect to the control cells, which can not be attributed to DNA relaxation induced by SSBs, as suggested for the first process. It appears that the high degree of condensation and supercoiling in G<sub>0</sub> and G<sub>2</sub>/M cells reduce the accessibility of the highly concentrated DNA in the comet head to the action of alkali, reducing the amount of unwinded DNA in the comet head and preventing the fluorescence decrement induced by SSBs suggested in the first process. This finding indicates that the most fluorescence decrement induced by X-rays in G<sub>0</sub> and late-G<sub>2</sub>/M cells are due to relaxation of DNA loops broken by DSBs, as suggested in the second process.

The fluorescence decrement at 5 Gy-dose, induced by the first process (i.e. by SSBs localized in the head region) decreases with increasing the degree of DNA supercoiling, with progression of cells from S to G<sub>2</sub>/M stages of the cell cycle. This effect can be attributed to a reduction of DNA accessibility to alkali with increasing the degree of DNA condensation, with progression of cells through the mitotic cycle. This reduction in DNA accessibility to alkali leads to a reduction in DNA unwinding and therefore the amount of single stranded DNA with the cell cycle, with a consequent decrease in the fluorescence decrement induced by the 5 Gy dose of X-ray, with respect to that of unirradiated nucleoids (Table 3.13).

On the basis of the last results, we expect that there are two main DNA relaxation processes induced by two different DNA-lesions SSBs and DSBs. The first one occurs at the level of DNA secondary structure, via SSB-induction, which leads to a partial unwinding of double stranded DNA, during the alkaline shock treatment and stabilization of this unwinding during the neutralization. Crosslinking and entangling induced by this process leads to an increase in DNA condensation after irradiation with 5 Gy of X-rays (Table 3.12 and Fig 3.17). This effect leads to a reduction in DNA relative size at this dose of X-rays (Table 3.16 and Fig 3.18). The approximate saturation of this process at 5 Gy and the effect of second process of the full DNA relaxation induced by DSBs leads to a significant decrease in DNA condensation after irradiation with 10 Gy of X-rays. This effect leads to a significant increase in DNA relative size at this dose of X-rays:

The observed approximate saturation of the fluorescence decrement, induced by this DNA relaxation process, at 5 Gy, indicates a saturation of SSB-induced decondensation, at this dose of ionizing radiation. This means that no further increase in DNA decondensation is induced by SSBs, with increasing dose of ionizing radiation more than 5 Gy. If there were no decondensation process other than this, the DNA condensation would be constant with increasing dose of X-ray, which was not observed. Otherwise, the results of condensation-dose response curves showed a gradual decrease in DNA condensation with dose, which cannot be attributed to SSB-induced DNA relaxation. Rather, it reflects other decondensation (relaxation) process induced by DSBs (the dose-response measured under the neutral conditions of the present protocol). The significant decrease in DNA condensation with dose induced by this process (Table 3.14) demonstrates the significance of DNA double strand breaks in reducing the DNA supercoiling and chromatin condensation in irradiated cells, with respect to SSBs. This is expected, since a single DSB induces a full relaxation of the DNA loop from the supercoiling, as compared to SSBs, which

leads to a slight relaxation of the solenoid fiber, while the DNA loop remains in the circular supercoiled DNA configuration.

By calculating the fluorescence decrement induced by partial alkaline unwinding of DNA in nucleoids, after electrophoresis, at different doses of ionizing radiation, we obtained the results shown in (Table 3.18) and (Fig 3.17). These results showed two different behaviors for cells at various stages of the cell cycle. The first one occurs in interphase cells, which is characterized by a considerably high fluorescence decrement, after irradiation with 5 Gy dose of ionizing radiation, followed by a slower rate of fluorescence decrement, with a further increase in the dose of ionizing radiation. The second one occurs in G0 cells characterized by a linear increase in the fluorescence decrement with dose, in the whole range of X-ray doses.

The difference in EB-stainability between the single stranded (alkaline unwinded) DNA and double stranded DNA, observed in this study, is attributed to the metachromatic properties of EB which fluorescence weakly in the 590 nm region, and emit fluorescence of a longer wavelength (>600 nm), on binding to single stranded DNA. It is known that EB forms two different complexes with DNA; it may form a fluorescent complex with double stranded DNA by intercalation between the base pairs of the double helix; this complex has strikingly enhanced fluorescence quantum yield. Ethidium bromide may also form a complex with single stranded DNA by electrostatic binding of the cationic dye to negatively charged phosphate groups (*LE Pecq and Paoletti, 1967*).

Ethidium bromide fluoresces about 100 and 400 times more intensively on binding to intact double stranded DNA, than when bound to partially DNase-degraded DNA or fully single stranded DNA, respectively (*LE Pecq and Paolett 1966*). On this basis, we can consider the relative fluorescence decrement as a measure of the fraction of damaged DNA.

On the other hand, the relative fluorescence decrements  $dF(ssb)/F_0$  and  $dF(dsb)/F_0$  represent the fractions of damaged DNA induced by degradation of DNA, at the SSB-sites, made accessible to the alkaline action by relaxation of DNA, induced by radiation SSB and DSB-inductions, respectively. Results reported by (*Olive et al., 1994*), revealed reduction in the comet fluorescence induced by strand break induction in irradiated nucleoids pretreated with 5  $\mu\text{g/ml}$  nitrogen mustard, lysed under the alkaline conditions and subjected to alkaline microgel electrophoresis. Exposure of cells to the crosslinking compound (nitrogen mustard) concealed the presence of subsequent radiation-induced strand breaks and also prevented the loss of fluorescence observed after 15 Gy-irradiation, confirming that the most of the fluorescence reduction induced by ionizing radiation is caused by DNA strand breaks and the subsequent degradation during the alkaline treatment. A striking observation in this study is that, this reduction in comet fluorescence reaches a plateau level at the 5 Gy-dose of X-ray, consistent with the present study on diploid nucleoids treated for a short period with alkaline solution, after neutral electrophoresis, which revealed a near plateau reduction in comet fluorescence at the same dose of X-ray (Fig 3.17).

During the short period of alkaline unwinding, followed by overnight neutralization, there is a high probability of unwinding and tangling of DNA, at the SSB-sites in the tail than in the head region. Since, the DNA localized in the tail represent the DNA loops, relaxed by the DSB-induction, we can propose that a high fraction of the fluorescence decrement,  $dF$ , induced by

alkaline unwinding of DNA relaxed into the tail, after neutral electrophoresis, represents the amount of DSB-damaged DNA induced by ionizing radiation. Since, the fluorescence decrement,  $dF$ , represents not only the amount of DSB-damaged DNA in the tail region, but also the amount of DSB-damaged DNA remained tangled in the head region, it gives an actual measure for the total DSB-damaged DNA induced by ionizing radiation.

Therefore, the total fraction of DSB-damaged DNA as a percentage value can be calculated by using the following equation:

$$\% \text{ Damaged DNA} = \frac{F - F_0}{F^*_0} \cdot 100$$

Where,  $F$  is the total fluorescence of irradiated nucleoids,  $F_0$  is the total fluorescence of unirradiated nucleoids (the intercept value of the fluorescence-dose response relationship calculated in the dose range (5-20 Gy) (Table 3.12) and  $F^*_0$  is the total fluorescence of intact DNA in unirradiated nucleoids, before electrophoresis.

The results of DNA damage, measured by this method, (Table 3.15 and Fig 3.17), revealed a remarkable increase in DNA damage with dose of X-ray at all stages of the cell cycle. The results showed a fraction value of damaged DNA, in the range (2.183-6.949 %), at 5 Gy and (9.76-25.412 %), at 20 Gy, respectively. As compared to interphase cells, G<sub>0</sub> and G<sub>2</sub>/M cells showed extensive degradation of DNA, at all doses of ionizing radiation. The slope values of these lines (Table 3.16) revealed a remarkable increase in the rate of DNA damage in G<sub>0</sub> and late-G<sub>2</sub>/M-phase cells, as compared to cells in other phases of the cell cycle.

By calibrating the rate of DNA damage (Table 3.16), using the rate of DSB-induction in G<sub>1</sub>-phase cells (21 DSBs/Gy.cell) (*Iliakis et al., 1991b*), as a reference value, we obtain the rate values of DSB induction, at the various stages of the cell cycle, shown in (Table 3.17). As shown in this table, a maximum rate of DSB-induction is observed in G<sub>0</sub> phase of cell cycle. This rate decreases remarkably when cells enter the G<sub>1</sub> phase and increases again at the S stage of cell cycle. The results revealed rate values of 21 and 35 DSBs/Gy in cells at the G<sub>1</sub> and S stages, respectively. The value obtained for S cells is by a factor 1.6 higher as compared with the results obtained by *Iliakis et al. (1991b)*.

G<sub>2</sub>/M cells showed by a factor of 1.6 higher rate of strand break induction, as compared to S-phase cells. This finding is consistent with results reported previously by *Radford and Broadhurst (1988)*, who found a factor of 1.9 by using neutral elution. In contrast to these findings *Iliakis et al. (1991b)* observed an enhanced induction of DSB in G<sub>2</sub>/M cells relative to S cells by a factor of 1.3. *Olive and Banath (1993)* found no variation in DSB induction in G<sub>1</sub>, S and G<sub>2</sub>/M cells using Id Urd labeling. Approximately no variation in DSB induction in G<sub>1</sub>, S and G<sub>2</sub>/M cells was observed by *Iliakis et al. (1991b)*. It appears that the chromatin structure affects the results obtained by neutral elution or comet assay (tail moment and fluorescence decrement).

Variation in DSB yields (Table 3.17) has the consequence that the tail moment and also fluorescence decrement (this work) are not useful to measure DSB induction in dependence of the cell cycle. It is obvious that the comet assay (as is also for the neutral elution) may respond to the same cell cycle-associated alterations in the biophysical and/or biochemical properties of the DNA molecules. If this is true, then the variation in fluorescence decrement observed through the cycle should also be attributed to alterations in physicochemical properties of the DNA that

affect the changes in fluorescence by ionizing radiation and not to alterations in the induction of DSB throughout the cell cycle. Therefore, calibration in various phases of the cell cycle is required for a meaningful quantification and interpretation of the results obtained with synchronous cells.

\*\*\*



# ***CONCLUSIONS***

---

## **Conclusions**

The new approaches of the neutral comet assay have been successfully used to study the effects of ionizing radiation on the nuclear morphology and DNA structure in individual cells at various stages of the cell cycle. The results demonstrated a remarkable reduction in the nuclear size after X- ray irradiation.

A considerable reduction in DNA fluorescence induced by X-ray irradiation reflects an extensive breakage of DNA induced by ionizing radiation. The percentage decrement in comet fluorescence can be used as a measure of the DNA damage in individual cells at various stages of the cell cycle. Using the rate value 21 DSB/Gy. Cells for G1 cells (*Iliakis et al. , 1991b*) as a reference value , the rate values of damaged DNA can be calculated for S, G2/M and G0 cells.

Using the comet fluorescence as comet parameter, rather than the tail parameters, a lower sensitivity for measuring the DNA damage at the S and G2/M phases of the cell cycle in both irradiated and unirradiated nucleoids, indicating that the variation in these parameters with the cell cycle is not caused by the radiation damage, rather it reflects intrinsic differences in DNA structure between cells in various stages of the cell cycle. It is concluded that caution needs to be exercised before differences observed in the fluorescence decrement between various phases of the cell cycle after exposure to a given dose of radiation are interpreted as suggesting differences in the induction of DSB.

\*\*\*

# ***Summary***

## Summary

The present study reports improvements in the neutral comet assay first introduced by (*Singh and Stephans, 1997; Olive et al., 1998*) to measure radiation induced DNA damage. Different biochemical steps, including microgel preparation, lysis and enzymatic/chemical treatments have been modified and optimised to estimate the fraction of cells in different phases of the cell cycle and to determine the dose-response relationship.

Among all tail parameters that were used to measure the DNA damage induced by ionising radiation, the tail length was found to be the most sensitive. In this study DNA damage induced by X-ray doses as low as 5 Gy was detected.

The developed analytical method has been used for the simultaneous estimation of the fraction of cells and of DNA damage at different stages of the cell cycle. By using the tail intensity as a comet parameter, results showed a linear dose response relationship in the dose range between 0-20 Gy. The tail length on shows only a small radiation effect. This indicates that the tail intensity is the best descriptor of the response of DNA in only G0 and G1 cells to ionising radiation among all parameters studied in individual cells within the range of the X-ray doses used. The reproducibility of the method was statistically investigated and shown to be a very useful method.

The effects of ionizing radiation on the degree of DNA condensation in individual skin fibroblasts at different stages of the cell cycle was investigated using the developed comet assay method. The results of this study revealed a considerable condensation of the nuclear DNA after irradiation with 5 Gy and decondensation after irradiation with 10Gy of X-rays. This decondensation was attributed to a relaxation of the DNA from the supercoiling induced by the DSB-damage.

A significant increase in the tail length, concomitant with insignificant changes in the tail intensity, after electrophoresis of unirradiated nucleoids was recorded. These results provide an evidence for electrostretching of DNA loops extruded into the halo region of unirradiated nucleoids.

The results of dose response curves showed a decrease in the comet fluorescence with the X-ray dose, at all stages of the cell cycle. This reduction in comet fluorescence was attributed to partial unwinding of DNA at the SSB-sites of DNA loops relaxed from supercoiling, via DSB-induction, during neutral lysis and electrophoresis and consequently have a higher accessibility to alkaline action, during the short period of alkaline shock treatment, after electrophoresis. This observation provides a basis for estimating the fraction of damaged DNA, based on the fluorescence decrement induced by ionising radiation.

\*\*\*

## Zusammenfassung

Die vorliegende Untersuchung berichtet über Verbesserungen in der neutralen Kometenprobe, die zuerst durch (*Singh und Stephans 1997; Olive et al., 1998*) zum Messen der von Strahlung verursachten DNA-Beschädigung verwendet wurde. Unterschiedliche biochemische Schritte, einschließlich der Microgelvorbereitung, der Lysis und der enzymatisch-chemischen Behandlungen sind modifiziert und optimiert worden, um den Anteil der Zellen in den unterschiedlichen Phasen des Zellzyklus einzuschätzen und das Dosis-Antwort-Verhältnis festzustellen.

Unter allen Schweifparametern, die verwendet wurden, um die DNA-Beschädigung zu messen, welche durch die ionisierende Strahlung verursacht wurde, wurde die Schweiflänge dafür befunden, die empfindlichste zu sein. In dieser Studie wurde die DNA-Beschädigung, die durch die Röntgenstrahlung verursacht wurde, welche niedriger als 5 Gy war, ermittelt.

Die entwickelte analytische Methode ist für die simultane Einschätzung des Anteils der Zellen und der DNA-Beschädigung in den unterschiedlichen Stadien des Zellzyklus verwendet worden. Die Resultate ergaben, unter Benutzung der Schweifintensität als Kometenparameter, ein lineares Dosierungs-Reaktionsverhältnis im Dosierungsbereich von 0-20 Gy. Die Schweiflänge zeigt nur einen kleinen Strahlungseffekt. Dieses zeigt, dass die Schweifintensität die beste Beschreibung der Reaktion der DNA in den Zellen G0 und G1 ist, um Strahlung zu ionisieren innerhalb aller Parameter, die in den einzelnen Zellen innerhalb des Bereiches der benutzten Röntgenstrahldosen studiert wurden. Die Reproduzierbarkeit der Methode wurde statistisch berechnet und es zeigte sich, dass sie eine sehr nützliche Methode ist.

Die Effekte der ionisierenden Strahlung auf den Grad der DNA-Kondensation in den einzelnen individuellen Hautfibroblasten in den unterschiedlichen Stadien des Zellzyklus wurden mit dem entwickelten Kometenprobeverfahren erforscht. Die Resultate dieser Studie wiesen eine beträchtliche Kondensation der Kern-DNA nach der Bestrahlung mit 5 Gy und eine Dekondensation nach Bestrahlung mit 10 Gy Röntgenstrahlen auf. Diese Dekondensation wurde einer Entspannung der DNA zugeschrieben, welche durch das Supercoiling inklusive DSB-Zerstörung verursacht wurde.

Eine bedeutende Zunahme der Schweiflänge, zusammenfallend mit bedeutungslosen Änderungen in der Schweifintensität, wurde nach der Elektrophorese der unbestrahlten Nukleotide notiert. Diese Resultate stellen einen Beweis für das Elektrostretching der DNA-Schleifen dar, welche in die Haloregion der unbestrahlten Nukleotide gedrängt wurden.

Die Resultate der Dosis-Reaktionskurven zeigten eine Abnahme in der Kometenfluoreszenz mit der Röntgenstrahldosis, in allen Stadien des Zellzyklus. Diese Verringerung der Kometenfluoreszenz wurde dem teilweisen Abwickeln von DNA in den SSB-Stellen der DNA-Schleifen zugeschrieben, die vom Supercoiling über DSB-Induktion während der neutralen Lysis und der Elektrophorese entspannt wurden und infolgedessen eine höhere Zugänglichkeit zur alkalischen Reaktion, während der kurzen Periode der alkalischen Schocktherapie, nach der Elektrophorese hatten. Diese Beobachtung stellt eine Grundlage für die Einschätzung des Anteils der beschädigten DNA zur Verfügung dar, basierend auf der Fluoreszenzverminderung, die durch ionisierende Strahlung verursacht wurde.

---

## References

Alberts, B.; Bray, D.; Lewis, J.; Raff, M.; Roberts, K. and Watson, J. D. (1983): *Molecular biology of the cell*, Garland, New York.

Ager, D. D.; Dewy, W. C.; Gardiner, K.; Harvey, W.; Johanson, R. T. and Waldren, C. A. (1990): Measurement of radiation-induced DNA double strand breaks by pulsed-field gel electrophoresis. *Radiat. Res.*, 122: 181-187.

Baily Norman, T. J. (1959): *Statistical methods in Biology*. Wiley, New York, pp.173, 193.

Banath, J. P.; Fushiki, M. and Olive, P. L. (1998): Rejoining of DNA double-strand breaks in human white blood cells exposed to ionizing radiation. *Int. J. Radiat. Biol.* 73 (6): 649-660.

Baserga, R. and Nicolini, C. (1976): Chromatin structure and function in proliferating cells. *Biochem. and Biophys. Acta*, 458: 109-134.

Bliss, C. I. (1976): *Statistical methods for research in the natural sciences*. (Vol II). McCraw. Hill Book Company. New York, St Louis, San Francisco, Düsseldorf, London, Mexico, Toronto. PP. 564-565.

Blöcher, D. (1990): Rapid communication in CHEF electrophoresis: a linear induction of dsb corresponds to a nonlinear fraction of extracted DNA with dose. *Int. J. Radiat. Biol.* 57 (1): 7-12.

Blöcher, D. and Pohlit, W. (1982): Double-strand breaks in Ehrlich ascites tumor cells at low doses of X-rays. II. Can cell death be attributed to double strand breaks ? *Int J. Radiat. Biol.*, 42: 329-338.

Blow, J. J. (1992): Chromosome pathology. The regulation of chromosome replication. *J. of Pathology*, 167: 175-179.

Bryant, P. E. (1984): Enzymatic restriction of mammalian cell DNA using Pvu II and Bam HI: evidence for the double-strand break origin of chromosomal aberrations. *Int. J. Radiat. Biol.* 46: 57-65.

- 
- Chiu, N. and Baserga, R. (1975): Changes in template activity and structure of nuclei from WI-38 cells in the pre-replicative phase. *Biochemistry*, 14 (14): 3126-3132.
- Collins, J. M. (1974): Structural changes in deoxyribonucleic acid during early stages of lens regeneration. *J. of Biol. Chem.*, 25: 1839-1847.
- Collins, J. M.; Berry, D. E. and Baywell, C. B. (1980): Different rates of DNA synthesis during the S-phase of log phase HeLa S3, WI-38 and 2RA cells. *J. Biol. Chem.* 255 (8): 3585-3590.
- Collins, A. R.; Dobson, V. L.; Dusinska, M.; Kennedy, G. and Stetina, R. (1997): The comet assay: What can it really tell us? *Mutation Res.* 375: 183-193.
- Coquerelle, T. and Hagen, U. (1978): Radiation effects on the biological function of DNA. "Effects of ionizing radiation on DNA. physical, chemical and biological aspects." (Hüttermann, J.; Köhlein, W.; Teoule, R. and Bertinchamps, A. J. Eds). Springer-Verlag, Berlin, Heidelberg New York, PP.261-303.
- Darzynkiewicz, Z.; Traganos, F. and Melamed, M. R. (1980): New cell cycle compartments identified by multiparameter flow cytometry. *Cytometry*, 1 (2): 98-108.
- Darzynkiewicz, Z.; Traganos, F.; Carter, S. P. and Higgins, P. J. (1987): In situ factors affecting stability of the DNA helix in interphase nuclei and metaphase chromosomes. *Exp. Cell Res.* 172: 168-179.
- Dean, P. N. and Jett, J. H. (1974): Mathematical analysis of DNA distributions derived from flow microfluorometry. *J. of Cell Biol.* 60: 523-527.
- Dean, F.; Bullock, P.; Murakami, Y.; Wobbe, R.; Weissbach, L. and Hurwitz, J. (1987): DNA replication: SV40 large T-antigen unwinds DNA containing the SV40 origin of replication. *Proc. Natl. Acad. Sci. U.S.A.* 84: 16.
- Dodson, M.; Dean, F.; Bullock, P.; Echols, H. and Hurwitz, J. (1987): Unwinding of duplex DNA from the SV40 origin of replication by T-antigen. *Science*, 238: 964.
- Earnshaw, W. C. and Heck, M. M. S. (1988): DNA topoisomerase II facilitated degradation accompanies chromosome decondensation during early-G1. *Current Communications in Molecular Biology*. Cold Spring Harbor Laboratory. Cell cycle control in eukaryotes (Beach, D.; Basilico, C. and Newport, J. Eds.). PP: 176-183.

---

Elgin, S. C. R. and Weintraub, H. (1975): Chromosomal proteins and chromatin structure. *Ann. Rev. Biochem.* 44: 725-774.

Estey, E.; Adlakha, R. C.; Hittelman, W. N. and Zwellung, L. A. (1987): Cell cycle stage dependent variations in drug-induced topoisomerase II mediated DNA cleavage and cytotoxicity. *Biochemistry*, 26: 4338-4344.

Fairbairn, D. W.; Olive, P. L. and O'Neil, K. L. (1995): The comet assay: a comprehensive review. *Mutation Res.* 339: 37-59.

Farber, J.; Rovera, G. and Baserga, R. (1971): Template activity of chromatin during stimulation of cellular proliferation in human diploid fibroblasts. *Biochem. J.* 122: 189-195.

Flick, M.; Warters, R. L.; Yasur, L. S. and Krisch, R. E. (1989): Measurement of radiation-induced DNA damage using gel-electrophoresis or neutral filter elution shows an increased frequency of DNA strand breaks after exposure to PH 9,6. *Radiat. Res.*, 119: 452-465.

Fox, M. H.; Arndt-Jovin, T. M.; Baumann, P. H. and Robert-Nicoud, M. (1991): Spatial and temporal distribution of DNA replication sites localized by immunofluorescence and confocal microscopy in mouse fibroblasts. *J. of Cell Sci.*, 99: 247-253.

Frankenberg, D.; Frankenberg-Schwager, M.; Blöcher, D. and Habrich, R. (1981): Evidence for DNA-double strand breaks as the critical lesions in yeast cells irradiated with sparsely ionizing radiation under oxic and anoxic conditions. *Radiat. Res.*, 88: 524-532.

Friedl, A. A.; Friederike, A. K. and Schupp, E. (1995): An electrophoretic approach to the assessment of the spatial distribution of DNA double strand breaks in mammalian cells. *Electrophoresis*, 16: 1865-1874.

Giaretti, W.; Nüsse, M.; Bruno, S.; Di Vinci, A. and Geido, E. (1989): A new method to discriminate G1, S, G2, M and G1 postmitotic cells. *Exp. Cell Res.* 182: 290-295.

Gordon, D. J.; Milner, A. W.; Beaney, R. P.; Gridina, D. J. and Vaughan, A. T. M. (1990): The increase in radioresistance of V79 cells cultured as spheroids is correlated to changes in nuclear morphology. *Radiat. Res.* 121: 174-179.



- 
- Goswami, P. C.; Hill, M.; Higashikubo, R.; Right, W. D. and Roti Roti, J. L. (1992): The suppression of the synthesis of a nuclear protein in cells blocked in G2 phase: identification of NP-170 as topoisomerase II. *Radiat. Res.* 132: 162-167.
- Heck, M. M. S.; Hittelman, W. N. and Earnshaw, W. C. (1989): In vivo phosphorylation of the 170 kDa form of eukaryotic DNA topoisomerase II. *J. Biol. Chem.* 264: 1561-1564.
- Hill, B. T. (1978): Cancer chemotherapy. The relevance of certain concepts of cell cycle kinetics. *Biochem. Biophys. Acta*, 516: 389-417.
- Hill, B. T. and Baserga, R. (1974): Changes in the number of binding sites for ribonucleic acid polymerase in chromatin of WI-38 fibroblasts stimulated to proliferate. *Biochem. J.* 1974 141 (1): 27-34.
- Holland, J. M.; Wright, W. D.; Higashikubo, R. and Roti Roti, J. L. (1990): Effects of irradiation on nuclear protein synthesis in G2-phase of the cell cycle. *Radiation Res.* 122 (2): 197-208.
- Iliakis, G. E.; Metzger, L.; Denko, N. and Stamato, T. D. (1991a): Detection of DNA double-strand breaks in synchronous cultures of CHO cells by means of asymmetric field inversion gel electrophoresis. *Int. J. Radiat. Biol.*, 59(2): 321-341.
- Iliakis, G. E.; Cicilioni, O. and Metzger, L. (1991b): Measurement of DNA double-strand breaks in CHO cells at various stages of the cell cycle using pulsed field gel electrophoresis: calibration by means of I decay. *Int. J. of Radiat. Biol.* 59 (2): 343-357.
- Iliakis, G. E.; Cicilioni, O. and Metzger, L. (1993): Measurement of DNA double strand breaks in CHO cells at various stages of the cell cycle using pulsed-field gel electrophoresis: calibration by means of I-decay. *Int. J. Radiat. Biol.*, 64: 265-273.
- Jaberaboansari, A.; Nelson, G. B.; Roti Roti, J. L. and Wheeler, K. T. (1988): Post-irradiation alterations of neutral chromatin structure. *Radiat. Res.* 114: 94-104.
- Kendall, F. and Swenson, R. (1976): Nuclear morphometry during the cell cycle. *Science*, 196: 1106-11109.

- 
- Kendall, F. M.; Wu, C. T.; Giaretti, W. and Nicolini, C. A. (1977): Multiparameter geometric and densitometric analysis of the Go-G1 transition of WI-38 cells. *J. of Histochem. and Cytochem.* 25 (7): 724-729.
- Klaude, M.; Rriksson, S.; Nygren, J. and Ahnstöm, G. (1996): The comet assay: mechanisms and technical considerations. *Mutation Res.* 363: 89-96.
- Kornberg, A. (1988): DNA replication. *J. Biol. Chem.*, 263: 1.
- Larsen, J. K.; Birgitte, M. P.; Christiansen, J. and Jörgensen, K. (1986): Flow-cytometric discrimination of mitotic cells: Resolution of M<sub>2</sub> as well as G<sub>1</sub>, S and G<sub>2</sub> phase nuclei with mithramycin, propidium iodide and ethidium bromide after fixation with formaldehyde. *Cytometry*, 7: 54-63.
- Le Becq, J. B. and Paoletti, C. (1967): A fluorescent complex between ethidium bromide and nucleic acids: physical-chemical characterization. *J. Mol. Biol.* 27: 87-106.
- Leenhouts, H. P. and Chadwick, K. H. (1981): An analytical approach to the induction of translocations in the spermatogonia of the mouse. *Mutation Res.* 82(2): 305-321.
- Lett, J. T. and Sun, C. (1970): The production of strand breaks in mammalian DNA by X-rays at different stages in the cell cycle. *Radiat. Res.*, 44: 771-787.
- Löbrich, M.; Ikpeme, S.; Haub, P.; Weber, K. J. and Kiefer, J. (1993): Double-strand break induction in yeast by X-rays and  $\alpha$ -particles measured by pulsed-field gel electrophoresis. *Int. J. Radiat. Biol.*, 64: 539-546.
- Mason, R. L.; Gunst, R. F. and Hess, J. L. (1989): Statistical design and analysis of experiments, with applications to engineering and Science. John Wiley and Sons. New York, Chichester, Brisbane and Singapore. PP. 552-555.
- Mateos, S. and Grdon, A. T.; Steel, G. G. and McMillan, J. J. (1996): Cell-cycle variation in DNA migration in pulsed-field gel electrophoresis. *Int. J. Radiat. Biol.* 69 (6): 687-693.
- McKelvey-Martin, V. J.; Green, M. H. L.; Schmerzer, P.; Pool-Zobel, B. L.; DeMeo, M. P. and Collins, A. (1993): The single cell gel electrophoresis assay ( comet assay ): A European review. *Mutat. Res.* 288: 47-63.

- 
- Milner, A. E.; Vaughan, A. T. M. and Clarke, I. P. (1987): Measurement of DNA damage in mammalian cells using flow cytometry. *Radiat. Res.* 110 (1): 108-117.
- Mullenders, L. H. F.; Van Kersteren, A. C.; Bussman, C. J. M.; Van Zeeland, A. A. and Natarajan, A. T. (1984): Preferential repair of nuclear matrix associated DNA in Xeroderma pigmentosum: Complementation group C. *Mutation Res.* 141: 75-82.
- Natarajan, A. T. and Obe, G. (1978): Molecular mechanisms involved in the production of Chromosomal aberrations: I. Utilization of *Neurospora* endonuclease for the study of aberration production in G2 stage of the cell cycle. *Mutation Res.* 52: 137-149.
- Nicolini, C. and Baserga, R. (1975): Circular dichroism and ethidium bromide binding studies of chromatin from WI-38 fibroblasts stimulated to proliferate. *Chem-biol. Interactions*, 11:101-116.
- Nicolini, C.; Ajiro, K. and Thaddeus, W. B. (1975 a): Chromatin changes during the cell cycle of HeLa cells. *J. Biol. Chem.* 250 (9): 3381-3385.
- Nicolini, C.; NG, S. and Baserga, R. (1975 b): Effect of chromosomal proteins extractable with low concentrations of NaCl on chromatin structure of resting and proliferating cells. *Proc. Natl. Acad. Sci. USA.*, 72 (6): 2361-2365.
- Nicolini, C.; Kendall, F. and Giaretti, W. ( 1977 a ): Objective identification of cell cycle phases and subphases by automated image analysis. *Biophys. J.* 19: 163-178.
- Nicolini, C.; Kendall, F.; Baserga, R.; Dessaive, C.; Clarkson, B. and Fried, J. (1977 b) The Go-G1 transition of WI38 cells: 1. Laser flow microfluorometric studies. *Exp. Cell Res.* 106: 111-118.
- Nelson, W. G.; Pienta, K. J.; Barack, R. E. and Coffey, D. S. (1986): The role of the nuclear matrix in the organization and function of DNA. *Annu. Rev. Biophys. Biophys. Chem.* 15: 457-475.
- Nüsse, M.; Beisker, W.; Hoffman, C. and Tarnok, A. (1990): Flow cytometric analysis of G1- and G2/M-phase subpopulations in mammalian cell nuclei using side scatter and DNA content measurements. *Cytometry*, 11: 813-821.

- 
- Okayasu, R.; Bloecher, D. and Iliakis, G. (1988): Variation through the cell cycle in the dose-response of DNA neutral filter elution in X-irradiated synchronous CHO cells. *Int. J. Radiat. Biol.* 53: 729-747.
- Olive, P. L.; Hilton, J. and Durand, R. E. (1986): DNA conformation of Chinese hamster V79 cells and sensitivity to ionizing radiation. *Radiat. Res.*, 107: 115-124.
- Olive, P. L.; Banath, J. P. and Durand, R. E. (1990): Heterogeneity in radiation-induced DNA damage and repair in tumor and normal cells. *Radiat. Res.* 122: 86-94.
- Olive, P. L.; Wlodek, D. and Banath, J. P. (1991): DNA double-strand breaks measured in individual cells subjected to gel electrophoresis. *Radiat. Res.* 51: 4671-4676.
- Olive, P. L. (1992): DNA organization affects cellular radiosensitivity and detection of initial DNA strand breaks. *Int. J. Radiat. Biol.*, 62 (4), 389-396.
- Olive, P. L. and Banath, J. P. (1992): Growth fraction measured using the comet assay. *Cell Prolif.*, 25: 447-457.
- Olive, P. L.; Wlodek, D.; Durand, R. E. and Banath, J. P. (1992): Factors influencing DNA migration from individual cells subjected to gel electrophoresis. *Exp. Cell Res.*, 198: 259-267.
- Olive, P. L. and Banath, J. P. (1993 a): Induction and rejoining of radiation-induced DNA single-strand breaks: "tail moment" as a function of position in the cell cycle. *Mutation Res., DNA repair*, 294: 275-283.
- Olive, P. L. and Banath, J. P. (1993 b): Detection of DNA double-strand breaks through the cell cycle after exposure to X-rays, bleomycin, etoposide and Id Urd. *Int. J. Radiat. Biol.*, 64 (4), 349-358.
- Olive, P. L., Banath, J. P. and Evans, H. H. (1993): Cell killing and DNA damage by Etoposide in Chinese hamster V79 monolayers and spheroids: Influence of growth kinetics, growth environment and DNA packaging. *Br. J. Cancer*, 67: 522-530.
- Olive, P. L.; Banath, J. P. and Fjell, C. D. (1994 a): DNA strand breakage and DNA structure influence staining with propidium iodide using the alkaline comet assay. *Cytometry*, 16: 305-312.

---

Olive, P. L.; Banath, J. P. and Macphail, H. S. (1994 b): Lack of a correlation between radiosensitivity and DNA double strand break induction or rejoining in six human tumor cell lines. *Cancer Res.* 54: 3939-3946.

Olive, P. L. and Banath, J. P. (1995): Radiation-induced DNA double-strand breaks produced in histone-depleted tumor cell nuclei measured using the neutral comet assay. *Radiat. Res.* 142: 144-152.

Olive, P. L.; Johanson, P. J.; Banath, J. P. and Durand, R. E. (1998): The comet assay: a new method to examine heterogeneity associated with solid tumours. *Nature (Medicine)*, 4: 103-105.

Olive, P. L. (1999): Review. DNA damage and repair in individual cells: applications of the comet assay in radiobiology. *Int. J. Radiat. Biol.* 75 (4): 395-405.

Östling, O. and Johanson, K. (1984): Microelectrophoretic study of radiation-induced DNA damage in individual cells. *Biochem. and Biophys. Res. Commun.*, 123: 291-298.

Östling, O. and Johanson, K. (1987): Bleomycin, in contrast to gamma irradiation induces extreme variation of DNA strand breakage from cell to cell. *Radiat. Biol.* 52 (5): 683-691.

Paranjape, S. M.; Kamakaka, R. T. and Kadonaga, J. J. (1994): Role of chromatin structure in the regulation of transcription by RNA polymerase II. *Annu. Rev. Biochem.*, 63: 265-297.

Pederson, T. (1972): Chromatin structure and the cell cycle. *Proc. Natl. Acad. Sci. USA.* 69 (8):2224-2228.

Pederson, T. and Robbins, E. (1972): Chromatin structure and the cell division cycle. Actinomycin binding in synchronized HeLa cells. *J. of Cell Biol.* 55: 322-327.

Pettijohn, D. E. and Price, C. M. (1988): Nuclear proteins of the mitotic apparatus. In Adolph, K. W. (ed), "Chromosomes" Vol 3. Boca Raton, FL; CRC Press.

Pettijohn, D. E. and Coworkers (1984): Nuclear proteins that become part of the mitotic apparatus: a role in nuclear assembly. *J. Cell Sci. Suppl.* 1: 187.

- 
- Radford, I. R. and Broadhurst, S. (1988): Aphidocolin synchronization of mouse L cells perturbs the relationship between the cell killing and DNA double-strand breakage after X-irradiation. *Int. J. of Radiat. Biol.* 53: 205-215
- Rigler, R.; Killander, D.; Bolund, L. and Ringertz, N. R. (1969): Cytochemical characterization of deoxyribonucleoprotein in individual cell nuclei: techniques for obtaining heat denaturation curves with the aid of acridine orange microfluorometry and ultraviolet microspectro-photometry. *Exp Cell Res.*, 55: 205.
- Ringertz, N. R. and Bolund, L. (1969): Activation of Hen erythrocytes deoxyribonucleoprotein. *Exp. Cell Res.*, 55: 205.
- Roberts, J. and D' Urso, G. (1988): Positive control of DNA replication in the Eukaryotic cell cycle: Induction of a replication origin unwinding activity at the G1/S boundary. "Cell cycle control in Eukaryotes." *Current communication in molecular biology.* Cold Spring Harbor Laboratory, P. 90-99.
- Ross, G. M.; McMillan, T. J.; Wilcox, P. and Collins, A. R. (1995): The single cell microgel electrophoresis (comet assay): technical aspects and applications. Report on the 5th LH Gray trust workshop, Institute of cancer res., 1994. *Mutation Research*, 337: 57-60.
- Roti Roti, J. L. and Wright, W. D. (1987): Visualization of DNA loops in nucleoids from HeLa cells: Assays for DNA damage and repair. *Cytometry*, 8: 461-467.
- Roti Roti, J. L.; Taylor, Y. C.; Wright, W. D. (1992): Subnuclear structure in radiation and heat response. *Radiat. Res.* [ *Proc. Int. Congr.* ], 9 th 1991 (pub. 1992). 2: 160-165.
- Roti Roti, J. L.; Wright, W. D. and Taylor, Y. C. (1993): DNA loop structure and radiation response. *Advances in Radiat. Biol.* 17: 227-259.
- Rovera, G. and Baserga, R. (1971): Early changes in the synthesis of acidic nuclear proteins In human diploid fibroblasts stimulated to synthesize DNA by changing the medium. *J Cell Physiology*, 77 (2), 201-212.
- Ruiz De Almodovar, J. M.; Steel, G. G.; Whitaker, S. J. and McMillan, T. J. (1994): A comparison of methods for calculating DNA double strand break induction frequency in mammalian cells by pulsed field gel electrophoresis. *Int. J. Radiat. Biol.*, 65: 641-649.

- 
- Rydberg, B. (1984): Detection of DNA strand breaks in single cells using flow cytometry. *Int.J. of Radiat. Biol.*, 46: 521-527.
- Rydberg, B. and Johanson, K. J. (1978): Estimation of DNA strand breaks in single mammalian cells. In *DNA repair mechanisms*, ( Hanawalt, E. C.; Friedberg, E. C. and Fox, C. F., Eds ); New York, Academic Press, PP. 465-468.
- Salganik, R. I. and Dianov, G. L. (1992): Molecular mechanisms of the formation of DNA double-strand breaks and induction of genomic rearrangements. *Mutation Res.* 266: 163-170.
- Sapora, O.; Belli, M.; Maione, B.; Pazzaglia, S. and Tabocchini, M. A. (1991): The influence of genome structural organization on DNA damage and repair in eukaryotic cells exposed to ionizing radiation. ( Fielden, E. M. O. and Neill, P., Eds ). *The early effects of radiation on DNA (Vol H54)*.
- Sasaki, M. S. and Norman, A. (1966): DNA fibre from human lymphocyte nuclei. *Exp. Cell Res.* 44: 642-645.
- Sawicki, W.; Rowinski, J. and Swenson, R. (1974): Change of the chromatin morphology during the cell cycle detected by means of automated image analysis. *J. Cell Physiol.* 84: 423-428.
- Singh, N. P.; McCoy, M. T.; Tice, R. R. and Schneider, E. L. (1988): A simple technique for quantitation of low levels of DNA damage in individual cells. *Exp. Cell Res.*, 175: 184-191.
- Singh, N. P.; Danner, D. B.; Tice, R. R.; McCoy, M. T.; Collins, G. D. and Schneider, E. L. (1989): Abundant alkali-sensitive sites in DNA of human and mouse sperm. *Exp. Cell Res.* 184: 461-470.
- Singh, N. P.; Danner, D. B.; Tice, R. R.; Brandt, L. and Schneider, E. L. (1990): DNA damage and repair with age in individual human lymphocytes. *Mutation Res.*, 237: 123-130.
- Singh, N. P.; Tice, R. R.; Stephens, R. E. and Schneider, E. L. (1991): A microgel electrophoresis technique for the direct quantitation of DNA damage and repair in individual fibroblasts cultured on microscope slides. *Mutation Res.* 252: 289-296.
- Singh, N. P. and Stephens, R. E. (1997): Microgel electrophoresis: sensitivity, mechanisms and DNA electrostretching. *Mutation Res.* 383: 167-175.

- 
- Smets, L. A. (1973): Activation of nuclear chromatin and the release from contact inhibition of 3T3 cells. *Exp. Cell Res.* 79: 239-243.
- Stahl, H.; Droge, P. and Knippers, R. (1986): DNA helicase activity of SV40 large tumour antigen. *EMBO J.*, 5: 1939.
- Sweigert, S. E.; Rowley, R.; Waters, R. L. and Dethlefsen, L. A. (1988): Cell cycle effect on the induction of DNA double strand breaks by X-rays. *Radiat. Res.*, 116 (2): 228-244.
- Tempel, K. (1990): Changes in nucleoid viscosity following X-irradiation of rat thymic and splenic cells in Vitro. *Radiat. Environ. Biophys.* 29: 19-30.
- Terasima, R.; Tolmach, L. J. (1963): X-ray sensitivity and DNA synthesis in synchronous populations of HeLa cells. *Science*, 140: 490-492.
- Tice, R. R.; Andrews, P. W. and Singh, N. P. (1990): A sensitive technique for evaluating intercellular differences in DNA damage and repair. ( Sutherland, B. M. and Woodhead, A. D., Eds.), *DNA damage and repair in human tissues*. Plenum, New York, PP. 291-301.
- Tobey, R. A.; Vadez, j. G. and Grissmann, H. A. (1988): Synchronization of human diploid fibroblasts at multiple stages of the cell cycle. *Exp. Cell Res.* 179: 400-416.
- Van Der Velden, H. M. W and Wanka, F. (1987): The nuclear matrix. Its role in the spatial organization and replication of eukaryotic DNA. *Mol. BioL. Rep.* 12: 69-77.
- Vogelstein, B.; Pardoll, D. M. and Coffey, D. S. (1980): Supercoiled loops and eukaryotic DNA replication. *Cell*, 22: 79-85.
- Von Sonntag, C. (1987): *The chemical basis of radiation biology*. Taylor and Francis, London.
- Wagner, R. P.; Maguire, M. P. and Stallings, R. L. (1993): *Chromosomes. A synthesis*. A John Wiley and Sons, INC., publication, New York, Chichester, Brisbane, Toronto, Singapore. PP. 66-77, 114-121.
- Watanabe, M. and Horikawa, M. (1977): Analysis of differential sensitivities of synchronized HeLa S3 cells to radiation and chemical carcinogenesis during the cell cycle. *Mutation Res.*, 44: 413-426.



---

Withers, H. R.; Mason, K.; Reid, B. O.; DubRaysky, N.; Barkely, H. T.; Brown, B. W. and Smathers, J. B. (1974): Response of mouse intestine to neutrons and gamma rays in relation to dose fractionation and division cycle. *Cancer*, 34: 39-47

Wlodek, D. and Olive, P. L. (1990): Physical basis for detection of DNA double strand breaks using neutral filter elution. *Radiat. Res.*, 124: 326-333.

Wold, M.; Li, J. and Kelly, T. (1987): Initiation of Simian virus SV40 DNA replication in vitro: large tumour antigen and origin dependent unwinding of the template. *Proc. Natl. Acad. Sci. USA*. 84: 3643.

Worcel, A. and Benjayati, C. (1977): Higher order coiling of DNA in chromatin. *Cell*, 12: 83  
Zinkowski, R. P.; Meyne, J. and Brinkley, B. R. (1991): The centromere kinetochore complex: A repeat subunit model. *J. Cell Biol.* 113 (5): 1091-1110.

Zucker, R. M. and Elstein, K. H.; Easterling, R. E. and Massaro, E. J. (1988): Flow cytometric discrimination of mitotic nuclei by right-angle light scatter. *Cytometry*, 9:226-231.

## Curriculum Vitae

**Name:** Atef Mahmoud Mahmoud Attia

**Nationality:** Egyptian

**Date of birth:** 21. February, 1965

**Place of birth:** Giza, Egypt

**1982** High secondary school (Military Saedia) , Giza / Egypt

**1982-1986** B. Sc., Faculty of Science , Cairo University , Biophysics Department

**1986-1994** M. Sc., Faculty of Science , Cairo University , Biophysics Department

**1994-1997** Ph. D., Faculty of Science , Cairo University , Biophysics Department

**1997-2002** Ph. D. , Faculty of Biology , Georg- August- University , Goettingen

\*\*\*